BIOINSPIRED SYMMETRICAL LIPIDS FOR CONTROLLED DRUG DELIVERY

A Dissertation

Presented to the Faculty of the Graduate School

of Cornell University

In Partial Fulfillment of the Requirements for the Degree of

Doctor of Philosophy

by

Sara Yazdi

August 2009

BIOINSPIRED SYMMETRICAL LIPIDS FOR CONTROLLED DRUG DELIVERY

Sara Yazdi, Ph. D.

Cornell University 2009

Designing new drug delivery systems requires tight control of drug release kinetics. Historically, polymers have been strong contenders in the field. However, achieving a narrow polydispersity and reducing batch-to-batch variability in synthesis can be difficult. Therefore researchers have expanded to other materials such as lipids, which mat have more favorable drug release properties. Lipids are a chemically unique category of molecules that plays a role in functionality and architecture of all living cells. Thus when used as materials for design of drug delivery systems, they will be considered biodegradable and biocompatible. In addition they offer more robust control over design of molecular architecture and thus directly impact the release kinetics of model drugs.

The aim of this study was to better understand the mass transport mechanism involved in controlled release of a model drug from lipid based parenteral delivery systems. A family of dihydroxyacetone (DHA) derived symmetrical lipids with varying hydrocarbon chain length was synthesized to systematically analyze how lipid chain length influences drug release kinetics. Our results showed that microparticles prepared using solvent emulsification are porous and polydisperse in size. The effects of several formulation and processing parameters (lipid and surfactant concentration) on the resulting release kinetics were measured. As expected smaller particles (<25μm) showed faster release kinetics possibly due to shorter diffusion pathway length compared to the larger particles ([25-40] μm and >40 μm). Our results showed

that porosity controls the release kinetics of the anti-inflammatory drug piroxicam more strongly than hydrophobicity.

Further investigation of parenteral delivery systems made from DHA derived symmetrical diglcycerides showed that protein release is dependent on the hydrophobicity of the matrix. With lysozyme as a model protein drug, long chain diglycerides (C_{16} and C_{14}) showed slower release compared to short chain, less hydrophobic diglycerides (C_{10} and C_{12}). As with solid microparticles, the effect of varying formulation and processing parameters (e.g. lysozomal loading, compression force) was studied. SDS gel electrophoresis and enzymatic study in *M. lysodeikticus* suspensions were used to study the structural integrity and activity of dispersed model drug. The results showed that there is slight aggregation and loss of activity possibly as a result of heat generation during compression. Furthermore diglyceride implants showed acute inflammatory response in early time points of the biocompatibility study conducted using rat animal models. The inflammatory response subsided for later time points. Histological inspection of the tissues showed presence of granulomas but no sign of tissue necrosis.

BIOGRAPHICAL SKETCH

Sara Yazdi was born in Iran and moved to Newton, Massachusetts in October of 1998 when 17 years old. She is the eldest of all grand children in the Ghaffari family and the only one to be named by her beloved grandfather. Starting as a chemistry major at University of Massachusetts-Boston, she switched her major to chemical engineering and completed her baccalaureate degree in Chemical Engineering at University of Massachusetts -Amherst in May of 2004.

For Mother, Father and Omid, for their never ending love and patience

ACKNOWLEDGMENTS

I would like to first acknowledge my thesis advisor, Dr. David Putnam for guiding me through the scientific process while allowing me to develop my own skills as an independent researcher. I would also like to thank members of my committee, Professor Michael Shuler, and Professor Gerald Fiegenson for their direction and support of this research study. A large portion of this work would have not been possible without the help of generous collaborators and colleagues, particularly Professor Ursula Krotscheck of College of Veterinary Medicine who kindly provided laboratory space and expertise for the animal study, and Dr. Robert Padera of Brigham and Woman's Hospital in Boston, MA for his help with the pathology experiment and analysis. I would like to acknowledge my dear friends and colleague, Jordan Atlas. He and I were cohorts at University of Massachusetts-Amherst and his perspective on all scientific and life matters have proven to be of great value to me. My fond memories of Ithaca will always include culinary adventures with Conor and Tricia, long discussions about all things NPR related with David, and dinner and movie nights with Marina and John. I am glad that my best friends decided to remain on the eastern coast of US and did not run off to California and Ireland. I would like to close by thanking my family, for one can never ask for more patience, love and sacrifice than what they have offered me. My father's advice has been to pay attention to details and mother has always insisted on having patience in the face of adversity. My brother stands for hope, like his name, and for gradual but steady progress. I am proud to be their daughter and sister.

TABLE OF CONTENTS

LIST OF FIGURES

LIST OF TABLES

LIST OF ABBREVIATIONS

DDS	Drug Delivery Systems
Poly(lactic acid)	PLA
Poly(glycolic acid)	PGA
PLGA	Poly(lactic-co-glycolic acid)
PEG	Poly(ethylene glycol)
HPMA copolymer	*N*-(2-hydroxypropyl)methacrylamide copolymer
BDNF	Brain Derived Neurotrophic Factor
FDA	Food and Drug Administration
DHA	Dihydroxyacetone
N_2 gas	Nitrogen gas
PVA	Poly(vinyl alcohol)
^{1}H-NMR Spectroscopy	Proton Nuclear Magnetic Resonance spectroscopy
DSC	Differential Scanning Calorimetry
TGA	Thermo-gravimetric analysis
THF	Tetrahydrofuran
DCM	Dichloromethane
SDS-PAGE	Sodium dodecyl sulfate-polyacrylamide gel electrophoresis
UV	Ultra Violet

CHAPTER 1

SYNTHETIC AND BIOLOGICAL MATERIALS FOR DRUG DELIVERY

1. Introduction

In the past few decades medicine and pharmacy have faced many new challenges. These challenges, which range from the need for better and more effective cancer treatments[1, 2] to treatment of widespread and chronic disease that are caused by a combination of hereditary and environmental triggers (e.g. diabetes mellitus), have led to breakthrough innovations in the field of drug delivery. However, despite the role of fast-paced genomic and proteomic research in discovering the molecular basis for many diseases, and the use of tools such as combinatorial chemistry combined with computer-assisted rational design for high throughput synthesis of new biomaterials, the progress toward better therapies has been slow. Translation of innovative therapeutics from bench-top to bedside is often held back by lack of investment in developing new drug delivery technologies that can improve the efficacy of treatments [3, 4].

1.1. Drug delivery and importance of controlled release

The two most important aspects of controlled release drug delivery are spatial placement and temporal delivery of the therapeutic compound. Spatial placement refers to the targeting necessary to achieve a therapeutic dose of a particular drug within a specific tissue, while minimizing exposure of healthy tissue to the drug. Temporal delivery refers to controlling the timing of drug delivery to the targeted site. These two factors are important to incorporate in an optimal design for novel drug delivery systems[3]. An example of where temporal delivery can help includes the

delivery of protein and peptides. Their short in-vivo half lives and their sensitivity to physiological pH marks a challenge in their delivery[5]. Examples of where spatial delivery can help include cancer therapy drugs. The role novel delivery systems play in decreasing toxicity by their encapsulating matrices allow their local implantation at the tumor site and thus improving safety and efficacy of chemotherapy treatments [6, 7].

Drug release rates have direct implications on the therapeutic effect of drug delivery systems (DDS). Failure to release the drug in a timely manner could result in drug levels below the therapeutic window; while rapid release of the drug from the carrier could lead to drug levels exceeding the maximum tolerated dose or even enter the toxic range[3]. Table 1.1 gives examples of problems exhibited by free drugs that can be addressed through use of DDS. In controlled drug delivery, drug release from the carrier generally occurs by one of three mechanisms (or a combination thereof): (i) diffusion, (ii) chemical reaction, and (iii) solvent activation and transport. In the case of (i) diffusion-controlled system, two main geometries exist, either a reservoir that encapsulates the drug within a barrier, or a matrix in which the drug is uniformly distributed. In either case, diffusion through the matrix is the rate-limiting step. For delivery systems that (ii), release the drug as a result of a chemical reaction, the drug is released due to chemical degradation of the matrix. Alternatively, the drug can be attached to a polymer/lipid by a covalent bond that can be either hydrolyzed or enzymatically cleaved, thus resulting in drug release. A third mechanism is (iii) solvent activation. In such systems, the matrix containing the drug swells because of osmotic effects and external water entering the drug delivery systems pushes the drug out [8-13]. A number of materials have been used in the design of controlled delivery systems, including both lipids and polymers. The following is a brief review of particles, implants, and vesicles made from polymers and lipids and their advantages and shortcomings.

Table 1.1. Non-ideal properties of drugs and their therapeutic implication (modified from [3])

Problem	Implications	Effect of DDS
Poor solubility	Human body is composed of 70% water, thus administrating hydrophobic drugs can result in precipitation in aqueous media. Use of excipients such Cremphor to solubilize highly hydrophobic drugs results in unacceptable side effects.	Using hydrophobic carriers, such as lipid micelles or liposomes provides both hydrophobic and hydrophilic environments, resulting in enhanced drug solubility.
Tissue damage on extravasation	Accidental burst release will expose the tissues to toxic concentrations of the drug, resulting in necrosis.	Regulated drug release from DDS, can reduces or eliminate tissue necrosis.
Quick breakdown of the drug in vivo	Loss of therapeutic activity upon administration, due to acidic pH, enzymatic processes	DDS protects the drug from premature degradation while functioning as a sustained release system. In addition, lower doses of the drug may be required.
Undesirable pharmacokinetic	Rapid clearance of the drug upon administration, thus requiring high doses or continuous infusion.	DDS can significantly alter the PK of the drug and reduce clearance rate.
Poor biodistribution and absence of selectivity for target tissue	Unnecessary exposure of healthy tissue to drugs because of widespread biodistribution can result in dose-limiting side effects.	DDS can lower the volume of distribution and help to reduce side effects. In return it can also increase drug concentration through the EPR effect.

1.2. Parenteral therapies

Drug delivery systems aim to enhance the pharmacological properties of conventional ("free") drugs. Parenteral therapies denote a category of DDS that are designed to bypass the body's natural defense against microbial invasion associated with skin and mucosal tissues[14]. Parenteral, from *para entron*, meaning to "avoid

intestines", refers to all administration principles for drugs that do not utilize the alimentary canal for the delivery of a drug to tissues. The advantages of parenteral delivery include predictable pharmacokinetic as well as the ability to interdict a rapidly progressing lethal process or disease (e.g., injection of adrenalin to prevent cardiac arrest) [14]. In addition parenteral delivery systems are designed to reduce the administration frequency, and to protect the drug against degradation upon administration, while accurately controlling the release rate. Examples of such systems include particulate carriers, implants, and emulsions[15].

1.2.1. Lipids

Lipids are one chemically unique category of drug delivery materials that play a fundamental role in the architecture and functionality of all living cells. The wealth of information that exists on lipid ingestion, solubilization, and subsequent processing, provides the basis for semi-empirical design of lipid-based delivery systems. Such systems cover a wide range of modalities such as liposomes, solid lipid particles (nano/micro), implants, emulsions, and nanostructured lipid carriers.

1.2.1.1. Liposomes

Liposomes, in the broadest sense, are colloidal particles composed of a phospholipid bilayer enclosing an aqueous core. The bilayer structure allows incorporation of hydrophilic drugs into the aqueous core and incorporation of hydrophobic drugs into the lipid bilayer. These formulations have played a significant role in improving delivery of potent drugs since their discovery in the 1960s. Today, the majority of drug delivery systems approved for parenteral administration are liposomal formulations, Table 1.2. Most of these formulations approved for use in humans contain phosphotidylcholine (neutral charge), with fatty acyl chains of varying lengths and degrees of saturation[16]. Important challenges associated with liposomal

formulation are limited physical stability of the dispersions, burst release, low activity due to non-specific tumor targeting, non-specific clearance by reticuloendothelial system (RES), and difficulties in production scale up[17]. Some of these limitations still remain as obstacles in developing new formulations.

The liposomal fate in vivo is greatly impacted by their size, charge, pH, and their lipid constituents. These properties can be adjusted to overcome some of the aforementioned limitations in liposomal delivery systems. For examples, leakage of small molecular weight drugs in presence of blood plasma prompted the insertion of cholesterol and high melting point lipids such as hydrogenated lecithin, distearyl phosphotidylcholine (DSPC) and sphingomyelin (SM) into the bilayer, thus resulting in a less permeable barrier [16, 18, 19].

Table 1.2. Examples of liposomal formulations

Agent	Administration	Formulation	Refs.	Application
Paclitaxel	Systemic	Liposome	[20, 21]	Antineoplastic agent
Monophosphoryl lipid A and QS21	Systemic	Liposomes	[22]	Vaccine adjuvant systems against hepatitis B
Cytarabine	Systemic	Liposomes	[23, 24]	Leukemic and lymphomatous meningitis
Doxorubicin	Systemic	PEGylated liposomes	[25, 26]	Metastatic breast cancer, mullerian carcinoma, cervical cancer, advanced soft tissue sarcomas
Daunorubicin	Systemic	Liposomes	[27]	Myelogenous leukemia
Recombinant factor VIII	Systemic	Liposomes	[28]	Hemophilia A
Human interferon beta	Systemic	Cationic liposomes	[29]	Gene therapy for advanced melanoma

Rapid clearance of liposomes by the RES has been addressed by insertion of more hydrophilic groups such as polyethylene glycol (PEG). The hydrophilic shield

provided by the PEG groups increases the circulation time of liposomes in the system by reducing the rate of plasma protein adsorption on the hydrophilic surface. The therapeutic potential of liposomal formulation was expanded when a detailed understanding of lipid polymorphisms, physiological mechanisms of in vivo liposome deposition, and lipid-drug and lipid-protein interaction emerged. These data resulted in enhanced design of liposomal systems with increased in vivo stability and improved biodistribution[16].

1.3. Particles

Particulate drug delivery systems are the principle drug carrier in experimental pharmaceutics and clinical medicine. The critical factor affecting in vivo particle distribution is size; particles with diameters larger than 1 μm are best described as microparticles and those smaller than 1 μm are referred to as nanoparticles. The size distinction causes major differences at various levels, from formulation to in vivo usage [30].

1.3.1. Lipid particles

Solid lipid particles are made from solid lipids (i.e. lipids that are solid at room and body temperature) and are stabilized by surfactants. By definition, the lipids can be purified triglycerides, complex glyceride mixtures (mono-, di-), and waxes[31-33]. Key advantages of solid lipid particles include their excellent physical stability, their ability to protect encapsulated labile drugs from degradation, and their amenability to function as controlled release systems [17].

1.3.2. Solid lipid nanoparticles

Solid lipid nanoparticles (SLN) are usually made by means of high-pressure homogenization and are mainly characterized by their less than 500 nm size. A clear advantage of SLN is the use of physiological lipids, which lower the risk of acute and

chronic toxic responses. Furthermore, the absence of organic solvents in the production of SLN makes these delivery systems suitable candidates for parenteral delivery. Characterization of SLN has shown that methods of preparation, lipid composition, and choice of emulsifier, have a direct impact on the final size, charge, and stability of these particles. In addition, the degree of lipid crystallinity and the modification of lipids are strongly correlated with drug incorporation, and the release rates from SLN [33]. However, the rapid clearance of nanoparticles from the body by liver and spleen has limited the usefulness of SLN. While this response is advantageous for those particular cases where the spleen and liver are the targeted delivery sites, for delivery to other major organs and to prolong the circulation time, polymers such as block polyoxyethylene polypropylene copolymer are used to create a hydrophilic coating on the SLN[34].

1.3.3. Solid lipid microparticles

Similar to SLN, solid lipid microparticles (SLM) are prepared from lipids that are solid at body and room temperature. The methods of preparation range from solvent evaporation, to oil in water (O/W) and water in oil (W/O) melt dispersion, multiple emulsion techniques, and high-pressure homogenization. The chemical and physical characteristics of the drug candidate dictate the preparation technique of SLM. Studies have shown that SLM show high encapsulation efficiencies for lipophilic drugs. Jaspart et al. reported successful encapsulation of salbutamol acetonide, a bronchodilator agent, for pulmonary delivery via SLM[35, 36]. Reithmeir et al. reported successful encapsulation of thymocartin and insulin for parenteral release, and Saraf et al. demonstrated encapsulation and delivery of hepatitis B surface antigen for mucosal immunization[37, 38]. The shortcomings associated with SLM delivery include low encapsulation efficiency of hydrophilic drugs and lipid polymorphism

during storage. However, studies have shown that SLM are non-toxic in vivo, thus more research is needed to fully exploit the therapeutic potential of SLM[36, 39].

1.4. Lipid implants

The use of lipid implants as a parenteral controlled drug delivery system provides an interesting alternative for protein and peptide drugs. The acidic microenvironment within traditional polymeric delivery systems, and the preparation steps of these matrices can compromise the stability and functionality of protein and peptide drugs, while preparation methods of lipid implants offer a less caustic approach to encapsulation of proteins and peptides [15, 40-46]. In addition to providing protection for drug molecules, and allowing accurate control of the release rate, lipid implants can be used to obtain locally restricted drug distribution. Formation of biofilm on the surface of prosthetic implants often leads to persistent infection and inflammation, as well as local and systemic toxicity resulting in overall failure of the implant. To decrease and prevent these side effects, a locally high concentration of antibiotic is needed, but because of inadequate vascularization at the wound site, conventional routes of delivery such as intravenous and intramuscular delivery fail to achieve a sufficient drug concentration. The use of antibiotic loaded lipid implants has proven to be an effective delivery route. Implants not only offer local and proximal delivery at the wound site, but they can also decrease the unnecessary exposure of other organs to drug molecules[47, 48].

1.5. Polymeric systems

Polymers offer a vast array of versatile designs for drug delivery applications, for example, through covalent conjugation directly to a drug molecule, or via use of electrostatic forces to form polyplexes, or by encapsulating the drug within the polymer. Understanding the structure-function relationship between a polymer's

molecular architecture and its inherent properties is an important aspect for their design in drug delivery applications. Research has shown that molecular weight (M_w), polydispersity, charge, and the hydrophilic-hydrophobic character of polymer's main chain directly affects the biodistribution, clearance rate, toxicity, and biological activity of polymeric drug delivery matrices.

Polymers used as biomaterials can be naturally occurring, synthetic, or a combination of both. The characteristics of the main groups of polymeric materials used for drug delivery are summarized in Tables 1.3 and 1.4. Despite the abundance of naturally occurring polymers, their utilization has been limited by irreproducible production methods. Their structural complexity renders modification and purification tasks challenging. Additionally, significant batch-to-batch variations occur because of their "bio-preparation" in living organisms (plants, crustaceans). In contrast, synthetic polymers are available in a wide variety of molecular compositions with easily adjustable properties. Processing, copolymerization, and blending provide simultaneous means of optimizing a polymer's mechanical characteristics and its diffusive and biological properties. Their primary obstacle is the general lack of biocompatibility of the majority of the synthetic materials, although poly(ethyelene oxide) (PEO) and poly(lactic-*co*-glycolic acid) (PLGA) are notable exceptions. Therefore, synthetic polymers are often associated with inflammatory reactions, limiting their use to solid, unmoving, and impermeable devices[49].

Poly(lactic acid) (PLA), poly(glycolic acid) (PGA) and their copolymer PLGA are one of the most well-studied family of biomaterials with regard to use in drug delivery applications[50]. PLGA has been so extensively studied because of its biocompatibility and the ease of varying its properties by altering the copolymer composition, as well as its inclusion in a number of Food and Drug Administration (FDA) approved devices. Examples of drugs studied for delivery via encapsulation

within PLGA matrix include, piroxicam, neurotrophic growth factor (CNTF), leuprolide (LupronDepot) or triptorelin (Trelstar) [51-53]. However, despite successful encapsulation and delivery of the above drugs, polymeric drug delivery faces a challenge for delivery of protein therapeutics and peptides. Presence of acidic microclimates within the PLGA particles causes denaturation and aggregation and ultimately leads to incomplete release of inactive proteins, therefore, more research is needed to optimize the design and delivery of proteins and peptides using polymeric matrices [40, 54].

Table 1.3. Summary of the main properties and applications of the naturally occurring polymeric biomaterials (adapted from [49])

Polymer	Main application	Biodegradable
Protein and protein-based polymers	Absorbable, biocompatible, elastic properties allow use in implants and in tissue engineering.	
Collagen	Drug delivery microspheres, sponge wound dressing, and absorbable sutures	Yes
Albumin	Used as a model drug in microsphere encapsulations	Yes
Poly(amino acids)		
poly(α, L-amino acids)	Generally non-antigenic and biocompatible. Used as oligomeric drug carriers.	Yes
Polysaccharides and derivatives	Immobilization matrices for cells and bioactive molecules	Yes
Plant sourced		
Agarose	Major use as supporting materials in clinical analysis and as an immobilization matrix.	Yes
Alginate	Use as immobilization matrices for cells and enzymes, controlled release of bioactive molecules, injectable microcapsules for treating neurodegenerative disease.	
Carboxymethyl cellulose	Use in drug delivery systems and dialysis membranes. Utilizing a combination of ionotropic gelation and polyelectrolyte complex formation for cells immobilization.	No
Human/animal sourced		
Hylauronic acid	Important lubricant properties, potential therapeutic reagent.	Yes
Heparin and glycosaminoglycanes	Antithrombotic and anticoagulant properties utilized in surgical procedures. A major candidate for ionotropic gelation and capsule formation.	Yes
Microbial polysaccharides		
Dextrans and its derivatives	Widely used as a drug carrier with excellent rheological properties	Yes
Chitosan and its derivatives	Positively charged and biocompatible with major applications in controlled delivery systems (i.e. gels, microspheres, membranes).	Yes

Table 1.4. Summary of the main properties and applications of synthetic polymeric biomaterials (adapted from [49])

Polymer	Main application	Biodegradable
Aliphatic polyesters Poly(lactic acid), poly(glycolic acid) and their copolymers	Tunable degradation kinetics, used in drug delivery systems and tissue engineering applications.	Yes
Poly(hydroxy butyrate), poly(ε-caprolactone) and copolymers, poly(alkylene succinate), etc.	Utilized as a matrix for drug delivery system and cell microencapsulation. Properties can be changed through chemical modification and blending.	
Polyamides (Nylons)	Non-absorbent sutures, haemofilteration membranes.	No
Polyanhydrides	Biodegradable, used in tissue engineering and release of bioactive molecules.	Yes
Poly(ortho esters)	Surface eroding polymer, with applications in sustained delivery, ophthalmology.	Yes
Poly(cyano acrylates)	Biodegradable, depending on the length of the alkyl chain. Used widely as surgical adhesive.	Yes
Polyphosphazenes	Can be tailored for side chain functionality. Cast-able into films and hydrogels, with applications in drug release.	Yes
Thermoplastic polyurethanes	Elastomeric properties that can be tailored through composition change of the starting materials. Used as (prostheses, vascular grafts), catheters, and drug delivery systems.	No
Polyethylene (low density)	Surgical sutures, catheters, membranes.	No
Poly(vinyl alcohol)	Gels and blends are used in drug delivery and cell immunoisolation.	Yes
Poly(ethylene oxide)	Highly biocompatible. Derivatives and copolymers have been utilized in drug delivery applications.	Yes
Poly(hydroxyethyl methacrylate)	Soft contact lenses, skin coating and immunoisolation membranes.	No
Poly(methyl methacrylate)	Dental implants and bone replacements.	No
Poly(tetrafluroetheylene), Polydimethylsiloxanes	Vascular grafts, clips, sutures, and coatings.	No
Environmentally responsive polymers Poly(ethylene oxide-b-propylene oxide) Poly(vinyl methyl ether)	Surfactants with amphiphilic properties used in protein delivery and skin treatments. Non-toxic, temperature sensitive with excellent shape-memory properties.	Yes
Poly(N-alkylacrylamides)	Temperature-sensitive gels with adjustable lower critical solution temperature via co-monomer incorporation.	

1.6. Drug-conjugated delivery systems

Covalently conjugated delivery systems are designed to exploit the endocytosis pathway in cells. Endocytosis is a mechanism by which cells take up macromolecular nutrients (e.g. cholesterol in the form of lipoprotein particles, iron complexes with transferrin) that are unable to enter the cell through passive diffusion. Endocytosis is a general term describing three complex sub-pathways: (i) pinocytosis, by which a cell uptakes solutes and single molecules such as proteins; (ii) phagocytosis, by which cell ingests large objects such as viruses, apoptotic cell debris, and bacteria and (iii) receptor mediated endocytosis, by which a cell ingests compounds when triggered by specific ligand binding. Pinocytosis and phagocytosis are non-receptor mediated forms of endocytosis and may result in unspecific uptake of particles and/or proteins. In contrast, receptor mediated endocytosis is triggered by specific ligand binding. The combination of receptor mediated endocytosis and phagocytosis/pinocytosis is the basis for design of targetable polymeric carriers [55, 56].

A drug conjugated with a polymer is referred to as a "pro-drug", which is an inactive precursor of a drug that protects and delivers the drug to a specific site. Pro-drugs have several advantages: (i) an increased solubility of hydrophobic drug, serving to increase the bioavailability, (ii) protection and preservation of the drug's therapeutic activity during circulation, transport to a targeted organ and intracellular trafficking, (iii) reduced immunological response, (iv) improved drug targeting through functionalized moieties of the construct, and (v) the potential to form advanced drug delivery complexes. An ideal pro-drug structure, generally referred to as the Ringsdrof model, will contain the following components: an inert polymeric backbone, a functionally active spacer, a target moiety, and a drug molecule [57, 58].

Various molecular architectures of polymers have been studied for the design of drug conjugates, however two polymers have been most commonly examined,

poly(ethylene glycol) (PEG) and *N*-(2-hydroxypropyl)methacrylamide (HPMA) copolymer. Kopeček and colleagues developed *N*-(2-hydroxypropyl)metacrylamide (HPMA). It consists of a hydrophilic polymer that significantly increases water solubility of hydrophobic drugs, and has proven to be biocompatible. Insulin and ampicilin are examples of drugs that have been attached to HPMA through aminolysis of reactive polymeric precursors. Doxorubicin, an anthracyline antibiotic with a broad spectrum of antitumor activity, has been attached via a polypeptide spacer[56, 59, 60]. Other examples of HPMA-based prodrugs include chemotherapeutic agents such as *cis*-diamminedichloroplatinum(II) (cis-platin), which is widely used in treatment of solid tumors including ovarian, testicular, and head and neck cancers.

Frank Davis and colleagues developed the first generation of PEGylated proteins and peptides in the late 1970s. Their findings showed that the PEGylated complex was 5 to 10 times larger than the free drug form due to the binding of water molecules to the ethylene glycol subunits, which decreases renal clearance rates, and improves the pharmacodynamic and pharmacokinetic properties of PEGylated polypeptide drugs [61]. Weekly injections of IFN-α2 conjugated to a 40 kDa branched PEG for the treatment of chronic hepatitis C have resulted in near constant blood concentrations of IFN-α2, and a 100-fold decrease in renal clearance [62, 63].

1.7. Goals of this study:

The objective of this study was to investigate dihydroxyacetone-derived (DHA) diglycerides and their analogs as new materials for the preparation of parenteral controlled release matrices. The main goals were to characterize the biomaterial to facilitate the design and preparation of controlled release matrices, and to ensure the in vivo safety of these matrices. Herein we report the synthesis of a series of bioinspired symmetrical lipids comprised of two classes of biomolecules: fatty acids and DHA.

DHA is a constituent of the glycolysis pathway, and is FDA approved for oral and topical administration, making it an attractive building block for new biomaterials [64-66]. The particular advantage of using DHA as a lipid building block for this study is that the strong dipole moment of the DHA carbonyl maintains the lipids in the solid state while the lipid lengths are varied. Symmetrical glycerol analogues of the lipids reported herein are liquids and waxes, rather than solids. This study describes the synthesis and characterization of nine symmetrical lipids, with incrementally increasing aliphatic lipid tails, their fabrication into solid lipid microparticles, and the investigation of how the lipids influence particle morphology, and the controlled release kinetics of the model drug compound (Chapter 2).

We show that that the release kinetics of a hydrophobic drug model increased with increasing lipid length. SEM images, as well as particle density calculations collectively suggested that the microparticle porosity was the primary factor that controlled release kinetics, as microparticle porosity increased with increasing lipid length.

Chapter 3 focuses on the synthesis and characterization of the symmetrical analogues of these lipids, and their potential for delivery of proteins and peptides as model drugs. Our results demonstrate that wettability effects often play a crucial role in release of high molecular weight model compounds from lipidic matrices. Thus, release behavior of proteins can be tailored by varying the lipophilicity of the matrix material via selectively varying the fatty acid chain length. The symmetrical diglycerides showed excellent properties for retaining physical and chemical characteristics of these model pharmaceuticals. However, the burst effect in release behavior limits their use for prolonged drug release applications. The burst release, possibly due to less than desirable mechanical properties of diglyceride powders may be remedied through forming blends with other lipids such as cholesterol.

Biocompatibility studies of diglycerides implants in rats showed acute inflammatory response after the 2-day time point. However, implants for later time points showed no sign of tissue necrosis or damage (7,14 and 28 days). The final remarks (Chapter 4) focus on future experiments that can bring about a better understanding of mechanical behavior of diglycerides powders and its effects on the release of the macromolecules.

REFERENCES

[1] F. J. Martin and C. Grove 2001. Microfabricated drug delivery systems: concepts to improve clinical benefit. Biomedical Microdevices. 3, 2, 97-108.

[2] W. M. Saltzman and L. K. Fung 1997. Polymeric implants for cancer chemotherapy. Advanced Drug Delivery Reviews. 26, 209-230.

[3] T. M. Allen and P. R. Cullis 2004. Drug delivery systems: entering the mainstream. Science. 303, 1818-1822.

[4] R. Duncan 2003. The dawning era of polymer therapeutics. Nature-Drug Discovery. 22, 347-360.

[5] W. Wang 2005. Protein aggregation and its inhibition in biopharmaceutics. International Journal of Pharmaceutics. 289, 1-30.

[6] D. Mooney 2005. Cancer One step at a time. Nature. 436, 468-469.

[7] M. A. Moses, H. Brem, and R. Langer 2003. Advancing the field of drug delivery Taking aim at cancer. Cancer Cell. 4, 337-341.

[8] R. Langer 1990. New methods of drug delivery. Science. 249, 4976, 1527-1533.

[9] R. Langer 2006. Biomaterials for Drug Deliveryand Tissue Engineering. MRS bulletin. 31, 477-485.

[10] R. Langer and N. A. Peppas 1983. Chemical and physical structure of polymers as carriers for controlled release of bioactive agents: A review. Polymer Reviews. 23, 1, 61-126.

[11] R. Langer and N. A. Peppas 2003. Advances in biomaterials, drug delivery, and bionanotechnology. AIChE journal. 49, 12, 2990-3006.

[12] R. Langer and D. A. Tirrell 2004. Designing materials for biology and medicine. Nature. 428, 487-492.

[13] E. Mathiowitz, M. R. Kreitz, and L. Baranon-Peppas 1999. Microencapsulation. Encylopedia of Controlled Drug Delivery, Vol.2, 493-553.

[14] M. J. Groves 1999. Parenteral Drug Delivery Systems. Encylopedia of Controlled Drug Delivery-Vol.2, 743-777.

[15] F. Kreye, F. Siepmann, and J. Siepmann 2008. Lipid implants as drug delivery systems. Expert Opin. Drug Deliv. 5, 3, 291-307.

[16] T. Lian and R. J. Y. Ho 2001. Trends and developments in liposome drug delivery systems. Journal of Pharmaceutical Sciences. 90, 6, 667-680.

[17] S. A. Wissing, O. Kayser, and R. H. Müller 2004. Solid lipid nanoparticles for parenteral drug delivery. Advanced Drug Delivery Reviews. 56, 1257-1272.

[18] G. Gregoriadis 1995. Engineering liposomes for drug delivery: progress and problems. Trends in Biotechnology. 13, 527-537.

[19] F. Szoka Jr and D. Papahadjopoulos 1980. Comparative Properties and Methods of Preparation of Lipid Vesicles (Liposomes). Annual Reviews in Biophysics and Bioengineering. 9.

[20] P. Lim Soo, J. Cho, J. Grant, E. Ho, and M. Piquette-Miller … 2008. Drug release mechanism of paclitaxel from a chitosan–lipid implant system: Effect of swelling, degradation and morphology. European Journal of Pharmaceutics and Biopharmaceutics. 69, 149-157.

[21] K. M. Skubitz and P. A. Haddad 2005. Paclitaxel and pegylated-liposomal doxorubicin are both active in angiosarcoma. Cancer. 104, 2, 361-366.

[22] P. Vandepapeliere, Y. Horsmans, P. Moris, M. V. Mechelene, M. Janssens, M. Koutsoukos, P. Belle, F. Clement, E. Hanon, M. Wettendorff, N. Garcon, and G. Leroux-Roels 2008. Vaccine adjuvant systems containing monophosphoryl lipid A and QS21 induce strong and persistent humoral and T cell responses against hepatitis B surface antigen in healthy adult volunteers. Vaccine. 26.

[23] M. Benesch and C. Urban 2008. Liposomal cytarabine for leukemic and lymphomatous meningitis: recent developments. Expert Opin. Pharmacother. 9, 2, 301-309.

[24] S. Phuphanich, B. Maria, R. Braeckman, and M. Chamberlain 2007. A pharmacokinetic study of intra-CSF administered encapsulated cytarabine (DepoCyt®) for the treatment of neoplastic meningitis in patients with leukemia, lymphoma, or solid tumors as part of a phase III study. Journal of Neuro-Oncology. 18, 201-208.

[25] A. Gabizon, H. Shmeeda, and Y. Barenholz 2003. Pharmacokinetics of Pegylated Liposomal Doxorubicin: Review of Animal and Human Studies. Clinical pharmacokinetics. 42, 5, 419-436.

[26] I. Judson, J. A. Radfordb, M. Harrisb, J. Blayc, Q. v. Hoeseld, A. l. Cesnee, A. T. v. Oosteromf, M. J. Clemonsb, C. Kambyg, C. Hermansh, J. Whittakeri, E. D. d. Paolah, J. Verweijj, and S. Nielsenk 2001. Randomised phase II trial of

pegylated liposomal doxorubicin (DOXIL®/CAELYX®) versus doxorubicin in the treatment of advanced or metastatic soft tissue sarcoma: a study by the EORTC Soft Tissue and Bone Sarcoma Group. European Journal of Cancer. 37, 7, 870-877.

[27] A. Candoni, A. Michelutti, E. Simeone, and D. Damiani 2006. Efficacy of liposomal daunorubicin and cytarabine as reinduction chemotherapy in relapsed acute lymphoblastic leukaemia despite expression of multidrug resistance-related proteins. European journal of haematology. 77, 293-299.

[28] J. Spira, O. P. Plyushch, T. A. Andreeva, and R. N. Khametova 2008. Evaluation of liposomal dose in recombinant factor VIII reconstituted with pegylated liposomes for the treatment of patients with severe haemophilia A. Thromb Haemost. 6, 18, 277-283.

[29] K. J. Pulkkanen and S. Yla-Herttuala 2005. Gene therapy for malignant glioma: current clinical status. Molecular Therapy. 12, 4, 585-598.

[30] D. S. Kohane 2007. Microparticles and nanoparticles for drug delivery. Biotechnology and bioengineering. 96, 2, 203-209.

[31] R. H. Müller, K. Mäder, and S. Gohla 2000. Solid lipid nanoparticles (SLN) for controlled drug delivery–a review of the state of the art. European Journal of Pharmaceutics and Biopharmaceutics. 50, 1, 161-177.

[32] R. H. Müller, M. Radtke, and S. A. Wissing 2002. Solid lipid nanoparticles (SLN) and nanostructured lipid carriers (NLC) in cosmetic and dermatological preparations. Advanced Drug Delivery Reviews. 54, 1, 131-155.

[33] W. Mehnert and K. Mäder 2001. Solid lipid nanoparticles Production, characterization and applications. Advanced Drug Delivery Reviews. 47, 2-3, 165-196.

[34] P. Gershkovich, K. M. Wasan, and C. A. Barta 2008. A review of the application of lipid-based systems in systemic, dermal/ transdermal, and ocular drug delivery. Critical reviews in therapeutic drug carrier systems. 25, 6, 545-584.

[35] R. Cortesi, E. Esposito, G. Luca, and C. Nastruzzi 2002. Production of lipospheres as carriers for bioactive compounds. Biomaterials. 23, 11, 2283-2294.

[36] S. Jaspart, P. Bertholet, G. Piel, and J. M. Dogné 2007. Solid lipid microparticles as a sustained release system for pulmonary drug delivery. European Journal of Pharmaceutics and Biopharmaceutics. 65, 1, 47-56.

[37] H. Reithmeier, J. Herrmann, and A. Göpferich 2001. Lipid microparticles as a parenteral controlled release device for peptides. Journal of Controlled Release. 73, 2-3, 339-350.

[38] S. Saraf, D. Mishra, A. Asthana, R. A. Jain, and S. Singh 2006. Lipid microparticles for mucosal immunization against hepatitis B. Vaccine. 24, 1, 45-56.

[39] V. Sanna, N. Kirschvink, P. Gustin, and E. Gavini 2004. Preparation and in vivo toxicity study of solid lipid microparticles as carrier for pulmonary adminstration. AAPS PharmSciTech. 5, 2, 17-23.

[40] K. Fu, D. W. Pack, A. M. Klibanov, and R. Langer 2000. Visual Evidence of Acidic Environment Within Degrading Poly (lactic-co-glycolic acid)(PLGA). Pharmaceutical Research. 17, 1, 100-106.

[41] B. Appel, A. Maschke, B. Weiser, H. Sarhan, C. Englert, P. Angele, T. Blunk, and A. Gopferich 2006. Lipidic implants for controlled release of bioactive insulin: Effects on cartilage engineered in vitro. International Journal of Pharmaceutics. 314, 2, 170-178. DOI=10.1016/j.ijpharm.2005.11.049.

[42] N. Faisant, P. Menei, J. P. Benoit, and A. Goepferich 2006. In vitro investigation of lipid implants as a controlled release system for interleukin-18. International Journal of Pharmaceutics. 314, 145-152.

[43] S. Herrmann, G. Winter, S. Mohl, and F. Siepmann 2007. Mechanisms controlling protein release from lipidic implants: Effects of PEG addition. Journal of Controlled Release. 118, 161-168.

[44] Koennings, A. Sapin, T. Blunk, P. Menei, and A. Goepferich 2007. Towards controlled release of BDNF—Manufacturing strategies for protein-loaded lipid implants and biocompatibility evaluation in the brain. Journal of Controlled Release. 119, 163-172.

[45] S. Koennings, A. Berié, J. Tessmar, and T. Blunk 2007. Influence of wettability and surface activity on release behavior of hydrophilic substances from lipid matrices. Journal of Controlled Release. 119, 173-181.

[46] S. Koennings, J. Tessmar, T. Blunk, and A. Göpferich 2007. Confocal Microscopy for the Elucidation of Mass Transport Mechanisms Involved in Protein Release from Lipid-based Matrices. Pharmaceutical Research. 24, 7, 1325-1335.

[47] S. Allababidi and J. C. Shah 1998. Efficacy and pharmacokinetics of site-specific cefazolin delivery using biodegradable implants in in the Prevention of Post-operative Wound Infections. Pharmaceutical Research. 15, 2, 325-333.

[48] D. M. Chilukuri and J. C. Shah 2005. Local delivery of vancomycin for the prophylaxis of prosthetic device-related infections. Pharmaceutical Research. 22, 4, 563-572.

[49] N. Angelova and D. Hunkeler 1999. Rationalizing the design of polymeric biomaterials. Environ. Microbiol. 17, 409-421.

[50] S. Li and M. Vert 1999. Biodegradable Polymers:Polyesters. Encyclopedia of Controlled Drug Delivery, 71-93.

[51] C. Berkland, M. King, A. Cox, K. Kim, and D. W. Pack 2002. Precise control of PLG microsphere size provides enhanced control of drug release rate. Journal of Controlled Release. 82, 1, 137-147.

[52] D. Klose, F. Siepmann, K. Elkharraz, and J. Siepmann 2008. PLGA-based drug delivery systems: Importance of the type of drug and device geometry. International Journal of Pharmaceutics. 354, 95-103.

[53] M. K. Nkansah, S. Y. Tzeng, A. M. Holdt, and E. B. Lavik 2008. Poly(lactic-co-glycolic acid) nanospheres and microspheres for short-and long-term delivery of bioactive ciliary neurotrophic factor. Biotechnology and bioengineering. 100, 5, 1010-1019.

[54] M. van de Weert, W. E. Hennink, and W. Jiskoot 2000. Protein instability in poly (lactic-co-glycolic acid) microparticles. Pharmaceutical Research. 17, 10, 1159-1167.

[55] H. Lodish, A. Berk, P. Matsudaira, C. A. Kaiser, M. Krieger, M. P. Scott, L. Zipursky, and J. Darnell 2004. Molecular Cell Biology.

[56] D. Putnam and J. Kopecek 1995. Polymer conjugates with anticancer activity. Advances in Polymer Science. 122, 55-123.

[57] J. Khandare and T. Minko 2006. Polymer–drug conjugates: progress in polymeric prodrugs. Progress in Polymer Science. 31, 4, 359-397.

[58] H. Ringsdorf 1975. Structure and properties of pharmacologically active polymers. Journal of Polymer Science: Polymer Symposia. 51, 1, 135-153.

[59] J. Kopeček, P. Kopečková, T. Minko, and Z. R. Lu 2000. HPMA copolymer–anticancer drug conjugates: design, activity, and mechanism of action. European Journal of Pharmaceutics and Biopharmaceutics. 50, 61-81.

[60] T. K. Yeung, J. W. Hopewell, R. H. Simmonds, and L. W. Seymour 1991. Reduced doxorubicin given in the form ofN-(2-hydroxypropyl) methacrylamide conjugates: an experimental study in the rats. Cancer chemotherapy and pharmacology. 29, 105-111.

[61] J. M. Harris and R. B. Chess 2003. Effect of pegylation on pharmaceuticals. Nature-Drug Discovery. 2, 214-221.

[62] A. Kozlowski, S. A. Charles, and J. M. Harris 2001. Development of pegylated interferons for the treatment of chronic hepatitis C. BioDrugs. 15, 7, 419-429.

[63] K. Rajender Reddy, M. W. Modi, and S. Pedder 2002. Use of peginterferon alfa-2a (40 KD)(Pegasys®) for the treatment of hepatitis C. Advanced Drug Delivery Reviews. 54, 4, 571-586.

[64] P. N. Zawaneh, A. M. Doody, A. Zelikin, and D. Putnam 2006. Diblock Copolymers Based on Dihydroxyacetone and Ethylene Glycol: Synthesis, Characterization, and Nanoparticle Formulation. Biomacromolecules. 7, 11, 3245-3251.

[65] A. Zelikin, P. N. Zawaneh, and D. Putnam 2006. A functionalizable biomaterial based on dihydroxyacetone, an intermediate of glucose metabolism. Biomacromolecules. 7, 11, 3239-3244.

[66] A. N. Zelikin and D. Putnam 2005. Poly(carbonate-acetal)s from the dimer form of dihydroxyacetone. Macromolecules. 38, 13, 5532-5537. DOI=10.1021/ma050049v.

CHAPTER 2

SOLID LIPID MICROPARTICLES FOR CONTROLLED DRUG DELIVERY

2. Introduction

Microparticulates serve in the pharmaceutical field as injectable systems to control the spatial and temporal release of drugs[1-7]. A range of materials have been used for the microparticle matrix such as synthetic and natural polymers (i.e. poly(lactic-*co*-glycolic acid), collagen, gelatin and chitosan). More recently, lipids (i.e., cholesterol, phospholipids, lecithin, fatty acids, waxes and glycerides with fatty acids of variable chain length) have emerged as a new class of material that may be suitable for microparticle-based controlled drug delivery[8-18]. Lipid materials have a high variability of available structures permitting the design of predetermined drug release profiles. In addition, the use of physiological components in the design of lipid systems merges their multifunctional character with their potential to create a biocompatible material. Several studies support the potential use of solid lipids for the delivery of both hydrophobic and hydrophilic molecules, as well as the controlled release of peptides and proteins. Although the solid lipid matrix literature is fairly extensive, there has yet to be a systematic investigation of how the lipid matrix can be engineered at the molecular level to modulate the functional characteristics of the microparticle. Specifically, there is little understanding of how lipid structure, particularly lipid length, influences microparticle fabrication, microparticle morphology, and drug release kinetics.

Herein we report the synthesis of a series of bioinspired symmetrical lipids comprised of two classes of biomolecules, fatty acids and dihydroxyacetone (DHA). DHA is a constituent of the glycolysis pathway, and is FDA approved for oral and topical administration, making it an attractive building block for new biomaterials[28-31].

The particular advantage of using DHA as a lipid building block for this study is that the strong dipole moment of the DHA carbonyl maintains the lipids in the solid state while the lipids' lengths are varied. In fact, symmetrical glycerol analogues of the lipids reported herein are liquids and waxes, rather than solids. This study describes the synthesis and characterization of five symmetrical lipids with incrementally increasing aliphatic lipid tails, their fabrication into solid lipid microparticles, and the investigation of how the lipids influence microparticle fabrication, morphology and controlled release kinetics of a model drug compound.

2.1. Materials and Methods

Hexadecanoyl chloride, tetradecanoyl chloride, dodecanoyl chloride, decanoyl chloride, ocatanoyl chloride, 1,3-dihydroxyacetone dimer 97% (DHA), chloroform, anhydrous pyridine and piroxicam were all obtained from Sigma-Aldrich (Saint Louis, MO) and used without further purification. Poly(vinyl alcohol) (PVA, M_W~25,000, 88 mole% hydrolyzed) was purchased from Polysciences Inc. Dichloromethane (DCM), acetone, tetrahydrofuran (THF) and diethyl ether were purchased from J.T.Baker (West Chester, PA). All reagents and solvents were used as received without additional purification

2.1.1. Lipid synthesis and characterization

Symmetrical lipids were synthesized through modification of a previously reported method by Bentley and McCrae[32]. The general procedure is as follows, using the synthesis of C_{16} symmetrical lipid as an example: DHA (3.5 g, 39 mmole) was stirred in anhydrous chloroform (150 mL) under flow of N_2 at room temperature, followed by sequential dropwise (1 drop/sec) addition of hexadecanoyl chloride (22.1 mL, 80 mmol) and anhydrous pyridine (7.5 mL), in that order (Figure (2.1A)). The mixture was stirred at 800 rpm for 3 hrs at room temperature, and the color varied

from clear to slightly yellow. The reaction was extracted with deionized water (2 × 75 mL), the combined aqueous layers were washed with chloroform (1 × 75 mL). All chloroform layers were combined before removal by rotoevaporation in vacuo to a thick white/yellow residue. The residue was dissolved in dichloromethane:ether (1:1), in the lowest volume needed, and placed in the freezer to crystallize overnight (yield~70%). Uncorrected melting points were collected on a Fisher-Johns melting point apparatus. ^{1}H-NMR spectra were recorded at room temperature with a Brucker AF-300 spectrometer operating at 300.13 MHz, and elemental analyses were obtained through QTI (Whitehouse, NJ).

2.1.2. Fabrication of solid lipid microparticles (SLM) by spontaneous emulsification

Each lipid (0.1 g) was dissolved in a 3:2 (v:v) ratio of DCM:acetone by vigorous vortex for approximately 10 seconds. The lipid solution was transferred using a glass pipet into a stirring PVA solution as a slow and steady stream (450 mL, 2.5%). The suspension was stirred for 3 hrs to allow evaporation of the organic solvents and hardening of the microparticles. Microparticles were isolated by centrifugation at 4,800 RCF for 60 minutes followed by multiple washes (3×) with deionized water and centrifugation at 4,800 RCF for 45 minutes. The particles were resuspended in deionized water (5 mL), and lyophilized for a minimum of 12 hrs and were stored at -20 °C in the presence of desiccant. The final products were fine powders with approximate yields of 75% (relative to original weight of lipid). Particles containing the model drug (piroxicam) were prepared using the same method with the exception that the model drug and lipid were co-dissolved at 5:100 weight to weight ratios, in DCM:acetone before addition to the surfactant solution as noted above.

2.1.3. Particle characterization

The solid lipid microparticles were analyzed by two different methods to determine their geometric and aerodynamic size distributions. All measurements assume spherical geometry. The size distributions of each sample were collected until there were no changes in the overall shape of the distribution curve. For each method, the total number of counted particles was >100,000.

Geometric sizes of lipid particles in powder form were determined in isotonic diluent (Isoton II) by a Coulter Multisizer III (Beckman Coulter Inc.) equipped with a 100 μm aperture. About 5 mg of a given powder sample was added to 20 mL of Isoton II and each suspension was shaken for one minute to deagglomerate the particles. Any bubbles were allowed to dissipate prior to measurement.

Particle morphology was studied at low voltage (5 kV) using scanning electron microscopy imaging (LEICA 440) after coating with palladium. Surface charge on samples suspended in 1:10 diluted PBS was measured using a Malvern Zetasizer-Nano ZS (Malvern, UK).

2.1.4. Contact angle measurements

A PRECO Hydraulic press (Los Angles, CA) was used to make lipid pellets with approximate surface area of 25 mm^2. For contact angle measurements, a ramé-hart contact angle goniometer (100-FO) was used to measure the sessile contact angle of water on a lipid pellet surface. Unless otherwise stated, measurements were conducted in triplicate.

2.1.5. In vitro drug release

The encapsulation efficiency of lipid microparticles was determined via complete drug recovery from dissolved microparticles, followed by comparison with the theoretical maximum drug loading. Microspheres (1 mg) were dissolved in THF

(1 mL) and the piroxicam concentration was measured by UV absorbance at λ=276 nm using a microplate spectrofluorometer (Spectramax GeminiEM; Molecular Devices, Sunnyvale, CA). In vitro release kinetics were determined by suspending 5.0 mg of microspheres in 1 mL of PBS with 0.05% Tween-20 in microcentrifuge tubes (Eppendorf) and incubating at 37 °C under gentle rotation. The supernatant was collected in total for UV measurement at predetermined time intervals to determine the amount of release, and replenished with fresh buffer. Piroxicam concentration was measured at λ=276 nm and quantified according to a standard curve of piroxicam prepared by dissolving the drug in PBS with 0.05% Tween-20.

2.1.6. Kinetic analysis of the release data

The release mechanism of piroxicam from solid lipid microparticles was investigated using data corresponding to the 2-300 hours of drug released according to the following mathematical models, Tables 2.3-2.5.

Ritger-Peppas model: This model is often applied to describe drug release from matrices of various geometries using a simple power law relationship [33]:

$$\frac{M_t}{M_\infty} = kt^n \qquad (1)$$

where $\frac{M_t}{M_\infty}$ represents the fractions of released drug at time *t*, with *k* the release rate constant characteristic of the controlled-release device and *n*, the diffusional exponent, which also indicates the mechanism of the drug release. For spherical geometries, if $n \leq 0.43$, a Fickian diffusion, $0.43 \leq n \leq 0.85$, a non-Fickian transport mechanism, and $n \geq 0.85$, a zeroth-order drug release mechanism.

Jander equation model: This particular model considers the change in the interfacial area where the drug release from microspheres occurs through diffusion within the matrix[34].

$$1-\left(1-\frac{M_t}{M_\infty}\right)^{1/3}=\left(\frac{k_1}{r}\right)t^{1/2}=k_J t^{1/2} \qquad (2)$$

where k_1 and k_J denote rate constants and r, is the radius of the spherical matrix.

2.1.7. Lipid hydrolysis product analysis

Dihydroxyacetone, sodium butyrate and lipid C_4 were each separately suspended in hydrochloric acid (5 mL, 0.02 N, pH=1.67), and stirred at 37^o C for two days, after which the pH was adjusted to neutral by addition of NaOH (1 N) and the solutions lyophilized for 48 hrs. The resulting powder was dissolved in deuterium oxide for analysis by ^{1}H-NMR spectroscopy.

2.2. Results and Discussion

The symmetrical lipids were successfully synthesized via Schotten-Baumann acylation (following the method of Bentley and McCrae) with yields in excess of 70% (Figure 2.1(A)). The acyl chlorides were chosen so that the final product was derived from physiological lipids; for example hexadecanoyl chloride, derived from hexadecanoic acid, was selected to synthesize lipid C_{16}. Each symmetrical lipid is abbreviated C_x where "x" denotes the number of carbons in the corresponding fatty acid.

In addition, all of the synthesized lipids have melting points that are above room and body temperature, making them good candidates for fabrication into solid microparticles for controlled drug delivery. Elemental analysis obtained for C_8-C_{16} lipids is summarized in Table 1. ^{1}H-NMR (300 MHz, $CDCl_3$, δ): [C_8 lipid] 0.89 (t,6H), 1.27 (s,16H), 2.43 (t,4H), 4.76 (s,4H), [C_{10} lipid] 0.89 (t,6H), 1.27 (s,24H), 2.43

(t,4H), 4.76 (s,4H), [C_{12} lipid] 0.89 (t,6H), 1.27 (s,32H), 2.43 (t,4H), 4.76 (s,4H), [C_{14} lipid] 0.89 (t,6H), 1.27 (s,40H), 2.43 (t,4H), 4.76 (s,4H), [C_{16} lipid] 0.89 (t,6H), 1.27 (s,48H), 2.43 (t,4H), 4.76 (s,4H), (Figure 1(B)).

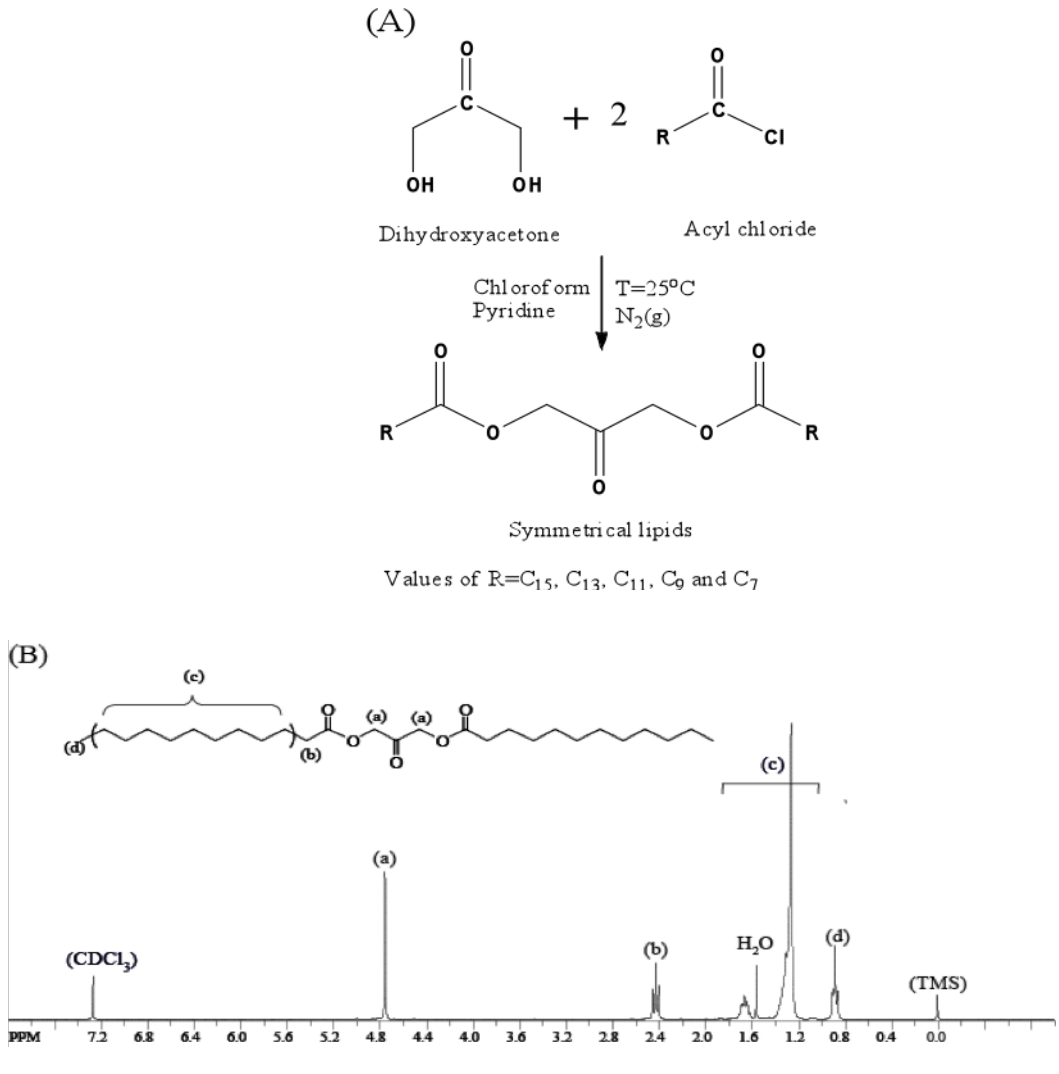

Figure 2.1. (A) Reaction pathway for the synthesis of symmetrical 1,3-lipids, (B) ^{1}H-NMR spectra of C_{12} lipid (dodecanoic acid 3-dodecanoyloxy-2-oxo-propyl ester). C_{12}'s spectrum serves as a representative of the remaining lipids.

Table 2.1. Melting point and elemental analysis of solid lipids

Lipid sample	Melting point (^{o}C)	Elemental analysis (Theoretical)		Elemental analysis (Experimental)	
		%C	%H	%C	%H
C_{16}	76-78	74.13	11.75	74.05	11.41
C_{14}	73-76	72.87	11.46	73.18	11.54
C_{12}	69-70	71.32	11.08	71.32	11.14
C_{10}	64-65	69.31	10.62	69.30	10.81
C_{8}	56-58	66.63	10.01	66.57	10.23

The sessile contact angle of water on each lipid surface was measured to establish the relative hydrophobicity differences among the lipids. The hydrophobic nature of each lipid is important for two reasons. First, lipids with insufficient hydrophobicity would be difficult to formulate into solid microparticles. Second, significant variability of the lipid hydrophobicity could be used to control the rate of drug release from the microparticles in the same way hydrophobicity is used to regulate hydrolytic drug release from polymer-based microparticles[35-36]. Generally, contact angles increased with increasing lipid length (Figure 2.2). The contact angles show an increasing trend in hydrophobicity among the lipids, with the series straddling 90°, the angle at which surfaces transition from "hydrophilic" for short chain lengths to "hydrophobic" for longer chain length lipids.

Microparticles containing piroxicam as a model drug were successfully fabricated from all lipids in the series using spontaneous emulsification. Encapsulation efficiencies for piroxicam were approximately 5-8% (w/w). The level of encapsulation efficiency is a result of hydrophilic drug partitioning into the outer aqueous phase from the inner oil phase during emulsification. The effect of lipid concentration and surfactant concentration (poly vinyl alcohol (PVA)) on the hydrodynamic particle size, with constant stirring rate and temperature, was determined by serial variation of both parameters. The results showed that increasing the lipid concentration led to an increasing trend in mean diameter, and increasing the

surfactant concentration led to a decreasing trend in the mean diameter (Table 2.2). Zeta potential measurements showed that lipid microparticles are negatively charged. The negative surface charge can be attributed to the presence of hydrolyzed ester groups at the particle surface or presence of residual PVA on the particles (Figure 2.3)[8].

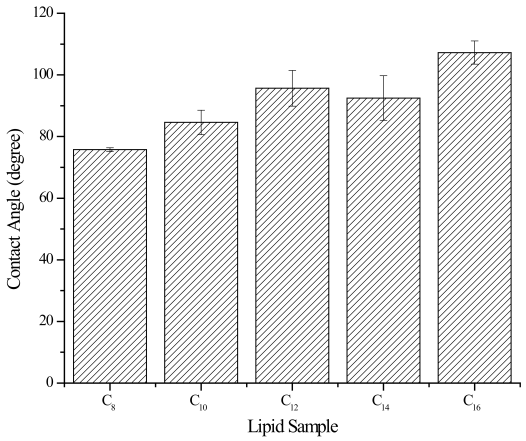

Figure 2.2. Sessile contact angle of water on each lipid surface.

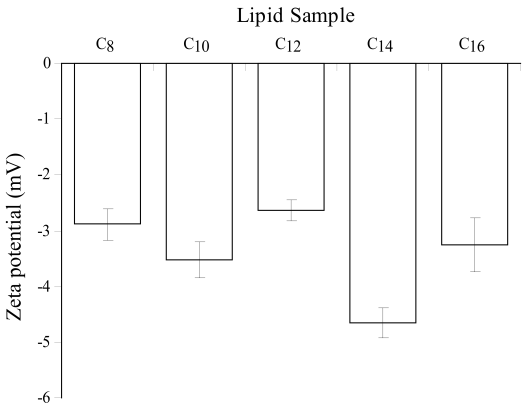

Figure 2.3. Zeta potential of lipid microparticles

Table 2.2. Average mean diameter of lipid microparticles

Lipid sample	**Lipid soln. (0.01 g/mL) 2.5% PVA**	**Lipid soln. (0.02 g/mL) 2.5% PVA**	**Lipid soln. (0.01 g/mL) 5% PVA**	**Lipid soln. (0.02 g/mL) 5% PVA**
C_8	39.6 ± 13	41.2 ± 12.3	28.8 ±11.3	37.8 ± 14.7
C_{10}	32.3 ± 13	35.6 ± 12.6	22 ± 9.36	33.6 ± 15.8
C_{12}	29.7 ± 13.5	36.6 ± 13.8	27.3 ± 12.1	28.4 ± 12.3
C_{14}	26.2 ± 14.1	29.7 ± 14	29 ± 12.3	17.6 ± 7.6
C_{16}	25.3 ± 11	24 ± 12.3	21.7 ± 9.75	26.1 ± 11.9

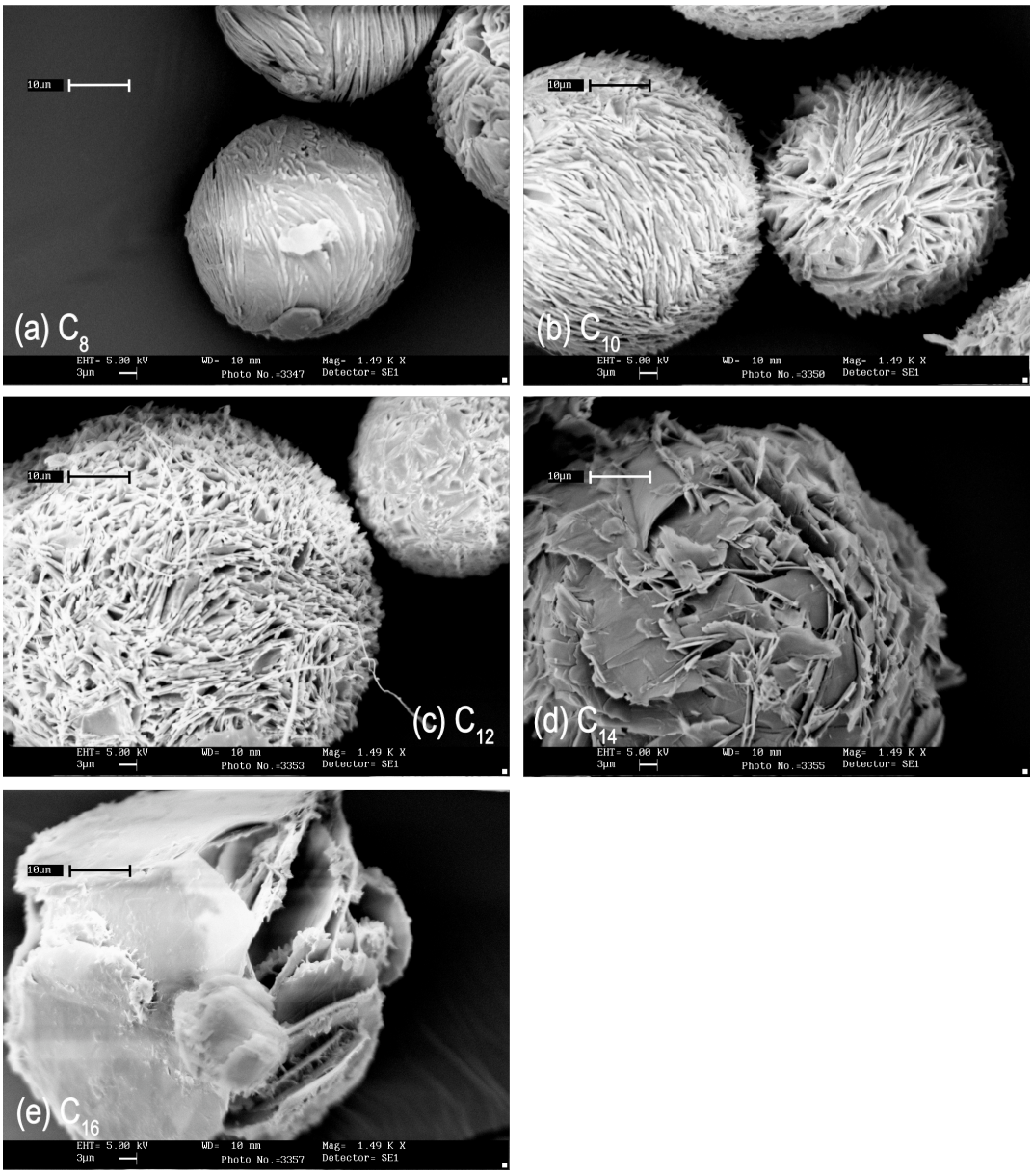

Figure 2.4. Lipid microparticle morphology as a function of lipid chain length. Clockwise from top-left, (A) C_8 particle morphology showing a tightly packed morphology followed by (B) $C_{10,}$, (C) C_{12}, (D) C_{14}, and (E) C_{16}. Note the increasing porosity trend with increasing lipid chain length, the scale bar in each picture is 10 µm.

Inspection of the particles by SEM showed porous structures on the surface and throughout the matrix (Figure 2.4). Particle porosity was a function of the lipid length, with the shorter lipids leading to denser particles. Particles from the C_8 lipid have a relatively smooth surface compared to C_{10} through C_{16} lipids. Additionally, the

surface structures became more prominent as the lipid chain length increased. The shape and structures of the pores formed are part of the inherent properties of the microparticle formulation method. During spontaneous emulsification, the lipid concentration in the organic phase constantly increases until reaching a solubility limit after which the lipid starts to precipitate. The rate at which the lipid precipitation takes place is a function of its solubility in the organic phase[37]. As evident by the SEM pictures, short and medium chain length lipid (C_8-C_{10} and C_{12}-C_{14}) result in coral shaped surfaces whereas longer chain lipid (C_{16}) results in sheet like surfaces.

Piroxicam, a non-steroidal anti-inflammatory molecule was chosen as a model drug because of its generalizable "drug-like" nature, thus presenting what is regarded as an accurate model for currently available therapeutic[38-39]. The in vitro release behavior of piroxicam-loaded lipid microparticles was observed over a 300 hr period at 37 °C. Because particle size can influence release kinetics, particles were sieved into three groups (>40 mm, 25-40 mm and <25 mm). As expected, based on the literature, larger particle sizes showed slower release rates in comparison to smaller particles, possibly due to an increased diffusion pathway length, or smaller surface to volume ratio[38,40-41]. The microparticles exhibited chain length-dependent release behavior, but in an unexpected manner with microparticles fabricated from longer chain lipid particles displaying faster release kinetics (Figure 2.5(A-C)). Based on the hydrophobic character of these lipids, we anticipated that the rate of lipid hydrolysis, and therefore drug release rate, would be inversely proportional to lipid chain length; however, based on the SEM images and particle density calculations, it appeared that this release behavior was governed more strongly by microparticle porosity, and subsequently the surface area, than by lipid hydrophobicity.

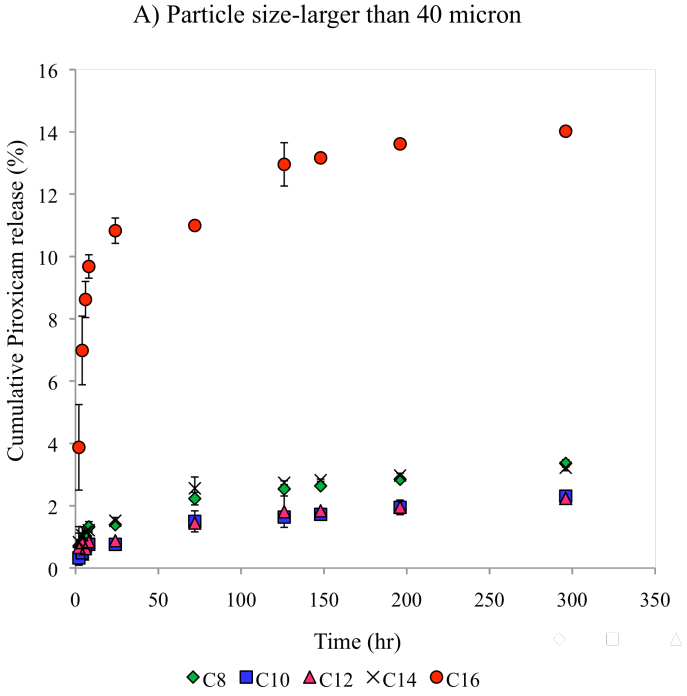

Figure 2.5(A). Cumulative release of piroxicam-loaded lipid microparticles sized 40 microns or larger.

B) Particle sizes between 25-40 microns

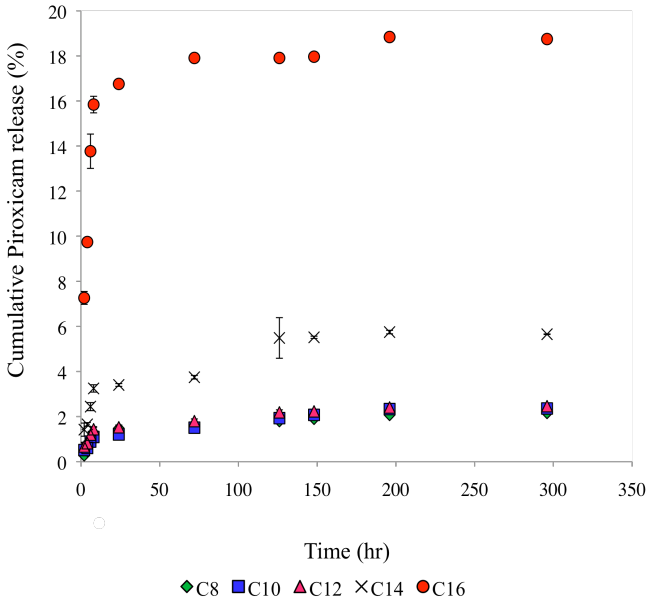

C) Particles smaller than or equal to 25 microns

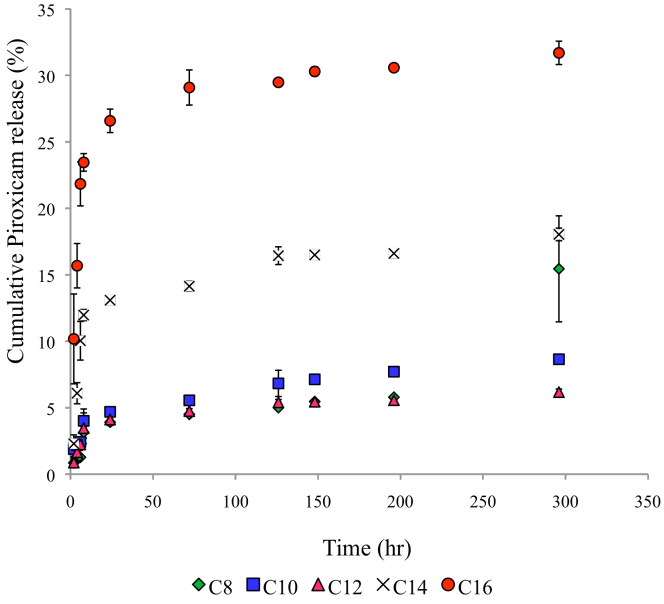

Figure 2.5(B). Cumulative release of particles sized between 25 to 40 microns, (C) cumulative release of particles smaller than 25 micron, showing faster release compared to the larger particles.

Table 2.3. Kinetic assessment of dissolution data for release of piroxicam (pH 7.4), for particles d≤25μm

Kinetic model	Regression parameters [a]	C_8	C_{10}	C_{12}	C_{14}	C_{16}
Ritger-Peppas	r^2	0.8863	0.95331	0.8514	0.7054	0.7708
	n	0.3903	0.3	0.3253	0.3903	0.1761
	k	0.8069	1.6132	1.1253	4.0218	12.945
Jander's equation	r^2	0.7914	0.8895	0.7343	0.596	0.6136
	$k_J \times 10^{-2}(h^{-1/2})$	1.15	1.06	0.95	1.19	0.96
	Intercept	0.2336	0.2796	0.2581	0.3966	0.5488

[a] Regression parameters (r^2: determination coefficients, n: diffusional release exponent, k_J: Jander's release rate constant)

Table 2.4. Kinetic assessment of dissolution data for release of piroxicam (pH 7.4), for particles d~[25-40]μm

Kinetic model	Regression parameters [a]	C_8	C_{10}	C_{12}	C_{14}	C_{16}
Ritger-Peppas	r^2	0.821	0.9564	0.9215	0.9144	0.731
	n	0.3424	0.2941	0.2393	0.2708	0.1508
	k	0.3652	0.4698	0.6789	1.3628	8.8729
Jander's equation	r^2	0.8265	0.9528	0.9052	0.8856	0.6221
	$k_J \times 10^{-2}(h^{-1/2})$	0.04	0.04	0.04	0.09	0.2
	Intercept	0.0019	0.0018	0.0028	0.0057	0.0391

[a] Regression parameters (r^2: determination coefficients, n: diffusional release exponent, k_J: Jander's release rate constant)

Table 2.5. Kinetic assessment of dissolution data for release of piroxicam (pH 7.4), for particles d≥40 μm

Kinetic model	Regression parameters [a]	C_8	C_{10}	C_{12}	C_{14}	C_{16}
Ritger-Peppas	r^2	0.983	0.9604	0.9807	0.9891	0.7949
	n	0.2996	0.354	0.2594	0.2809	0.194
	k	0.5981	0.3036	0.5527	0.6983	5.0808
Jander's equation	r^2	0.9431	0.926	0.9524	0.9239	0.9161
	$k_J \times 10^{-2}(h^{-1/2})$	0.79	0.78	0.64	0.75	0.5
	Intercept	0.1989	0.1613	0.191	0.2092	0.4422

[a] Regression parameters (r^2: determination coefficients, n: diffusional release exponent, k_J: Jander's release rate constant)

To achieve a better understanding of the underlying release mechanism, the results were evaluated using two models, Ritger-Peppas, and Jander[33-34]. The regression parameters for each model are listed in Table 2.3-2.5. The determination coefficients of Ritger-Peppas model represent a better fit for the kinetic analysis, thus we choose to limit our discussion to this model. The diffusional exponent for each release curve, for lipid particles across the length scale confirms the presence of Fickian diffusion mechanism of piroxicam ($n \leq 0.43$). In addition, the calculated rate constants verify the increasing trend with decreasing particle diameter.

Lastly, the lipids were designed to hydrolytically degrade to form DHA and free fatty acids, both of which are readily metabolized in the human body. To establish that the degradation products of the lipids are DHA and free fatty acid, C_8 lipid was allowed to hydrolyze in acidified distilled water. Dihydroxyacetone and sodium octoate were treated likewise and used as controls. Unfortunately no common solvent could be identified to solubilize the degradation products for analysis by NMR because of the relatively hydrophilic nature of DHA and the relative hydrophobic nature of octanoic acid. Because butyric acid and DHA are both water-soluble, we synthesized C_4 lipid to determine its hydrolytic products as a proof of concept to determine the degradation products of symmetrical DHA lipids.

Previous studies have shown that the dissolution of dihydroxyacetone in water results in formation of a dynamic equilibrium between dihydroxyacetone itself, its hydrated form and its cyclic hemiacetal dimer form. Dissolution of dihydroxyacetone in acidic conditions also leads to enolization and subsequent formation of monohydroxyacetone and its hydrated form as evident by ^{1}H-NMR analysis[43-45]. The ^{1}H-NMR of the C_4 lipid hydrolysis products showed overlapping peaks with that of DHA and sodium butyrate, indicating that the DHA lipids form the desired hydrolysis products (Figure 2.6(a) and (b), Figure 2.7) and (Table 2. 4(A-B)).

Table 2.6(a). Proton magnetic resonance chemical shifts for sodium butyrate structures in solution.

A-Compound	Solvent	Protons	δ(ppm)	Peak No.
Sodium butyrate 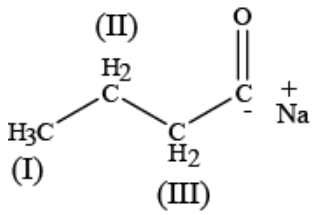	D_2O	--CH_3 --CH_2 --CH_2	0.9 (t) 1.6 (h) 2.2 (t)	(I) (II) (III)

Table 2.6(b). Proton magnetic resonance chemical shifts for di and monohydroxyacetone structures in solution.

B-Compound	Solvent	Protons	δ(ppm)	Peak No.
Dihydroxyacetone dimer 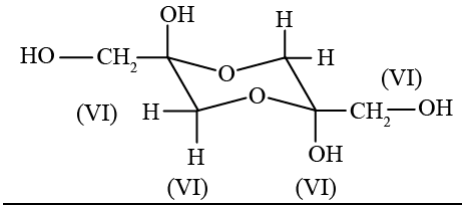	D_2O	--CH_2(ax) --CH_2(eq) --CH_2 --OH	3.82 (s) 3.82 (s) 3.7,3.9 (s) 3.65 (s)	(VI) (VI) (VI) (VI)
Dihydroxyacetone monomer 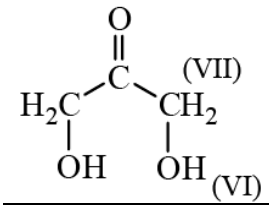	D_2O	--CH_2 --OH	4.4(s) 3.5-3.7 (m)	(VII) (VI)
Dihydroxyacetone monomer (hydrate) 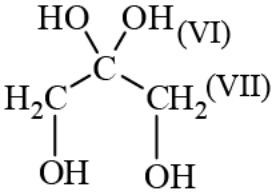	D_2O	--CH_2 --OH	4.4(s) 3.5-3.7 (m)	(VII) (VI)
Monohydroxyacetone 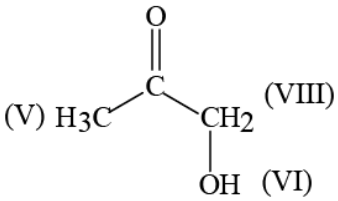	D_2O	--CH_2 --CH_3 --OH	5.25 (s) 2.29 (s) 3.65 (s)	(VIII) (V) (VI)
Monohydroxyacetone (hydrate) 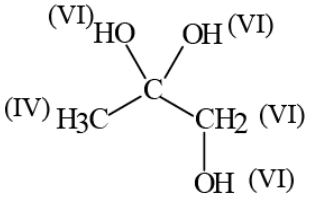	D_2O	--CH_2 --CH_3 --OH	3.8 (s) 1.32 (s) 3.65 (s)	(VI) (IV) (VI)

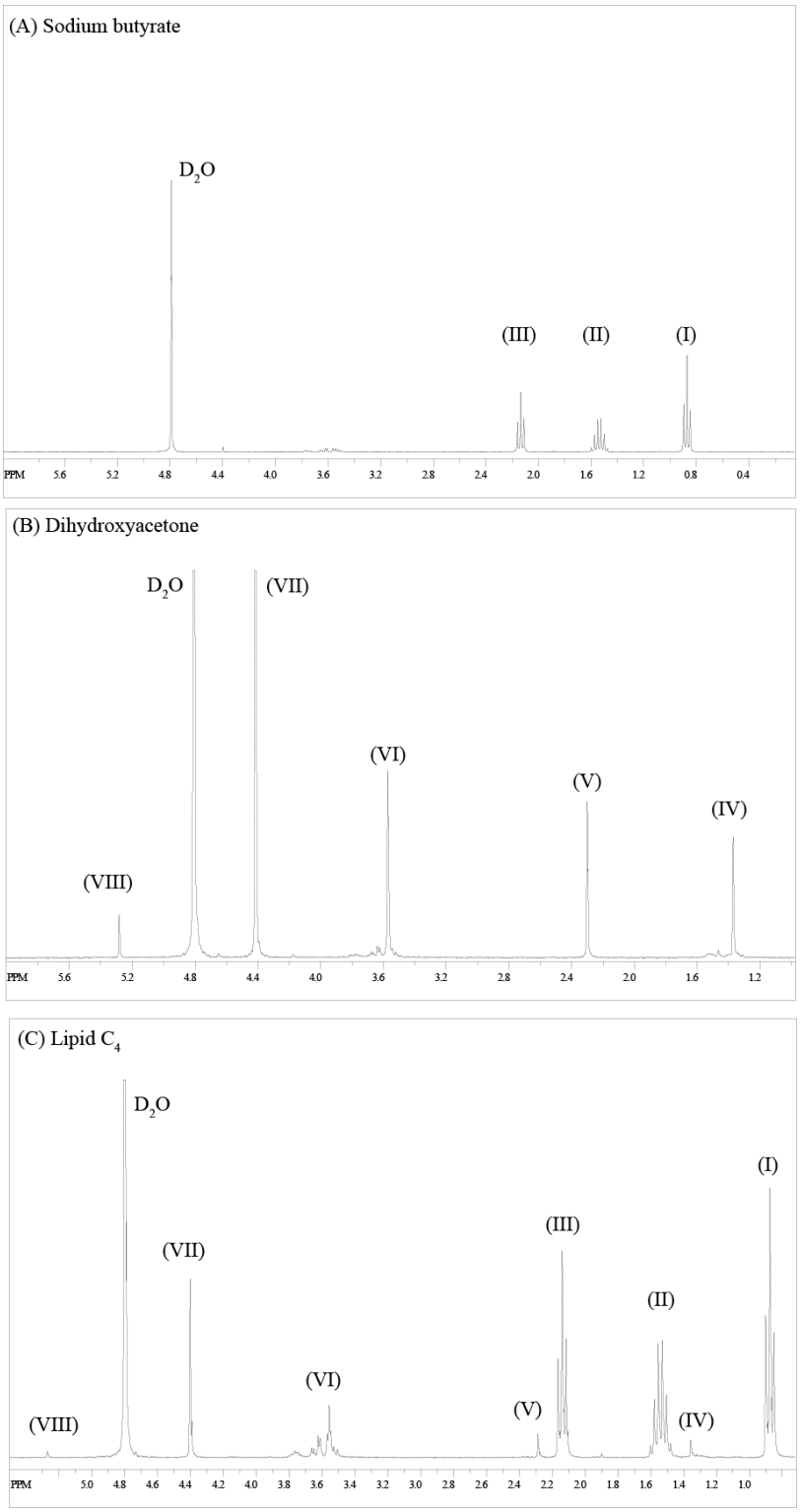

Figure 2.7. ^{1}H-NMR spectra of (A) sodium butyrate, (B) dihydroxyacetone and (C) hydrolyzed C_4 lipid.

2.3. Conclusion

In conclusion, a family of DHA derived symmetrical lipids with varying hydrocarbon chain lengths were synthesized to systematically analyze how lipid chain length influences microparticle fabrication, microparticle morphology, and drug release kinetics. Our results were somewhat surprising in that the release kinetics of a hydrophobic drug model increased with increasing lipid length. SEM images, as well as particle density calculations collectively suggested that the microparticle porosity was the primary factor that controlled release kinetics, as microparticle porosity increased with increasing lipid length. Future work with these lipids will focus on the controlled localized release of therapeutic drugs in animal models of disease.

REFERENCES

[1] R. Langer, Drug delivery: drugs on target, Science, 2001, 293, 58-59.

[2] H. Rosen, T. Abribat, The rise and rise of drug delivery, Nat. Rev. Drug Discov. 2005, 4, 381-385.

[3] D. Kohane, Microparticles and Nanoparticles for drug delivery, Biotechnology and Bioengineering, 2007, 96, 2, 203-209.

[4] W. Jiang, R.K. Gupta, M.C. Deshpande, S.P. Schwendeman, Biodegradable poly(lactic-co-glycolic acid) microparticles for injectable delivery of vaccine antigens, Adv. Drug Del Rev, 2005, 57, 391-410.

[5] V.R. Sinha, A. Trehan, Biodegradable microspheres for parenteral delivery. Crit Rev Ther Drug Carrier Syst, 2005, 22, 535-602.

[6] G. Jiang, B.H. Woo, F. Kang, J. Singh, P. DeLuca, Assessment of protein release kinetics, stability and protein polymer interaction of lysozyme encapsulated poly(D,L-lactide-co-glycolide) microspheres, J. Controlled Release, 2002, 79, 137-145.

[7] M.M. Arnolds, E.M. Gorman, L. J. Schieber, E.J. Munson, C. Berkland, NanoCipro encapsulation in monodisperse large porous PLGA microparticles, J. Controlled Release, 2007, 121,1-2, 100-109.

[8] S.S. Davis, Coming of age of lipid-based drug delivery systems, Adv. Drug Del. Rev., 2004, 56, 9, 1241-1242.

[9] S.A. Wissing, O. Kayser, R.H. Muller, Solid lipid nanoparticles for parenteral drug delivery, Adv. Drug Deliv. Rev., 2004, 56, 1257-1272.

[10] M. DelCurto, D. Chicco, M. D'Antonio, V. Ciolli, H. Dannan, S. D'Urso, B. Neuteboom, S. Pompili, S. Schiesaro, P. Esposito, Lipid microparticles as sustained release system for a GnRH antagonist (Antide), J. Controlled Release., 2003, 89, 297-310.

[11] R. Pandey, G.K. Khuller, Solid lipid particle-based inhalable sustained drug delivery system against experimental tuberculosis, Tuberculosis, 2005, 85, 227-234.

[12] S. Saraf, D. Mishra, A. Asthana, R. Jain, S. Singh, N. Jain, Lipid microparticles for mucosal immunization against hepatitis B, Vaccine, 2006, 24, 45-56.

[13] E. Gavini, V. Sanna, R. Sharma, C. Juliano, M. Usai, M. Marchetti, J. Karlsen, P. Giunchedi, Solid lipid microparticles (SLM) containing juniper oil as anti-acne topical carriers: preliminary studies, Pharm. Dev. Technol, 2005, 10, 479-487.

[14] S. Jaspart, P. Bertholet, G. Piel, J.-M. Dogne, L. Delattre, B. Evrard, Solid lipid microparticles as a sustained release system for pulmonary drug delivery, Eur. J. Pharm. Biopharm., 2007, 65, 47-56.

[15] S. Jaspart, G. Piel, L. Delattre, B. Evrard, Solid lipid microparticles: formulation, preparation, characterization, drug release and applications, Expert Opin. Drug Deliv., 2005, 2, 75-87.

[16] H. K. Frederiksen, H. G. Kristensen, M. Pedersen, Solid lipid microparticle formulations of the pyrethroid gamma-cyhalothrin-incompatibility of the lipid and the pyrethroid and biological properties of the formulations, J. Controlled Release, 2003, 86, 243-252.

[17] R. Cortesi, E. Esposito, G. Luca, C. Nastruzzi, Production of lipospheres as carriers for bioactive compounds, Biomaterials, 2002, 23, 2283-2294.

[18] C. Erni, C. Suard, S. Freitas, D. Dreher, H.P. Merkle, E. Walter, Evaluation of cationic solid lipid microparticles as synthetic carriers for the targeted delivery of macromolecules to phagocytic antigen-presenting cells, Biomaterials, 2002, 23, 4667-4676.

[19] B. Heurtault, P. Saulnier, B. Pech, J.-E. Proust, J.-P. Benoit, Physico-chemical stability of colloidal lipid particles, Biomaterials, 2003, 24, 4283-4300.

[20] W. Mehnert, K. Mader, Solid lipid nanoparticles: Production, characterization and applications, Adv. Drug Deliv. Rev. , 2001, 47, 165-196.

[21] H. Reithemeier, J. Herrmann, A. Gopferich, Development and characterization of solid lipid microparticles as drug carrier for somatostatin. Int. J. Pharm, 2001, 218, 133-143.

[22] M. Savolainen, J. Herder, C. Khooc, K. Lövqvist, C. Dahlqvist, H. Glad, A. M. Juppo, Evaluation of polar lipid-hydrophilic polymer microparticles, Int. J. Pharm, 2003, 262, 1-2, 47-62.

[23] N. Passerini, B. Perissutti, B. Albertini, D. Voinovich, M. Moneghini. L. Rodriguez, Controlled release of verapamil hydrochloride from waxy microparticles prepared by spray congealing, J. Controlled Release, 2003, 88, 263-275.

[24] Y. Akiyama, M. Yoshioka, H. Horibe, S. Hirai, N. Kitamori, H. Toguchi, Novel controlled-release microspheres using polyglycerol esters of fatty acids, J. Controlled Release, 1993, 26, 1-10.

[25] L. Rodriguez, N. Passerini, C. Cavallaria, M. Cinia, P. Sancinb and A. Finic, Description and preliminary evaluation of a new ultrasonic atomizer for spray-congealing process, Int. J. Pharm, 1999, 183, 133-143.

[26] M. Demirel, Y. Yazan. R. H. Muller, F. Killice and B. Bozan, Formulation and in vitro-in vivo evaluation of piribedil solid lipid micro-nanoparticles, J. Microencapsulation, 2001, 18, 359-371.

[27] S. Vanna , N. Kirschvink,P.Gustin, E. Gavini, I. Roland, L. Delattre, and B. Evrard, Preparation and In Vivo Toxicity Study of Solid Lipid Microparticles as Carrier for Pulmonary Administration, AAPS PharmSciTe, 2003, 5, Article 27.

[28] V. Esmann, Dihydroxyacetone as an intermediate during the metabolism of glycerol and glyceraldehyde in leukocytes from the rat. , Acta. Chemica. Scandinavica., 1968, 22, 2281-2288.

[29] P.N. Zawaneh, A.M. Doody, A.N. Zelikin, D. Putnam, Diblock copolymers based on dihydroxyacetone and ethylene glycol: synthesis, characterization, and nanoparticle formulation, Biomacromolecules, 2006, 7 ,3245-3251.

[30] A.N. Zelikin, D. Putnam, Poly(carbonate-acetal)s from the dimer form of dihydroxyacetone, Macromolecules, 2005, 38, 5532-5537.

[31] A.N. Zelikin, P.N. Zawaneh, D. Putnam, A functionalizable biomaterial based on dihydroxyacetone, an intermediate of glucose metabolism, Biomacromolecules, 2006, 7, 3239-3244.

[32] P.H. Bentley, W. McCrae, An efficient synthesis of symmetrical 1,3-diglycerides, J. Org. Chem., 1970, 35, 2082-2083.

[33] R. Gurny, E. Doelker, N.A. Peppas, Modeling of sustained release of water-soluble drugs from porous, hydrophobic polymers, Biomaterials, 1982, 27-32.

[34] Y. Yamagata, K. Iga and Y. Ogawa, Novel sustained-release dosage forms of proteins using polyglycerol esters of fatty acids, J. of Controlled Rel., 2000, 63, 319-329.

[35] M.A. Tracy, K.L. Ward, L. Firouzabadian, Y. Wang, N. Dong, R. Qian, Y. Zhang, Factors affecting the degradation rate of poly(lactide-co-glycolide) microspheres in vivo and in vitro, Biomaterials, 1999, 20, 1057-1062.

[36] K.Leong, J.Kost, E.Mathiowitz, and R.Langer, Polyanhydrides for controlled release of bioactive agents, Biomaterials 1986, 7, 364-371.

[37] I. Aranberri, B. Binks, J. Clint, P. Fletcher, Synthesis of macroporous silica from solid-stabilised emulsion templates, J Porous Mater 2009, 16, 429-437.

[38] N. Yüksel, A. Karataş, Y. Özkan, A. Savaşer, SA Özkan, T. Baykara, Enhanced bioavailability of piroxicam using Gelucire 44/14 and Labrasol: in vitro and in vivo evaluation, Eur. J. Pharm. Biopharm., 2003, 56, 453-459.

[39] C. Berkland, A. Cox, K. Kim and D.W. Pack, Three-month, zero-order piroxicam release from monodispersed double-walled microspheres of controlled shell thickness, J. of Biomed. Mat. Res. 2004, 70A, 576-584.

[40] R. Jain, The manufacturing techniques of various drug loaded biodegradable poly (lactide-co-glycolide)(PLGA) devices, Biomaterials, 2000, 21, 2475-2490.

[41] D. Klose, F. Siepmann, K. Elkharraz, S. Krenzlin, How porosity and size affect the drug release mechanisms from PLGA-based microparticles, Int. J. of Pharm., 2006, 314, 198-206.

[42] D. Klose, F. Siepmann, K. Elkharraz, J. Siepmann, PLGA-based drug delivery systems: Importance of the type of drug and device geometry, Int. J. of Pharm, 2008, 354, 95-103.

[43] O. Novotny, K. Cejpek, J. Velisek, Formation of α-hydroxycarbonyl and α-dicarbonyl compounds during degradation of monosaccharides, Czech J. Food Sci., 2007, 25, 3, 119-130.

[44] G.K. Glushonok, T.G.Glushonok, L.A. Maslovskaya, O.I. Shadyro, A 1H and 13C NMR and UV study of the state of hydroxyacetone in aqueous solutions, Russ J. Org. Chem., 2003, 73, 7, 1085-1089.

[45] L. Davis, The structure of dihydroxyacetone in solution, Bioorg. Chem., 1973, 2, 197-201.

CHAPTER 3

SYMMETRICAL DIGLYCERIDES FOR CONTROLLED DRUG DELIVERY OF PROTEINS

3. Introduction

In recent years, significant progress has been made in understanding the role of proteins and peptides in physiological and pathological processes. However, a range of problems raised by their physical and chemical properties has hindered the design of controlled release systems for delivery of such therapeutics. Their sensitivity to physical and chemical conditions as well as their short half-life requires frequent injection or intravenous infusion over an extended period of time, resulting in poor patient compliance.

Historically, the solution to the instability problem has been to encapsulate the drug within a matrix to protect it from degradation and elimination; however, the choice of matrix is of important consideration. Polymers have been largely considered the matrix of choice, especially poly(lactic-*co*-glycolic acid) (PLGA)-based devices. However, PLGA degrades into smaller chain acids upon contact with water, which can lead to significant drops in the environmental pH at the administration site[1]. Furthermore, protein based drugs can lose their activity during preparation procedures of polymeric matrices. For example, changes in the protein structure may occur at the liquid-liquid interface when using organic solvents using the solvent emulsification technique[2-7]. Protein based therapeutics often lose their activity under such harsh conditions, therefore use of lipid implants as parenteral drug delivery systems is a potential alternative for these types of drugs.

Various types of lipids have been reported in preparation of drug-loaded implants. Triglycerides in particular have been widely studied for the release of brain

derived neurotrophic factor (BDNF), interferon α-2a, bovine serum albumin, and interleukin-18[8-14]. In this study, we dedicate our efforts in illuminating the relationship between manufacturing conditions for protein-loaded implants and resulting matrix performance, such as release behavior and protein stability. The major objectives of this present study were: (i) to prepare lysozyme-loaded, lipidic matrix pellets, (ii) to investigate the effect of several formulation and processing parameters on the resulting protein release patterns, (iii) to better understand the underlying mass transport mechanisms, and (iv) to be able to predict the effects of processing variables on the resulting drug release kinetics in a quantitative way.

3.1. Materials and methods

Hexadecanoyl chloride, tetradecanoyl chloride, dodecanoyl chloride, decanoyl chloride, ocatanoyl chloride, 1,3-dihydroxyacetone dimer 97% (DHA), anhydrous chloroform, anhydrous pyridine, anhydrous tetrahydrofuran, sodium borohydride, chicken egg lysozyme (Grade I, M_w 14 kDa) and *M. lysodeikticus* were all obtained from Sigma-Aldrich (Saint Louis, MO) and used without further purification. Bicinchoninic acid disodium salt (BCA) protein assay kit was obtained from ThermoFisher Scientific.

3.1.1. Lipid synthesis and characterization

Symmetrical diglycerides were synthesized through modification of a previously reported method by Bentley and McCrae[15]. The general procedure is as follows, using the synthesis of C_{16} symmetrical lipid as an example: DHA (3.5 g, 39 mmole) was stirred in anhydrous chloroform (150 mL) under flow of N_2 at room temperature, followed by sequential drop-wise (1 drop/sec) addition of hexadecanoyl chloride (22.1 mL, 80 mmol) and anhydrous pyridine (7.5 mL), in that order (Figure (1A)). The mixture was stirred for 3 hrs at room temperature, and the color varied

from clear to slightly yellow. The reaction was extracted with deionized water (2 × 75 mL), and the combined aqueous layers were washed with chloroform (1 × 75 mL). All chloroform layers were combined before removal by rotoevaporation in vacuo to a thick white/yellow residue. The residue was dissolved in dichloromethane:ether (1:1), in the lowest volume needed, and placed in the freezer to crystallize overnight (yield~70%). The resulting product was dried in vacuo overnight and ^{1}H-NMR was recorded at room temperature with a Brucker AF-300 spectrometer operating at 300.13 MHz in preparation for the next step.

To make the final product, lipid C_{16} (1,3-dihydroxypropan-2-one 1,3-dipalmitate) (10.0 g) was dissolved in anhydrous tetrahydrofuran (250 mL) and benzene (50 mL) followed by the slow addition of water (15 mL). The heterogeneous emulsion was cooled externally using an ice bath (temperature ~5 ^{o}C), and neutral sodium borohydride (1.0 g) was added to the stirring emulsion. After 30 minutes, the excess sodium borohyride was reacted with glacial acidic acid (0.5 mL) by drop-wise addition to the reaction. The solution was diluted with equal reaction volume of chloroform, washed with sodium bicarbonate (1 M) and water in that order, the organic layer isolated and dried over sodium sulfate. Chloroform was removed by rotoevaporation in vacuo to yield a thick white/yellow residue, and further dried in vacuo overnight. The characterization steps taken afterward were exactly the same to those taken for symmetrical lipids.

3.1.2. Lipid matrix preparation

The true particle density of the single materials was obtained using helium pyncometry measurements (Quantachrome Instruments, Boynton Beach, FL). Diglyceride powders were ground and sieved using 200 μm USA standard sieves (Fisherscientific) and lyophilized for at least 24 hrs to remove excess moisture. The

binary mixtures of protein and diglyceride powders were combined carefully using geometric dilution. Protein loaded implants were prepared by using a hydraulic press (Carver, Model No. 3851-0, Wabash, IN) with a pressure gauge. The following protein loadings (1, 5 and 10%) and lipids were mixed geometrically in an agate mortar. The final powder mixture was compressed using a range of different pressures, first batch implants were compressed using 0.25 Ton force over 10 seconds, and second batch implants were compressed using 0.25 Ton force over 10 seconds, followed by gradual increase of force to 0.5 Ton force for an additional 10 seconds. For clarity, from here on the first batch is referred to as group A and second batch is referred to as group B. Implants were compressed under a range of different forces to achieve a controlled series of porosities, and cylinder heights were measured (n=3) using a digital sliding caliper (Marathon, Part No. CO030150). Porosity ε was calculated by the eq. 1 adapted from Siegel et al [16].

$$\varepsilon = \frac{(1-L)W}{\rho V} \tag{1}$$

where L is the protein loading, W is the mass of the implant, V denotes the volume calculated from Caliper measurements and ρ was obtained using helium pyncometry measurements (Quantachrome Instruments, Boynton Beach, FL). For the in vivo biocompatibility study, lyophilized and sieved lipid powder was compressed by applying a pressure of 0.5 tons over 10 seconds to produce 50 mg implants of 5 mm diameter. The implants were sterilized using UV irradiation on each side for 30 minutes.

3.1.3. Quantification of model substance release

3.1.4. In vitro release study

Lipid implants were incubated in 1.0 mL phosphate buffer saline pH 7.4 at 37 ^{o}C. Buffer was removed and replaced completely after each sampling interval and stored at -20 ^{o}C until further analysis. Bicinchoninic acid disodium salt (BCA) protein detection kit (FisherThermoscientific) was used to determine protein concentration in the release buffer through mixing of 25 μL of samples with 200 μL of working solution. The samples were mixed thoroughly for 30 second and incubated at 37 ^{o}C for 1 hr, after which the absorbance was measured at λ=562 nm using a microplate spectrophotometer (Spectramax GeminiEM; Molecular Devices, Sunnyvale, CA).

3.1.5. Sodium dodecyl sulfate-polyacrylamide gel electrophoresis (SDS-PAGE)

The protein released from the implants was analyzed using SDS-PAGE after the following time points: 2, 24, 168 and 288 hrs. All of the gels were run under reducing conditions. Each sample was mixed with an equal volume of sample buffer SDS (1% w/v), Tris-HCl (pH 6.8, 0.06 mM), glycerol (3 mM), bromophenol blue (0.01% w/v), and β-mercaptoethanol (0.05% v/v)). The samples were boiled for 5 minutes and cooled to room temperature before loading onto the gel. The samples were then resolved through a 4-18% polyacrylamide gradient gel at a constant voltage (125 V). Prestained molecular weight standards (BioRad Kelidoscope Precision Plus) were used to estimate the molecular weight of each protein sample. The gels were stained with Coomassie Blue dye and then photographed. The apparent molecular weights of the stained bands were then compared to that of the standards.

3.1.6. Biological activity of lysozyme

M. lysodeikticus (0.01%, w/v) was suspended in potassium phosphate buffer (66mM, pH 6.24). A 0.1 mL aliquot of appropriately diluted lysozyme samples was mixed with 2.5 mL of prepared *M. lysodeikticus* suspension in a quartz cell (path

length 1 cm), which was then immediately placed into a spectrophotometer (SpectraMax). The rate of decrease of absorbance at 450 nm was monitored by the UV spectrophotometer during a total period of 3 minutes at 25°C. The slope of the linear portion in the plot of absorbance against time provided the amount of lysozyme in enzyme unit (EU) [10, 17, 18]. Units of active lysozyme were calculated based on the EU, using eq. (2-3):

$$\text{Units of lysozyme/mL sample} = \frac{\left(\left(\Delta A_{450\text{ nm}}/\text{min Test}\right) - \left(\Delta A_{450\text{ nm}}/\text{min Blank}\right)\right) \times \left(\text{df}\right)}{0.001 \times 0.1} \qquad (2\text{-}3)$$

$$\text{Units of lysozyme/ mg} = \frac{\text{Units of lysozyme/mL sample}}{\text{mg lysozyme/mL sample}}$$

In the equation, df was the dilution factor and 0.001 was from the definition of lysozyme unit as one unit will produce $\Delta A_{450\text{ nm}}$ of 0.001 per minute at pH 6.24 and 25°C using a suspension of *M. lysodeikticus* as substrate in a 2.6 mL reaction mixture. The volume in milliliter of lysozyme sample used 0.1 mL. The biological activity of the released lysozyme sample was then compared with the native lysozyme sample to evaluate the effect of formulation on its biological activity.

3.1.7. In vivo biocompatibility and erosion studies

This study was conducted in accordance with the Cornell University Institutional Animal Care and Use Committee. The model animals were 8 weeks old female Sprague-Dawley rats (Harlan Sprague-Dawley, Inc. Indianapolis, IN). A total of 96 rats (4 per time point per group) were used for this study. Rats were weighed and pre-medicated using buprenorphine HCl (0.01 mg/kg s.q.) 20 minutes prior to anesthetic induction. Anesthesia was induced using isoflurane (2-3%) in oxygen via facemask and maintained through the surgical procedure (1-3% isoflurane in oxygen via face mask). Vital signs including heart rate and respiratory rate, as well as

response to stimulation and pedal reflex, were monitored throughout the anesthetic period. After induction, the dorsal intrascapular area was clipped and prepared using 2% chlorhexidine gluconate in standard aseptic technique.

Animals were divided into 6 groups of 16 animals each: control (sham surgery without implant placement), C_{10}, C_{12}, C_{14}, C_{16}, and PLGA. For surgery, standard aseptic technique was used. A 0.5 cm stab incision was made over the dorsal border of each scapula, 0.5 cm lateral to midline bilaterally. A small subcutaneous pocket was created using blunt dissection and the implant was placed. The incision was closed using 4-0 nylon.

The animals were allowed to recover in their cages and were monitored for pain, suture removal, or other adverse side effects every 2 hours the day of surgery and twice a day thereafter. All rats were housed two per cage in a temperature and humidity controlled room with a 12-hour on-off light cycle in accordance with the standard procedures. Rats in each group were euthanized on days 2, 7, 14, and 28 after surgery using pentobarbital sodium (0.4-0.75 mL) intraperitoneally. Immediately after euthanasia, a necropsy was performed. One of the implants and its surrounding tissues were randomly chosen, and representative samples of the liver, spleen, kidney, and lungs were also harvested and placed into 10% buffered formalin. The second implant site was also removed and weighed for in vivo water uptake and inspected for in vivo erosion study. The samples were shipped in formalin via overnight carrier to Brigham and Woman's Hospital-Boston for histopathology. The pathologist was blinded to the treatment groups.

To determine the degree of in vivo erosion, the excess tissue surrounding the retrieved implants were cleaned off as much possible and samples were dried under vacuum and weighed. The mass loss of an implant relative to its original weight was taken as a measure of erosion.

3.1.8. Tissue embedding, sectioning and staining

The harvested implants and the surrounding tissue were dehydrated through a series of graded ethanols and xyelen, and embedded in paraffin using standard histological technique. The samples were sectioned to a thickness of 5μm and stained with hematoxylin and eosin to reveal the histologic details.

3.1.9. Theory

Drug release was described using Fick's second law of diffusion, considering axial as well as radial mass transfer in a cylinder of a finite length,

$$\frac{\partial C_i}{\partial \mathrm{t}} = \frac{1}{\mathrm{r}}\left\{\frac{\partial}{\partial r}\left(rD_i\frac{\partial C_i}{\partial r}\right)+\frac{\partial}{\partial \theta}\left(\frac{D_i}{r}\frac{\partial C_i}{\partial \theta}\right)+\frac{\partial}{\partial z}\left(rD_i\frac{\partial C_i}{\partial z}\right)\right\} \qquad (2)$$

where c is the concentration of the drug; t represents time, r,z denote the radial and axial coordinates and θ the angle perpendicular to the r-z plane; D represents the apparent diffusion coefficient of the drug within the implant. Using infinite series of exponential functions this partial differential equation can be solved assuming initial boundary condition of homogenous drug distribution at $t=0$ (before the exposure to the release medium) and perfect sink conditions, leading to[19]:

$$\frac{M_t}{M_\infty} = 1-\frac{32}{\pi^2}\sum_{n=1}^{\infty}\frac{1}{q_n^2}\exp\left(-\frac{q_n^2}{R^2}Dt\right)\sum_{p=0}^{\infty}\frac{1}{(2p+1)^2}\exp\left(-\frac{(2p+1)^2\pi^2}{H^2}Dt\right) \qquad (3)$$

where M_t and M_∞ represent the absolute cumulative amounts of drug released at time t, and infinite time, respectively; q_n are the roots of the Bessel function of the first kind of zero order [$J_o(q_n)=0$], and R and H denote the radius and height of the cylinder.

3.2. Results and Discussion

The symmetrical diglycerides were successfully synthesized following the modified Schotten-Baumann acylation, and were further characterized in terms of physical and chemical characteristics, Scheme 3.1 and Table 3.1. All of the synthesized diglycerides have melting points that are above room temperature and body temperature, making them ideal candidates for fabrication into implants for controlled drug delivery. Elemental analysis obtained for C_{10}-C_{16} diglycerides is summarized in Table 3.1. A representative NMR spectrum of C_{14} diglyceride is shown in Figure 3.1. The ^{1}H-NMR peaks for the all lipid in increasing carbon number are: ^{1}H-NMR(300MHz, $CDCl_3$, δ): [C_{10} diglyceride], 0.86(t, 6H), 1.25 (s, 28H), 2.27 (t, 4H), 4.13 (m, 6H), [C_{12} diglyceride], 0.86(t, 6H), 1.25 (s, 36H), 2.27 (t, 4H), 4.13 (m, 6H), [C_{14} diglyceride], 0.86(t, 6H), 1.25 (s, 48H), 2.27 (t, 4H), 4.13 (m ,6H), [C_{16} diglyceride] 0.86 (t, 6H), 1.25 (s, 52H), 2.27 (t, 4H), 4.13 (m, 6H).

As mentioned in chapter 2, each symmetrical diglyceride is abbreviated as C_x where "x" is an indication of the number of carbons available on either side chain.

Table 3.1. Melting point and elemental analysis of solid diglycerides

Lipid	Melting point (^{o}C)	Theoretical Elemental Analysis		Experimental Elemental Analysis	
		%C	%H	%C	%H
C_{10} Diglyceride	43.05	68.69	11.07	68.88	11.17
C_{12} Diglyceride	57.10	71.01	11.48	71.04	11.57
C_{14} Diglyceride	61.88	72.61	11.79	72.52	12.01
C_{16} Diglyceride	69.41	73.89	12.05	74.15	12.29

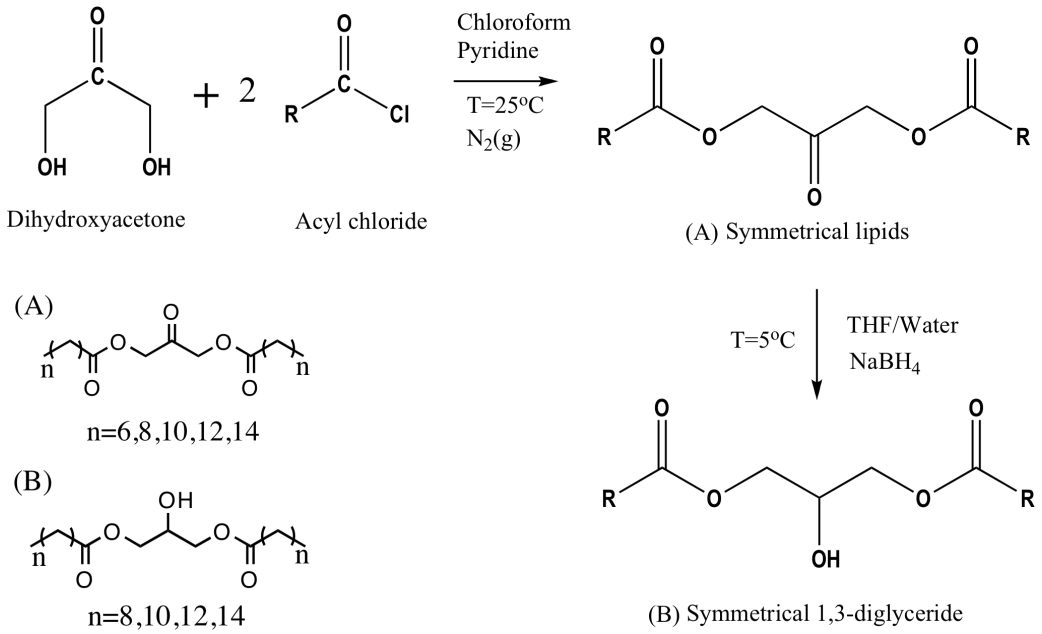

Scheme 3.1. Reaction pathway for the synthesis of symmetrical 1,3-diglycerides

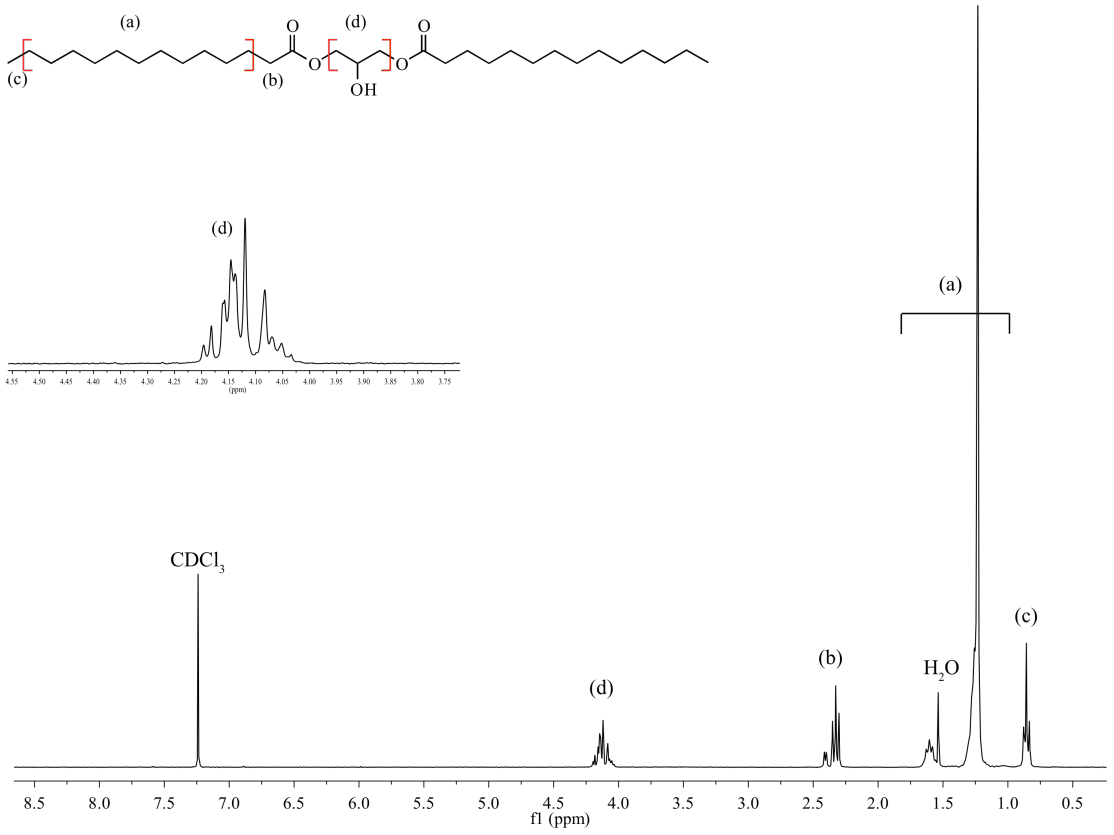

Figure 3.1. ^{1}H-NMR spectra of C_{14} lipid (2-hydroxy-3-(tetradecanoyloxy)propyl pentadecanoate). This spectrum serves as a representative of the remaining diglycerides.

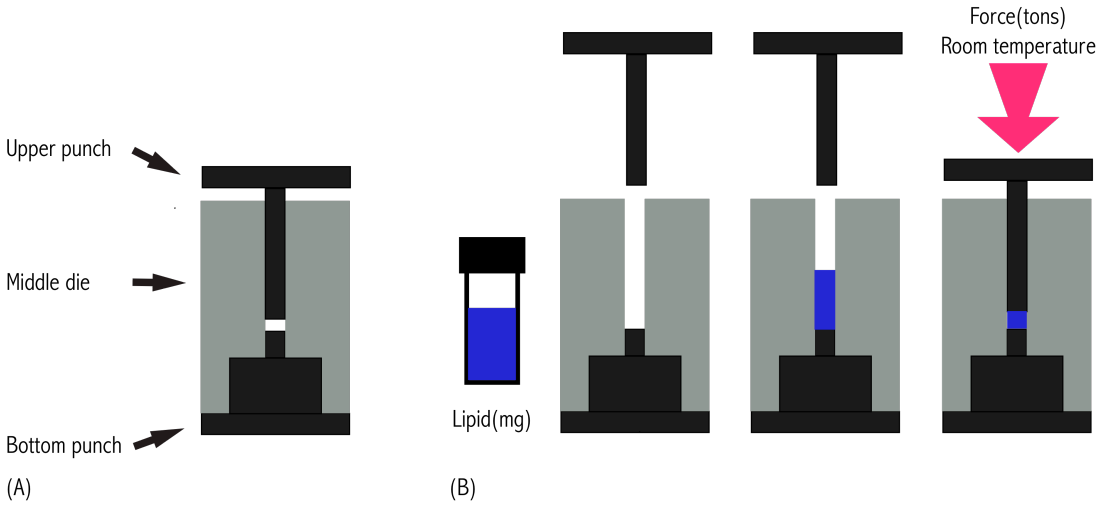

Scheme 3.2. Preparation of lipid implant through direct compression

3.2.1. Controlled release of lysozyme

The helium pyncometry measurements of diglyceride powders showed that they have similar densities, thus according to eq. (1) porosity of the same size implants is not a function of the lipid type, Table 3.2.

Table 3.2. True density results of He-pyncometry

Diglyceride	C_{10}	C_{12}	C_{14}	C_{16}
Density (g/mL)	1.0334	1.042	1.0225	1.0031

Our results showed that the diglyceride had a direct impact on the resulting release behavior of the model protein lysozyme, Figure 3.2-3.3. The amount of protein released over time decreased in the same order as the fatty acid chain length in the matrix increased. Studies have shown that drug release is a function of surface energy and thus matrix wettability [19, 20]. In the case of lipids, the longer fatty acid chain length leads to lower the overall wettability of the matrix. However, wettability can change during compression, moreover the surface roughness and penetration of the wetting liquid can distort the results. Therefore while wettability is a determining factor in onset of the release, the release behavior becomes more complex as wetting liquid penetrates further toward the center of the matrix.

3.2.2. Effects of drug loading

The effects of the initial lysozyme loading on drug release from diglyceride-based implants prepared by direct compression method are shown in Figures 3.2-3.3. An increase in the drug loading from 1 to 10% (w/w) resulted in a significant increase in the release rate, however all implants showed dramatic burst effect. This can be attributed to increase in lipid matrix porosity upon protein release. This effect is more pronounced at higher drug loadings (5-10%). Increased matrix porosity lead to higher drug mobility and thus an overall increase in absolute and relative release rates. It is

worth mentioning that the release rate was affected by initial drug loading as well as the underlying release mechanism. The drug release rate is primarily controlled by diffusion for lower drug loadings whereas for higher drug loadings (5-10%), the diffusion-controlled model systematically fails to fully describe the release mechanism. Upon contact with release medium, lysozyme starts to leach out of the matrix, resulting in increased matrix porosity and thus increased drug mobility. The increase in drug mobility compensates for the increase in the length of diffusion pathway.

3.2.3. Effects of the compression force

To address the effect of different porosities within the diglyceride resulting from different compression behavior, diglyceride powders were compressed under a range of different pressures to achieve a controlled series of porosities. Siegel et al[16] hypothesized that release from a monolithic matrix happens through a porous network of tortuous path created by drug particles. At high loading, the drug forms a complete interconnected network of its own, and release is a function of dissolution and diffusion through this network. Increased loading provides simpler pathways (low tortuosity) and greater porosity for diffusion[21]. At low loading, incomplete interconnected networks are formed and therefore release is incomplete although a burst release is observed because of dissolution of drug particles on the surface of the matrix.

Our results also indicate the burst effect in the early hours of the experiment, however it is possible that the burst effect is a result of low compression and subsequently low cohesion between the diglcyeride and drug particles, ultimately resulting in insufficient structural integrity of the implants when placed in the buffer. Higher drug loadings for both groups of A and B also showed burst effect and an overall faster release rate due to formation of the porous drug particle network. The

study outcome showed that for lower drug loading (1%), increasing compression force results in formation of less porous matrices and thus slower release rates, however for higher drug loadings (5-10%), increasing compression force does not significantly improve release behavior (Figure 3.4(a-c)). An interesting outcome in the study of the effect of compression force on release behavior was the apparent increase in brittleness of the implants. Increasing compression force resulted in formation of easily friable implants, particularly in case of C_{10}-C_{14} diglycerides with high lysozomal loading, (Figure 3.2.).

To better understand the underlying mass transport mechanism controlling lysozyme release from diglyceride implants, an analytical solution of Fick's second law of diffusion was fitted to the experimentally determined lysozyme release kinetic. Based on these calculations, the apparent diffusion coefficient of lysozyme released from diglyceride implants could be determined (Figure 3.5.). The gradual increase in diffusion coefficient allows us to assume that the buffer penetrates the implant through the submicron spaces between the lipid plates and drug release occurs via diffusion through these buffer filled channels. Thus the structure of this submicron void network determines the release pattern.

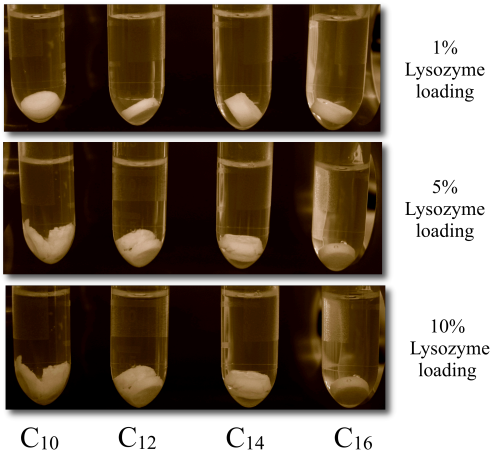

Figure 3.2. Increasing compression force results in friable implants, particularly in case of C_{10}-C_{14} diglycerides with high lysozomal loading.

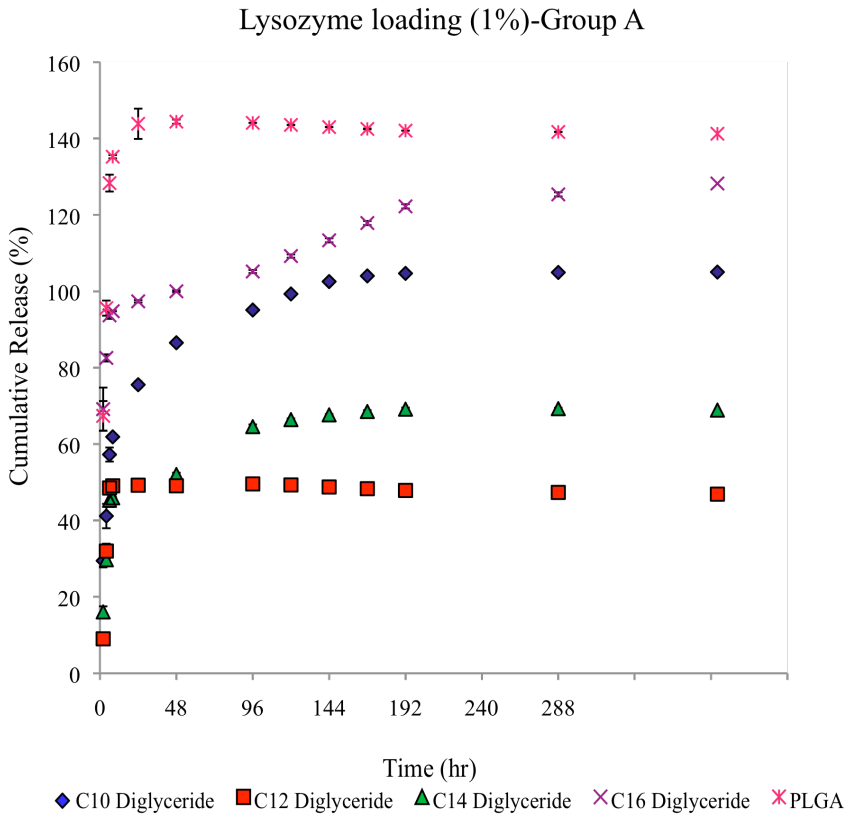

Figure 3.3(a). Lysozyme release behavior from lipid implants prepared with lower compression force with 1% lysozyme loading. Shorter chain diglycerides show faster release compared to more hydrophobic diglycerides. Increasing the drug loading also causes an increase in over release rate and shows immediate burst effect.

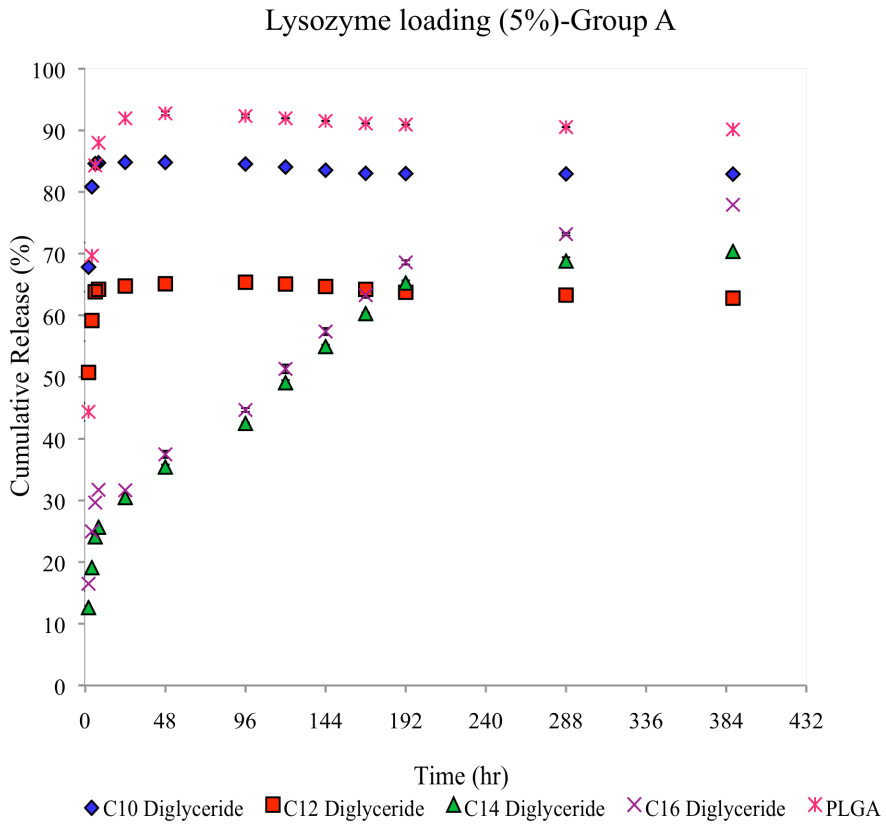

Figure 3.3(b). Lysozyme release behavior from lipid implants prepared with lower compression force with 5% lysozyme loading Shorter chain diglycerides show faster release compared to more hydrophobic diglycerides. Increasing the drug loading also causes an increase in over release rate and shows immediate burst effect.

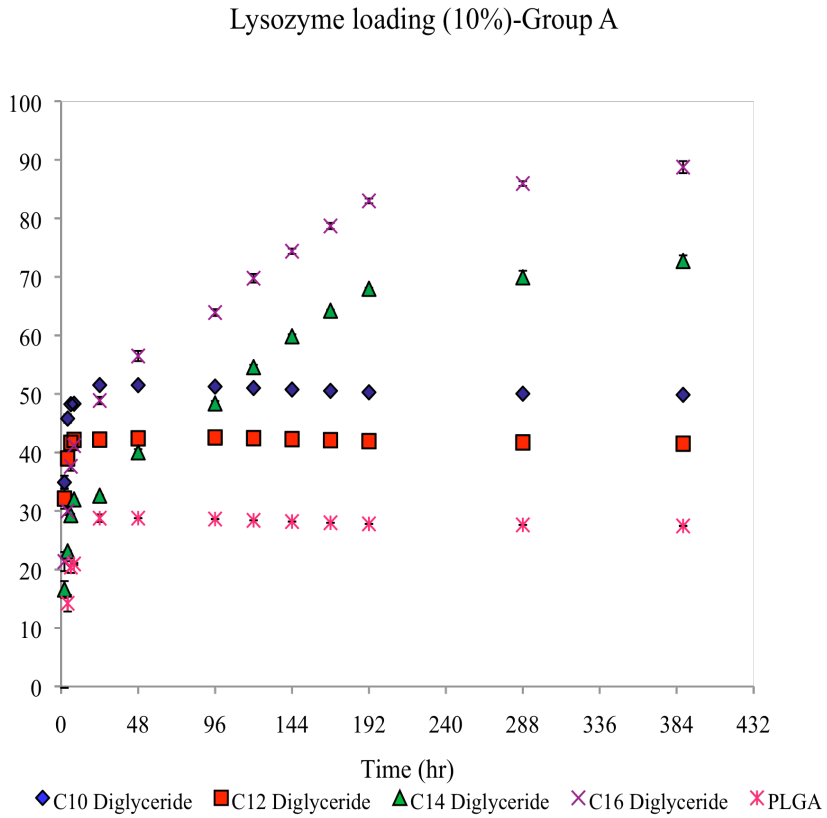

Figure 3.3(c). Lysozyme release behavior from lipid implants prepared with lower compression force with 10% lysozyme loading Shorter chain diglycerides show faster release compared to more hydrophobic diglycerides. Increasing the drug loading also causes an increase in over release rate and shows immediate burst effect.

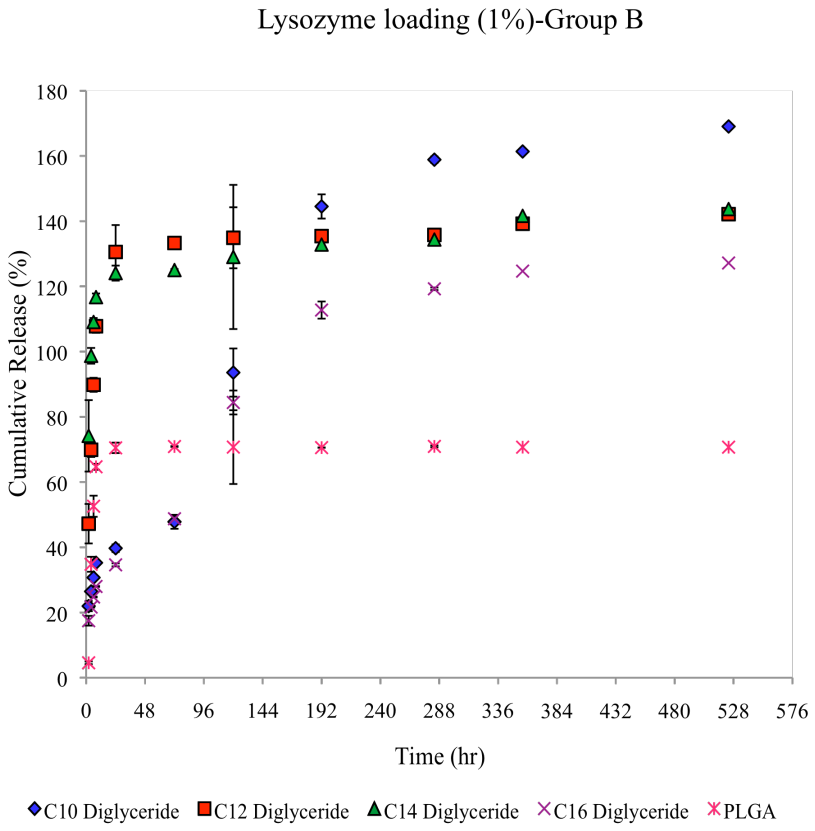

Figure 3.4(a). Lysozyme release behavior from lipid implants prepared with higher compression force with 1% lysozyme loading. Similar to group A, shorter chain diglycerides show faster release compared to more hydrophobic diglycerides, and increasing the drug loading also causes an increase in over release rate and shows immediate burst effect. Increasing the compaction force does not improve release behavior and burst effect appears to be more significant compared to group A.

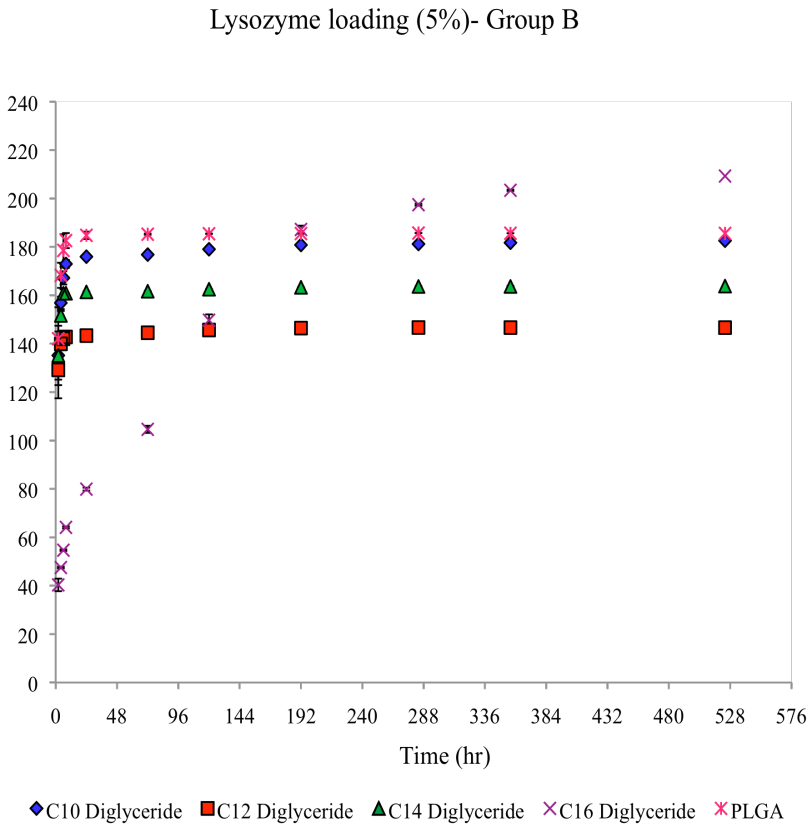

Figure 3.4(b). Lysozyme release behavior from lipid implants prepared with higher compression force with 5% lysozyme loading. Similar to group A, shorter chain diglycerides show faster release compared to more hydrophobic diglycerides, and increasing the drug loading also causes an increase in over release rate and shows immediate burst effect. Increasing the compaction force does not improve release behavior and burst effect appears to be more significant compared to group A.

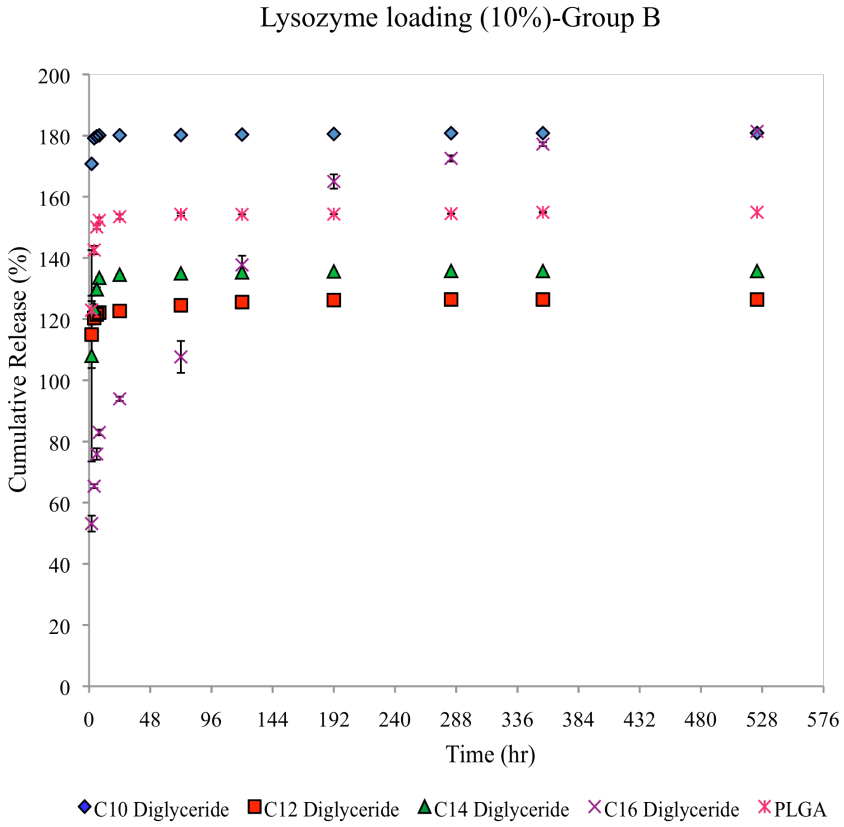

Figure 3.4(c). Lysozyme release behavior from lipid implants prepared with higher compression force with 10% lysozyme loading. Similar to group A, shorter chain diglycerides show faster release compared to more hydrophobic diglycerides, and increasing the drug loading also causes an increase in over release rate and shows immediate burst effect. Increasing the compaction force does not improve release behavior and burst effect appears to be more significant compared to group A.

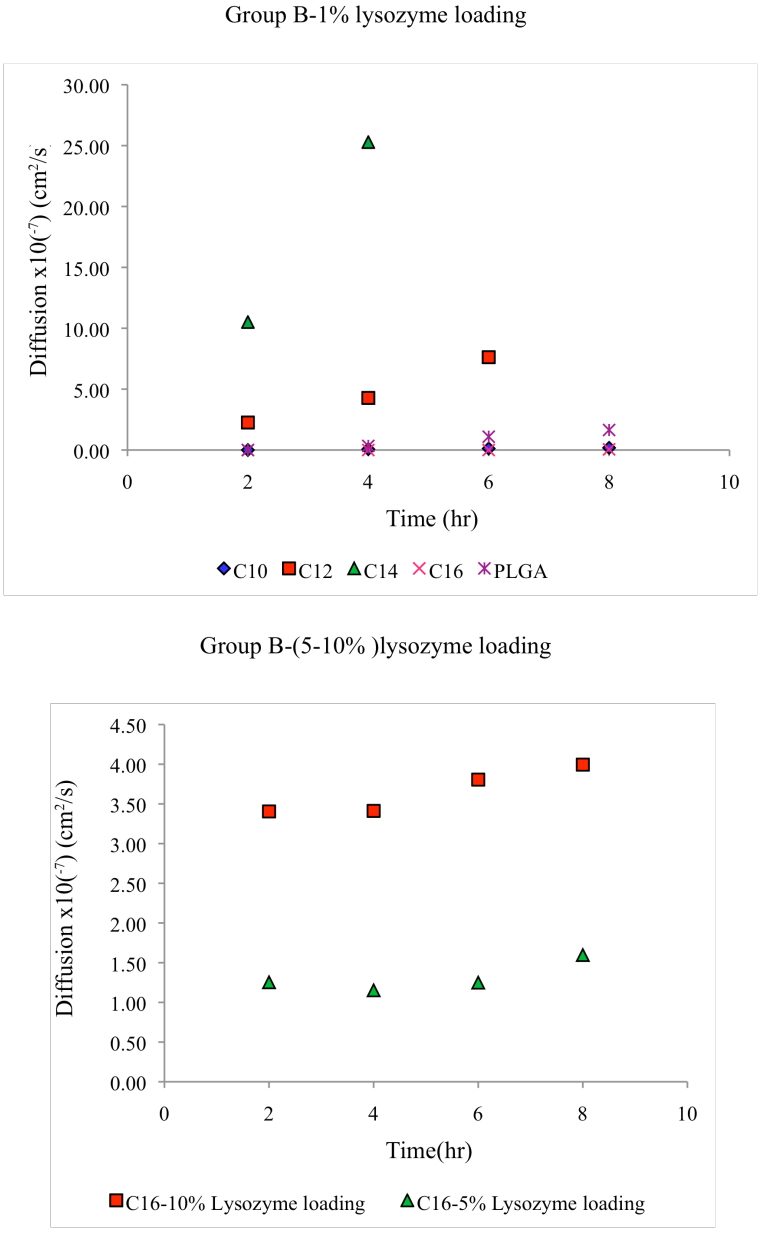

Figure 3.5. (Top) Apparent diffusion coefficient of lysozyme released from diglyceride implants. Burst release behavior from diglyceride implants C_{14} and C_{12} is noted with diffusion coefficients of order of 10^{-7} cm^2/s, C_{16} , C_{10} and PLGA show diffusion coefficient of order of 10^{-9} cm^2/s, (bottom) burst release behavior of C_{16} diglyceride implants with 5-10% lysozomal loading.

3.2.4. Influence of processing condition on protein stability

Released lysozyme from groups A and B were tested for structural integrity (Figures 3.5-3.6) and specific enzyme activity and compared with native lysozyme, (Figures 3.7-3.8)[17, 18, 20]. SDS-gel electrophoresis was used to test the stability of the protein structure, the resulting protein bands appeared alongside the control lysozyme band, suggesting that protein was not degraded or aggregated in the formulation step. The direct compression method seems to have small impact on the structural integrity of the lysozyme, (Figure 3.6-3.7). Enzymatic activity was tested using *M. lysodeikticus* suspensions in potassium phosphate buffer. Results indicated a decreased in enzymatic activity as time progresses possibly due to aggregation, especially with high lysozomal content (5-10%). Additionally, during compaction, the protein molecule is subjected to both pressure and shear (and possibly heat) that could result in reversible or irreversible denaturation. Interestingly, lysozyme released from C_{16} diglyceride implants showed higher enzymatic activity in comparison to other diglyceride, possibly due to lower wettability characteristics.

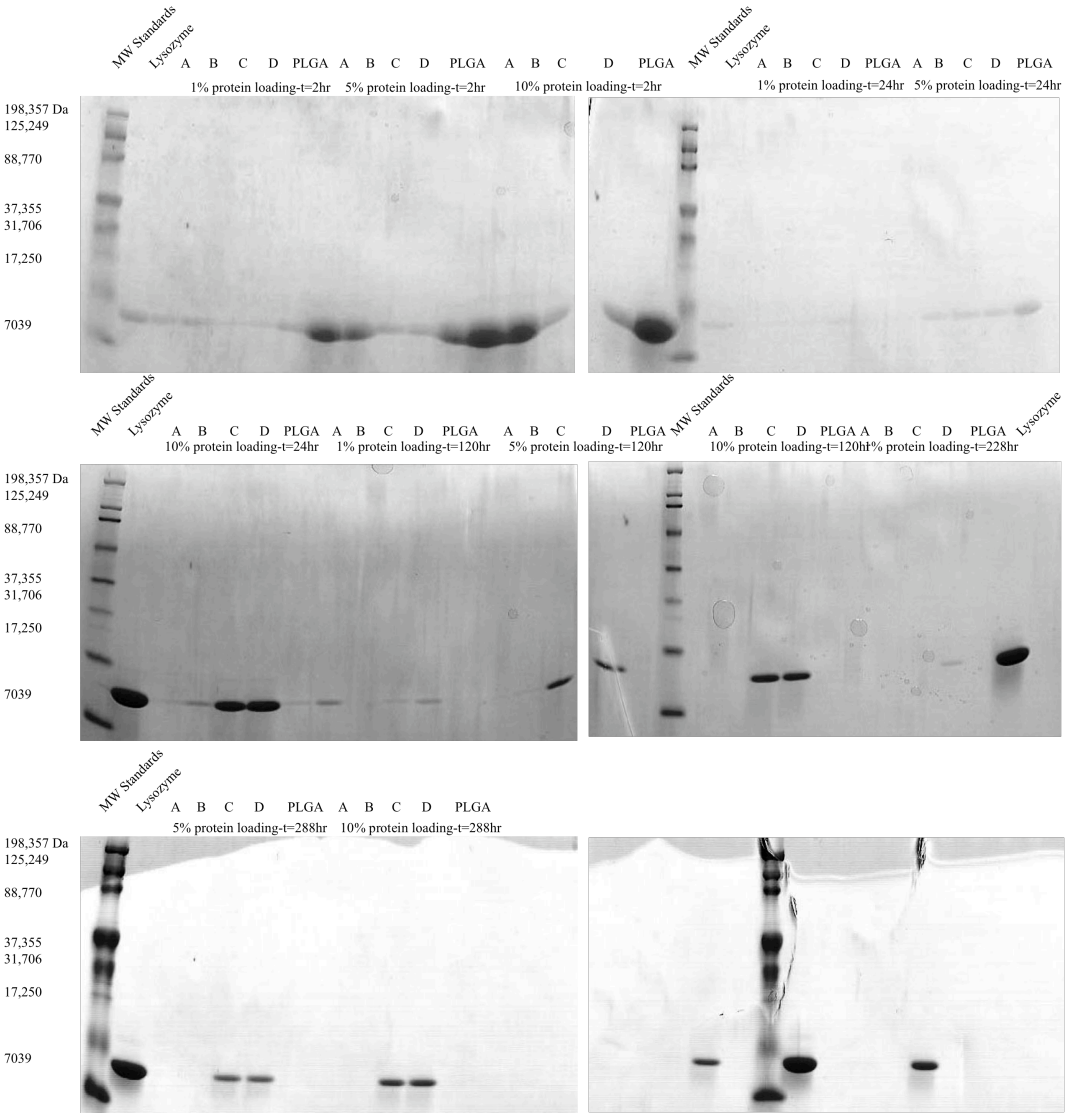

Figure 3.6. SDS-gel electrophoresis of protein present in release buffer, group A. Time points were 2hr, 24hr, 120hr and 228 hr after the start of the release experiments. Native lysozyme with molecular weight 14kDa was used as a control, (A) C_{10}, (B) C_{12}, (C) C_{14}, (D) C_{16} and PLGA bands are shown. The proteins showed minimal aggregation compared to the native, un-encapsulated lysozyme.

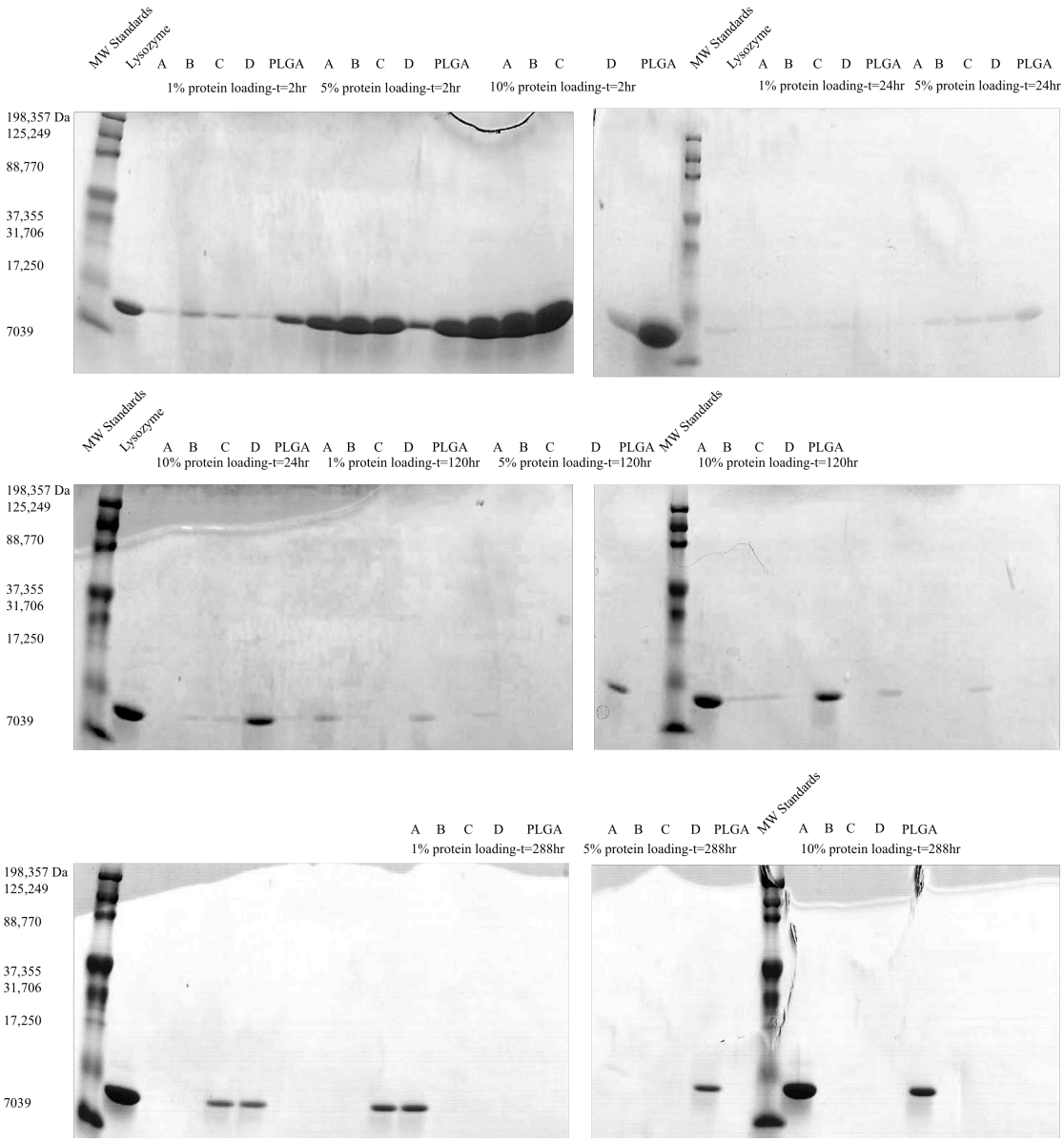

Figure 3.7. SDS-gel electrophoresis of protein present in release buffer, group B. Time points were 2hr, 24hr, 120 and 228 hrs after the start of the release experiments. Native lysozyme with molecular weight 14kDa was used as a control, (A) C_{10}, (B) C_{12}, (C) C_{14}, (D) C_{16} and PLGA bands are shown. Similar to group A, the proteins showed minimal aggregation compared to the native, un-encapsulated lysozyme.

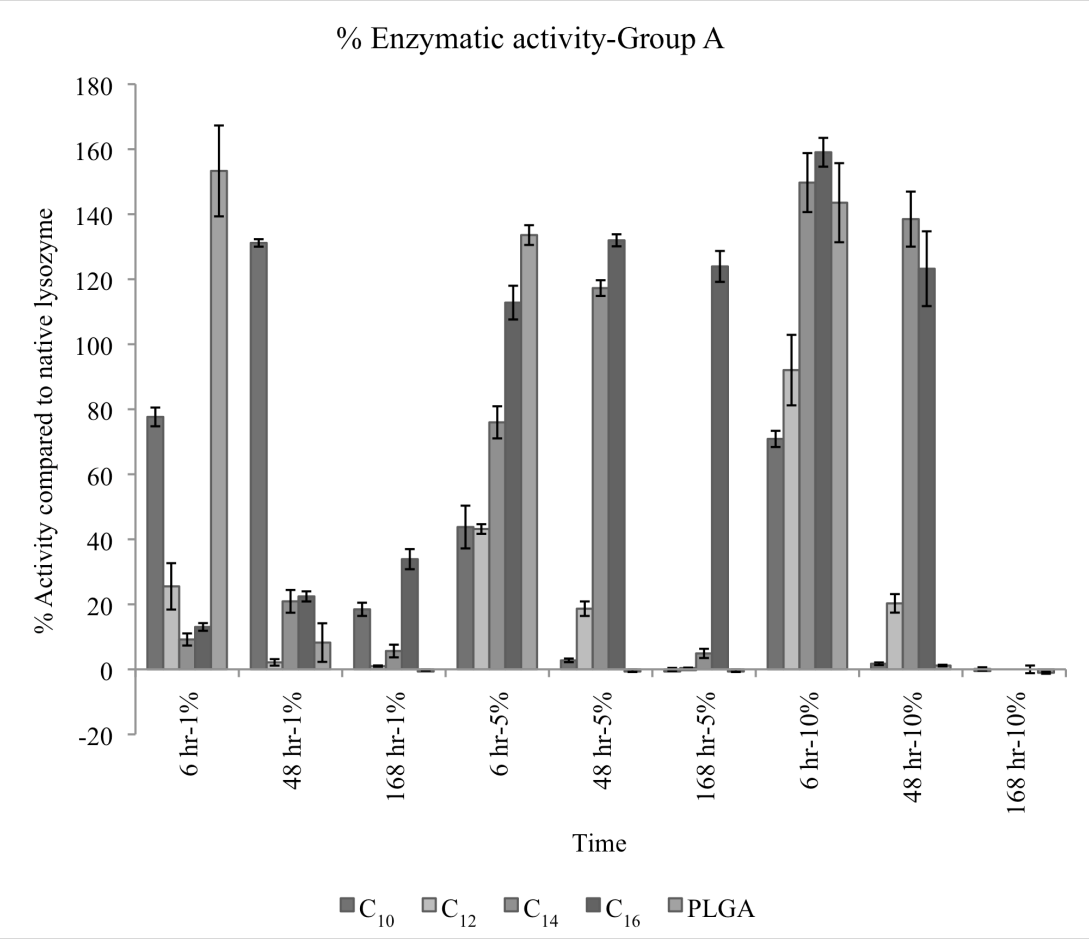

Figure 3.8. Enzymatic activity testing using *M. lysodeikticus* suspensions for group A revealed that the activity decreases with increasing time, possibly due to aggregation within lipid implants. Increasing lysozomal loadings seems to decrease the enzymatic activity of the proteins, possibly due to shear compaction forces and induced heat during processing.

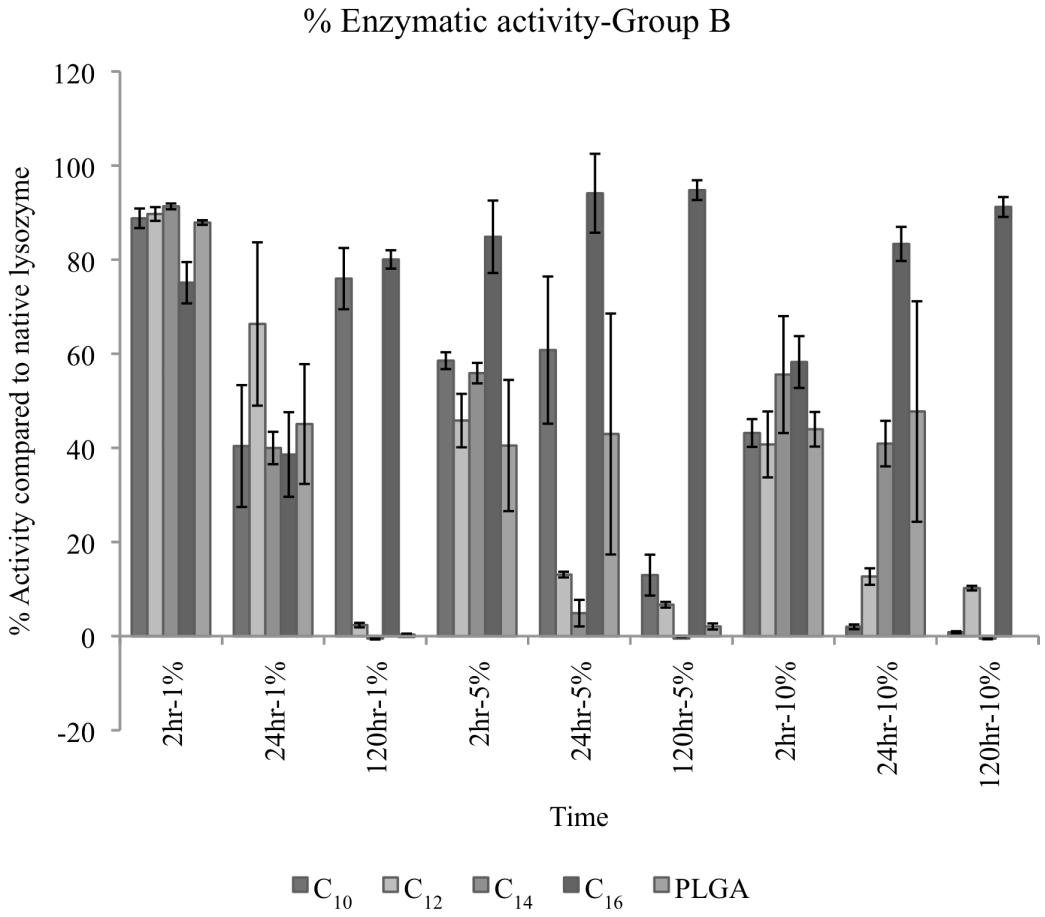

Figure 3.9. Enzymatic activity testing using *M. lysodeikticus* suspensions for group B also showed that the activity decreases with increasing time, possibly due to aggregation within lipid implants.

3.2.5. In vivo biocompatibility and in vivo erosion

In vivo biocompatibility of the diglyceride implants was evaluated in female Sprague-Dawley rats after subcutaneous administration. Figure 3.10 shows images of subcutaneous histology of poly(lactic-*co*-glycolic acid) implant that was prepared under the exact conditions and used as a positive control, in addition to the existing negative control. None of the animals died unexpectedly, exhibited abnormal behavioral changes, or experienced obvious weight loss, suggesting no gross toxicity from the surgical procedures or from the implants. An acute inflammatory type response was observed for the 2-day and 7-day time points, characterized by increased permeability of the capillaries and presence of foreign body giant cells (FBGC) and formation of granulomas. The 14-day and 28-day samples displayed minimal fibrosis and the presence of thin fibrous capsule. To understand the in vivo erosion behavior of these materials, changes in implant weight was recorded and plotted against lipid type and time, (Figure 3.10-3.11). Low wettability diglycerides such as C_{16} and C_{14} displayed less in vivo erosion compared to more hydrophilic C_{10} and C_{12}. The longer chain diglyceride were less water-soluble thus significant in vivo erosion was not observed until later time points in the study. Overall results of the study showed minimal fibrosis, no muscle damage, or necrosis, indicating the acceptable biocompatibility of the diglyceride delivery systems.

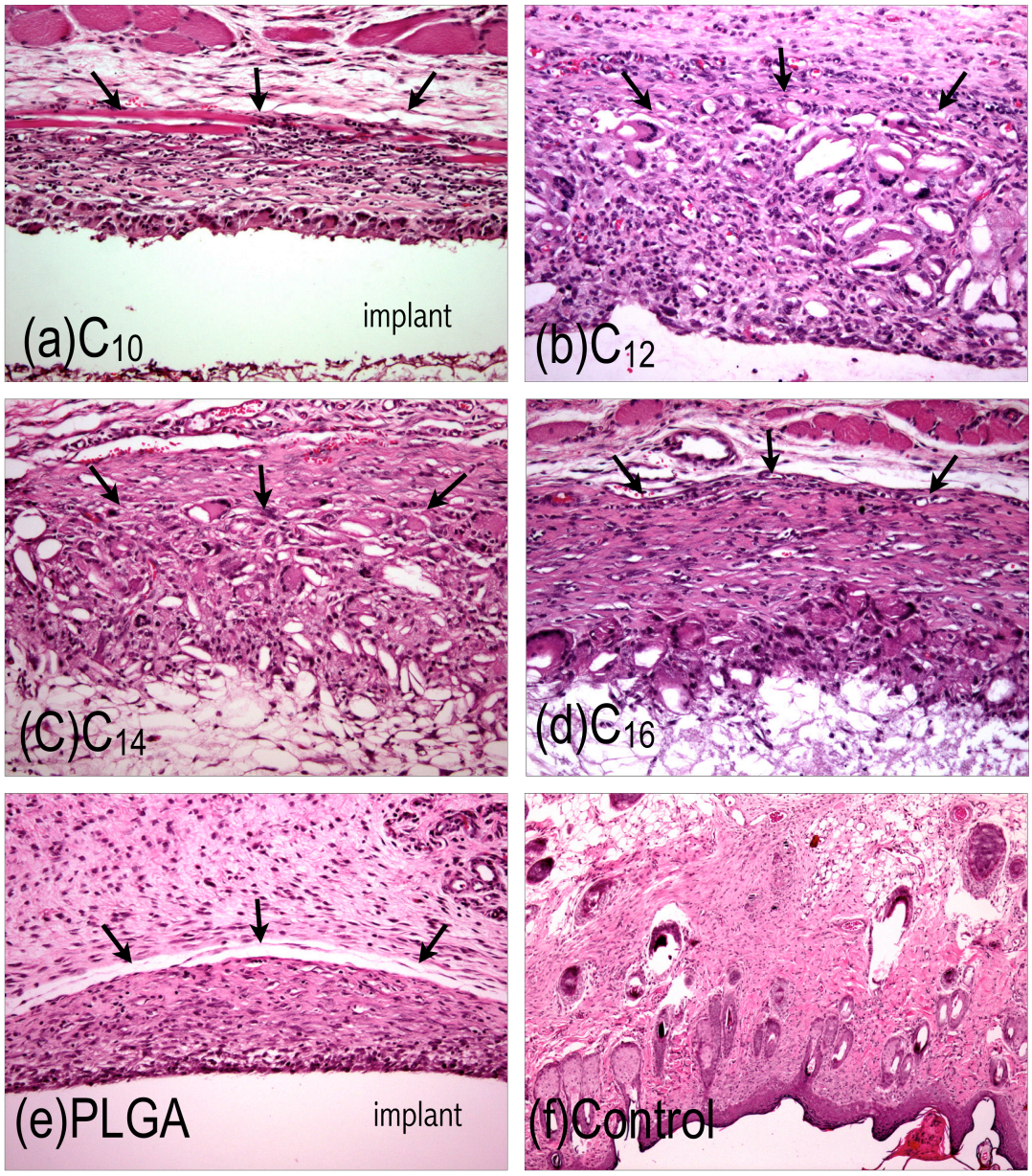

Figure 3.10. In vivo biocompatibility of the diglyceride implants showed increased permeability of the capillaries and presence of foreign body giant cells (FBGC) and formation of granulomas compared to PLGA control implant. Histology results of (a) PLGA, (b) C_{10} diglyceride, (c) C_{12} diglyceride, (d) C_{14} diglcyeride, (e) C_{16} diglyceride, after 14 days time point. . Arrows mark the tissue-implant interface.The magnification on this slide is 100X.

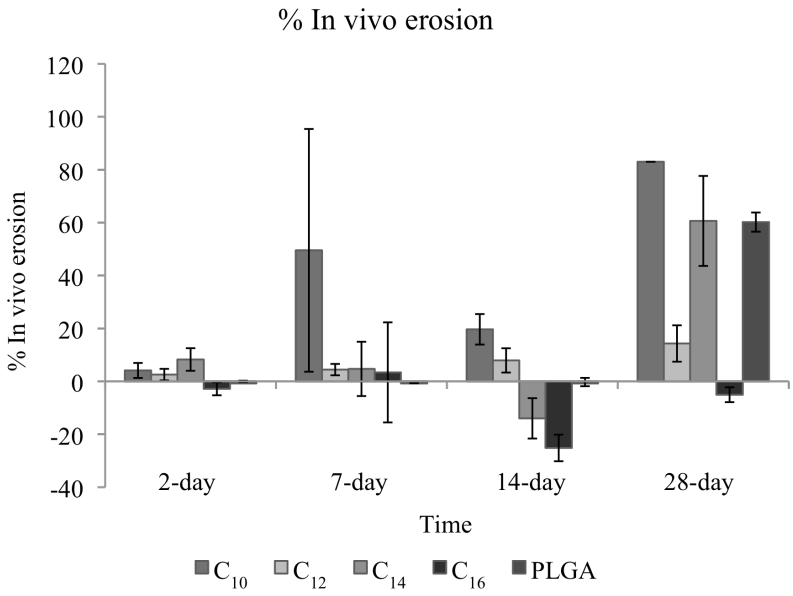

Figure 3.11. In vivo erosion of diglyceride implants with PLGA as control. Results showed that more hydrophobic lipids show slower in vivo erosion compared to more hydrophilic lipids, high in vivo erosion at 28 days time points is possibly due to formation of fibrous capsule around implants.

3.3. Conclusion

Wettability effects often play a crucial role in release of high molecular weight model compounds from lipidic matrices. Thus release behavior of proteins can be tailored by varying the lipophilicity of the matrix material via selectively varying the fatty acid chain length. The symmetrical diglycerides showed excellent properties for retaining physical and chemical characteristics of the model compound, however the burst effect in release behavior limits their use for prolonged drug release applications. The burst release, possibly due to less than desirable mechanical properties of diglyceride powders can be remedied through forming blends with other lipids such as cholesterol. The biocompatibility of diglycerides implants in rats showed acute inflammatory response however implants for earlier time points showed no sign of tissue necrosis or damage. Further work with the diglycerides will focus on achieving

a better understanding of their mechanical behavior and its effect on the release of macromolecules.

REFERENCES

[1] K. Fu, D. W. Pack, A. M. Klibanov, and R. Langer 2000. Visual Evidence of Acidic Environment Within Degrading Poly (lactic-co-glycolic acid)(PLGA). Pharmaceutical Research. 17, 1, 100-106.

[2] M. Iwata, T. Tanaka, Y. Nakamura, and J. W. McGinity 1998. Selection of solvent system for the the preparation of poly (D, L-lactic-co-glycolic acid) microspheres containing tumor necrosis factor alpha (TNF-alpha). International Journal of Pharmaceutics. 160, 145-156.

[3] F. Kang, G. Jiang, A. Hinderliter, P. P. DeLuca, and J. Singh 2002. Lysozyme stability in primary emulsion for PLGA microsphere preparation: effect of recovery methods and stabilizing excipients. Pharmaceutical Research. 19, 5, 629-633.

[4] R. Krishnamurthy, J. A. Lumpkin, and R. Sridhar 2000. Inactivation of lysozyme by sonication under conditions relevant to microencapsulation. International Journal of Pharmaceutics. 205, 23-34.

[5] M. van de Weert, W. E. Hennink, and W. Jiskoot 2000. Protein instability in poly (lactic-co-glycolic acid) microparticles. Pharmaceutical Research. 17, 10, 1159-1167.

[6] M. van de Weert, J. Hoechstetter, and W. E. Hennink 2000. The effect of a water/organic solvent interface on the structural stability of lysozyme. Journal of Controlled Release. 68, 351-359.

[7] W. Wang 2005. Protein aggregation and its inhibition in biopharmaceutics. International Journal of Pharmaceutics. 289, 1-30.

[8] N. Faisant, P. Menei, J. P. Benoit, and A. Goepferich 2006. In vitro investigation of lipid implants as a controlled release system for interleukin-18. International Journal of Pharmaceutics. 314, 145-152.

[9] S. Herrmann, G. Winter, S. Mohl, and F. Siepmann 2007. Mechanisms controlling protein release from lipidic implants: Effects of PEG addition. Journal of Controlled Release. 118, 161-168.

[10] Koennings, A. Sapin, T. Blunk, P. Menei, and A. Goepferich 2007. Towards controlled release of BDNF—Manufacturing strategies for protein-loaded lipid implants and biocompatibility evaluation in the brain. Journal of Controlled Release. 119, 163-172.

[11] S. Mohl and G. Winter 2004. Continuous release of rh-interferon α-2a from triglyceride matrices. Journal of Controlled Release. 97, 67-78.

[12] H. Reithmeier, J. Herrmann, and A. Göpferich 2001. Development and characterization of lipid microparticles as a drug carrier for somatostatin. International Journal of Pharmaceutics. 218, 133-143.

[13] W. Vogelhuber, E. Magni, A. Gazzaniga, and A. Goepferich 2003. Monolithic glyceryl trimyristate matrices for parenteral drug release applications. European Journal of Pharmaceutics and Biopharmaceutics. 55, 133-138.

[14] W. Vogelhuber, E. Magni, M. Mouro, T. Spruss, and C. Guse 2003. Monolithic triglyceride matrices: a controlled-release system for proteins. Pharmaceutical development and technology. 8, 1, 71-79.

[15] P. H. Bentley and W. McCrae 1970. Synthesis of symmetrical 1, 3-diglycerides. The Journal of Organic Chemistry. 35, 6, 2082-2083.

[16] R. A. Siegel, J. Kost, and R. Langer 1989. Mechanistic studies of macromolecular drug release from macroporous polymers. I: Experiments and preliminary theory concerning the completeness of drug release. Journal of Controlled Release. 8, 223-236.

[17] Y. C. Lee and D. Yang 2002. Determination of lysozyme activities in a microplate format. Analytical Biochemistry. 310, 223-224.

[18] D. Shugar 1952. The measurement of lysozyme activity and the ultra-violet inactivation of lysozyme. Biochimica et biophysica acta. 8, 3, 302-309.

[19] C. Guse, S. Koennings, F. Kreye, and F. Siepmann 2006. Drug release from lipid-based implants: elucidation of the underlying mass transport mechanisms. International Journal of Pharmaceutics. 314, 137-144.

[20] S. Koennings, A. Berié, J. Tessmar, and T. Blunk 2007. Influence of wettability and surface activity on release behavior of hydrophilic substances from lipid matrices. Journal of Controlled Release. 119, 173-181.

[21] W. D. Rhine, D. S. T. Hsieh, and R. Langer 1980. Polymers for sustained macromolecule release: procedures to fabricate reproducible delivery systems and controlled release kinetics. Journal of Pharmaceutical Sciences. 69, 265-270.

CHAPTER 4

FUTURE DIRECTIONS

4. Introduction

A considerable amount of research has been carried out in the past few years in order to obtain novel biomaterials with improved specific properties for controlled drug delivery. Lipids and in particular triglycerides, have gained growing attention in this context due to their desirable properties: as physiological substances they have displayed good biocompatibility subcutaneously, and in brain; they are easily compactable and display long term stability during storage, thus marking this group of materials as strong alternatives to polymeric matrices[1-4]. Diglycerides in return have received attention as matrix blends and participants in binary matrices, therefore a through study of their potential as single component monolithic matrices remains to be done[5, 6].

We investigated the potential of symmetrical 1,3-lipids and their glyceride analogs as matrices for controlled drug delivery applications. We synthesized a family of DHA derived symmetrical lipids with varying hydrocarbon chain lengths to systematically analyze how lipid chain length influences device fabrication, its morphology, and the resulting drug release kinetics. Our study showed that wettability effects often play a crucial role in the release of high molecular weight model compounds from lipidic matrices. Thus release behavior of proteins from lipid matrices, can be tailored by varying the lipophilicity of the matrix material via selectively varying the fatty acid chain length. The symmetrical diglycerides showed excellent properties for retaining physical and chemical characteristics of the model compound, however the burst effect in release behavior may limit their use for

prolonged drug release applications. The burst effect is possibly due to structural integrity of the implants, thus the future work of this study would benefit from focusing on mechanical characterization of diglycerides for compaction and tabletting to improve release behavior, in addition to quantitative measurements of pore size and distribution within the matrix.

4.1. Mechanical characterization of diglyceride powders

Successful compaction and tabletting of powders requires a full understanding of fundamental mechanical properties of powders, which dictates how formulations will behave during compaction. During the tabletting process, powders go through initial packing and rearrangement of particles, formation of temporary structures, elastic deformation, plastic deformation followed by breakage of particles, bond formation and consequently elastic recovery during the decompression process[7]. The deformation characteristics may be elastic, plastic, brittle fracture or a combination of these mechanisms. The factors that determine the deformation behavior also include Young's modulus, yield stress, and fracture toughness. However, deformation behavior of powder is predominantly a function of applied stress. Thus a study of stress-strain behavior of tablets can provide more information on a powder's response to mechanical stress.

4.2. Porosity measurements as a function of compression force

Porosity is a measure of void spaces in a material and can be evaluated using a variety of techniques such as density, gas adsorption, water displacement and porosimetry[8, 9]. Quantitative measurements of pore size and distribution can provide invaluable insight into disintegration, dissolution, adsorption and diffusion of drugs. The gas adsorption method is limited to pore diameters less than 2000 ^{o}A, thus mercury porosimetry, is the most suitable method for measuring the pore size. This

method is based on intrusion of mercury into the pores of a solid sample and it is explained using the Washburn equation:

$$\mathrm{Pr} = -2\gamma \cos\theta \qquad (1)$$

where P the pressure (psia), r is the pore radius (μm), γ is the surface tension of the mercury (dynes·cm^{-1}), and θ denotes the contact angle of the mercury. Mercury penetration under pressure, determines the size and quantity of the void spaces and pores. Additionally, decreasing pressure causes mercury to expel from the pores when therefore providing information on pore shape and structure [8, 9].

4.3. Summary

The mechanical characterization of these biomaterials would provide invaluable information regarding the intrinsic physical properties of symmetrical 1,3-diglycerides. The initial demonstration of release behavior of model drugs from these biomaterials combined with the additional insight into their behavior provides the ground for exploring further scientific opportunities in controlled release.

REFERENCES

[1] C. Guse, S. Koennings, F. Kreye, and F. Siepmann 2006. Drug release from lipid-based implants: elucidation of the underlying mass transport mechanisms. International Journal of Pharmaceutics. 314, 137-144.

[2] Koennings, A. Sapin, T. Blunk, P. Menei, and A. Goepferich 2007. Towards controlled release of BDNF—Manufacturing strategies for protein-loaded lipid implants and biocompatibility evaluation in the brain. Journal of Controlled Release. 119, 163-172.

[3] W. Vogelhuber, E. Magni, A. Gazzaniga, and A. Goepferich 2003. Monolithic glyceryl trimyristate matrices for parenteral drug release applications. European Journal of Pharmaceutics and Biopharmaceutics. 55, 133-138.

[4] W. Vogelhuber, E. Magni, M. Mouro, T. Spruss, and C. Guse 2003. Monolithic triglyceride matrices: a controlled-release system for proteins. Pharmaceutical development and technology. 8, 1, 71-79.

[5] Y. Yamagata, K. Iga, and Y. Ogawa 2000. Novel sustained-release dosage forms of proteins using polyglycerol esters of fatty acids. Journal of Controlled Release. 63, 3, 319-329.

[6] Y. Yamagata, Y. Yuasa, K. Yamamoto, and K. Okamoto 2000. Pharmacologic Effect of Recombinant Human IFN-alpha, Continuously Released from a Matrix Prepared from a Polyglycerol Ester of Fatty Acids, on 2',5'-Oligoadenylate Synthetase Activity in Murine Liver. Journal of Interferon & Cytokine Research. 20, 153-160.

[7] M. J. Adams and R. McKeown 1996. Micromechanical analyses of the pressure-volume relationships for powders under confined uniaxial compression. Powder Technology. 88, 155-163.

[8] S. Jain 1999. Mechanical properties of powders for compaction and tableting: an overview. Pharmaceutical Science & Technology Today. 2, 1, 20-31.

[9] K. A. Mehta, M. S. Kislalioglu, and W. Phuapradit 2000. Effect of formulation and process variables on porosity parameters and release rates from a multi unit erosion matrix of a poorly soluble drug. Journal of Controlled Release. 63, 201-211.

APPENDIX A

SOLID LIPID MICROPARTICLES' CHARACTERIZATIONS

A. Introduction

A.1. Controlled release drug delivery-Polymeric systems

The goal of controlled drug delivery is to develop a system that delivers drugs in a predictable and effective manner [1-4]. Various synthetic and natural materials such as polymers, cyclodextrins, and lipids have been investigated (i.e. poly(lactic acid-*co*-glycolic acid), polyanhdyrides, collagen, polysaccharides). In recent years the focus of drug delivery has shifted toward lipid based formulations despite the ubiquitous presence of polymers in this field [5-31]. Polymers present specific obstacles for pharmaceutical development. A manufactured drug needs to be homogenous and consist of one species. In contrast polymers by nature are heterogeneous, thus as macromolecules they present specific characterization challenges. The average molecular weight of a polymer is described as 'weight average molecular weight' (M_w), and 'number average molecular weight' (M_n). The ratio of these two parameters (M_w/M_n) gives a measure of polydispersity (PDI), meaning that a particular polymer sample may contain individual molecules of various chain lengths resulting in less than optimal conditions. The presence of a distribution of molecular weights directly impacts the kinetics of drug delivery and introduces variability amongst batches [5].

A.2. Lipid-based drug delivery systems

Lipids circumvent the difficulties associated with achieving a narrow polydispersity when it comes to chemical synthesis, inadvertently reducing the batch to batch variability. Previous results highlighting lipids as excipients or prodrugs set

the stage for further investigation of lipid-derived systems [13-16, 26-31]. Our aim for this project is to design a lipid-derived drug delivery vehicle for which the rate of release of the drug correlates with the level of hydrophobicity of the vehicle. In doing so, our goal is twofold. First to synthesize biomolecules with varying degrees of hydrophobicity with dihydroxyacetone (DHA) as a starting material, second to take advantage of the physical nature (i.e. solid, liquid) of these biomolecules for various controlled release drug devices (i.e. microparticles, implants, injectable depots).

Here we report the synthesis of a series of bioinspired symmetrical lipids, comprised of two classes of biomolecules, fatty acids and dihydroxyacetone (DHA). DHA a constituent, of the glycolysis pathway, and is FDA approved for oral and topical administration, making it an attractive building block for new biomaterials [34-37]. The particular advantage of using DHA as a lipid building block for this study is that the strong dipole moment of the DHA carbonyl maintains the lipids in the solid state while the lipids lengths are varied. In fact the further synthesized symmetrical glycerol analogues of the lipids are in liquid form. The solid state of the DHA lipids allows their use as microparticles or implants, and the liquid state of the glycerol analogs makes room for use as injectable formulations.

A.3. Applications of solid lipids

Microparticulates are used in the pharmaceutical field as injectable systems to control the spatial and temporal release of drugs [3-4,10-11]. Historically, materials that comprise the microparticle matrix are composed of synthetic polymers such as poly(lactic-*co*-glycolic acid), and the polyanhydrides, or natural polymers such as collagen, gelatin and chitosan. These materials have been successfully marketed in devices for controlled drug release systems. Recently, solid lipids have emerged as a new class of material that may be suitable for microparticle-based controlled drug

delivery [13-20]. A number of solid lipids are reported, such as fatty acids and alcohols, as well as the mono-, di- and tri-esters of glycerol [17, 26]. These reports support the potential use of solid lipids for the delivery of hydrophobic and hydrophilic small molecules, as well as the controlled release of peptides and proteins. Although the solid lipid matrix literature is fairly extensive, there has yet to be a systematic investigation of how the lipid matrix can be engineered at the molecular level to modulate the functional characteristics of the microparticle. Specifically, there is little understanding of how lipid structure, particularly lipid length, influences microparticle fabrication, microparticle morphology, and drug release kinetics.

Few studies exist on the use of saturated diglycerides alone as drug delivery vehicles. Lipid based delivery systems range from simple oil solutions to complex mixtures of oil, surfactants, cosurfactants and cosolvents, also described as microemulsions. However most of the studies have focused on the use of triglycerides or lipids with complex phase behavior [23, 26]. Earlier results obtained have shown that bioavailability of poorly water soluble drug is significantly enhanced when administered with food rich in fat. Diglyceride prodrugs of ibuprofen and an HIV protease inhibitor have also been reported [27-28]. Diglycerides are overlooked as liquid hydrophobic matrices for controlled drug delivery in lipidic systems, noting their dissolution abilities encompass a wide range of hydrophobic and highly hydrophobic drugs.

This study describes the synthesis and characterization of symmetrical lipids and their glyceride analogs with incrementally increasing aliphatic lipid tails, their application as drug delivery vehicles, and the investigation of how the hydrophobicity influences controlled release kinetics of a model drug compound. The first part of this report describes the experimental design and results associated with solid lipid

microparticles; the second part illustrates the experimental approach toward synthesis and characterization of liquid hydrophobic matrices derived from solid lipids.

B. Solid lipid microparticles for controlled drug delivery

B.1. Materials and methods

Hexadecanoyl chloride, tetradecanoyl chloride, dodecanoyl chloride, decanoyl chloride, ocatanoyl chloride, 1,3-Dihydroxyacetone dimer 97% (DHA), chloroform, anhydrous pyridine and nile red were all obtained from Sigma-Aldrich (Saint Louis, MO) and used without further purification. Poly(vinyl alcohol) (PVA, M_W~25,000, 88 mole% hydrolyzed) was purchased from Polysciences Inc. Dichloromethane (DCM), acetone, tetrahydrofuran (THF) and diethyl ether were purchased from J.T.Baker (West Chester, PA). All reagents and solvents were used as received without additional purification.

B.2. Lipid synthesis

1,3-dihydroxypropan-2-one 1,3-dialkylate

Symmetrical lipids were synthesized through modification of a previously reported method by Bentley and McCrae [39]. The general procedure is as follows, using the synthesis of C_{16} symmetrical lipid as an example: DHA (3.5 g, 39 mmole) was stirred in anhydrous chloroform (150 mL) under flow of N_2 at room temperature, followed by sequential dropwise (1drop/sec) addition of hexadecanoyl chloride (22.1 mL, 80 mmol) and anhydrous pyridine (7.5 mL), in that order. The mixture was stirred for 3 hrs at room, and its color varies from clear to slightly yellow due to dihydroxyacetone degradation. The reaction was extracted with deionized water (2 × 75 mL), the organic layers from each wash were combined and the combined aqueous layers were washed with chloroform (1 × 75 mL). All chloroform layers were combined before removal by rotoevaporation in vacuo to a thick white/yellow residue. The residue was dissolved in dichloromethane:ether (1:1), in the lowest volume

needed, and placed in the freezer to crystallize overnight. Melting points were collected on a Fisher-Johns melting point apparatus. ^{1}H-NMR spectra were recorded at room temperature with a Brucker AF-300 spectrometer operating at 300.13 MHz, and elemental analyses were obtained through QTI (Whitehouse, NJ).

B.3. Fabrication of solid lipid microparticles (SLM) by the spontaneous emulsification

Each lipid (0.1 gm) was dissolved in a 3:2 (v:v) ratio of DCM:acetone by vigorous vortex for approximately 10 seconds. The lipid solution was transferred using a glass pipet into a stirring PVA solution as a slow and steady stream (450 mL, 2.5%). The suspension was stirred for 3 hrs to allow evaporation of the organic solvents and hardening of the microparticles. Microparticles were isolated by centrifugation at 4,800 RCF for 60 minutes followed by multiple washes (3×) with deionized water and re-centrifugation at 4,800 RCF for 45 minutes. The particles were resuspended in small volumes of deionized water and lyophilized for a minimum of 12 hrs and were stored at -20 °C in the presence of desiccant. The final products were fine powder particles with approximate yield of 75% (relative to original weight of lipid).

B.4. Particle characterization

The solid lipid microparticles were analyzed by two different methods to determine their geometric and aerodynamic size distributions. All measurements assume spherical geometry. The size distributions of each sample were collected until there were no changes in the overall shape of the distribution curve. For each method, the total number of counted particles was >10,000. Geometric sizes of lipid particles in powder form were determined in isotonic diluent (Isoton II) by a Coulter Multisizer III (Beckman Coulter Inc.) equipped with a 100 μm aperture. About 5 mg of a given powder sample was added to 20 mL of Isoton II and each suspension was shaken for

one minute to deagglomerate the particles. Any bubbles were allowed to dissipate prior to measurement. Aerodynamic size distributions of the particles were determined directly from powder samples via time-of-flight measurements using an Aerosizer LD (Amherst Instruments) with a 700 μm aperture assuming a material density of 1 g/cm^3. About 5 mg of sample was introduced to the apparatus, and subject to a pneumatic shear force of 2 PSI. All cavities in the apparatus were cleaned with compressed air after each run so that the overall count within a minute of empty performance was reduced to <100.

Particle morphology was studied at low voltage (5 kV) using scanning electron microscopy imaging (LEICA 440) after coating with palladium. Surface charge on samples suspended in 1:10 diluted PBS were measured using a Malvern Zetasizer-Nano ZS (Malvern, UK). A PRECO Hydraulic press (Los Angles, CA) was used to make lipid pellets with approximate surface area of 25 mm^2. For contact angle measurements, a ramé-hart contact angle goniometer (100-FO) was used to measure the sessile contact angle of water on a lipid pellet surface. Unless otherwise stated, measurements were conducted in triplicate.

B.5. In vitro drug release and model drug distribution

The encapsulation efficiency of lipid microparticles was determined via complete drug recovery from dissolved microparticles, followed by comparison with the theoretical maximum drug loading. Microspheres (5 mg) were dissolved in acetonitirile:THF (1 mL) and nile red concentration measured by UV absorbance at λ=535 nm using a microplate spectrofluorometer (Spectramax GeminiEM; Molecular Devices, Sunnyvale, CA). In vitro release kinetics were determined by suspending 5.0 mg of microspheres in 1- mL of PBS in amber microcentrifuge tubes (Eppendorf) and incubating at 37 °C under gentle rotation. The supernatant was collected in total for fluorescence measurement after certain time intervals to

determine the amount of release, and replenished with fresh buffer. Nile red concentration was measured at λ_{Ex}= 550 nm and λ_{Em}=650 nm quantified according to a standard curve. Distribution profiles of nile red within lipid microparticles were obtained by laser confocal microscopy (Leica TCS SP2) with a helium-neon laser excitation source (543 nm). Samples were placed on microscope slides and sealed with cover slips. Fluorescence intensity profiles were determined with image analysis software (Image J).

B.6. Nomenclature

IUPAC nomenclature for the symmetrical lipids is of the form, using the octanoic acid lipid as an example, octanoic acid 3-octanoyloxy-2-oxo-propyl ester. To improve the readability of the text, each symmetrical is abbreviated C_x where "x" denotes the number of carbons in the corresponding fatty acid.

B.7. Statistical Analysis

The statistical significance of experimental results was determined using the two sample Students' t-test with significance set to samples with $p<0.05$. The calculated errors were set to standard mean error for all experimental results.

C. Results and Discussion

A series of symmetrical lipids were successfully synthesized by Schotten-Baumann acylation following the method of Bentley and McCrae with yields in excess of 70% [39] (Scheme C.1). The acyl chlorides were chosen such that the final product was derived from physiological lipids; for example palmitoyl chloride (IUPAC: hexadecanoyl chloride), derived from hexadecanoic acid, was selected to synthesize lipid C_{16}. In addition, all of the synthesized lipids have melting points that are above room and body temperature, making them good candidates for fabrication into solid

microparticles for controlled drug delivery. Elemental analysis obtained for C_8-C_{16} lipids are summarized in Table C.1.

Table C.1. Elemental analysis of symmetrical solid lipids

Sample name	Lipid	Melting point (°C)	E. analysis - theoretical		E. analysis - experimental	
			%C	%H	%C	%H
C_{16}	$C_{35}H_{66}O_5$	76-78	74.13	11.756	74.05	11.41
C_{14}	$C_{31}H_{58}O_5$	73-76	72.87	11.46	73.18	11.54
C_{12}	$C_{27}H_{50}O_5$	69-70	71.32	11.08	71.32	11.14
C_{10}	$C_{23}H_{42}O_5$	64-65	69.31	10.62	69.30	10.81
C_8	$C_{19}H_{34}O_5$	56-58	66.63	10.01	66.57	10.23

Figure C.1. ^{1}H NMR (300 MHz, $CDCl_3$, δ) of C_{12} solid lipid. Other lipids decidedly look exactly the same with the exception of the broad peak at 1.27 ppm. In increasing order of hydrophobicity the lipids peaks are: [C_8 lipid] 0.89 (t,6H), 1.27 (s,16H), 2.43 (t,4H), 4.76 (s,4H), [C_{10} lipid] 0.89 (t,6H), 1.27 (s,24H), 2.43 (t,4H), 4.76 (s,4H), [C_{12} lipid] 0.89 (t,6H), 1.27 (s,32H), 2.43 (t,4H), 4.76 (s,4H), [C_{14} lipid] 0.89 (t,6H), 1.27 (s,40H), 2.43 (t,4H), 4.76 (s,4H), [C_{16} lipid] 0.89 (t,6H), 1.27 (s,48H), 2.43 (t,4H), 4.76 (s,4H).

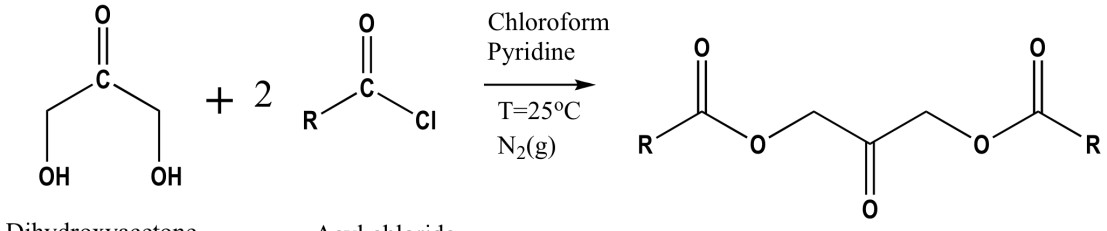

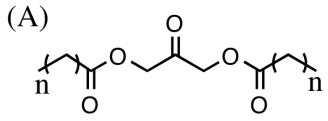

Scheme C.1. Reaction schematic for synthesis of lipids C_8 to C_{16}

The sessile contact angle of PBS buffer on each lipid surface was measured to establish the relative hydrophobicity differences among the lipids (Figure C.2a. left). The hydrophobic nature of each lipid is important for two reasons. First, lipids with insufficient hydrophobicity would be unable to form solid microparticles. Second, significant variability of the lipid hydrophobicity could be used to control the rate of drug release from the microparticles in the same way hydrophobicity is used to regulate drug release from polymer-based microparticles [40]. The contact angles show an increasing trend in hydrophobicity among the lipids, with the series straddling 90°, the angle at which surfaces transition from "hydrophilic" to "hydrophobic".

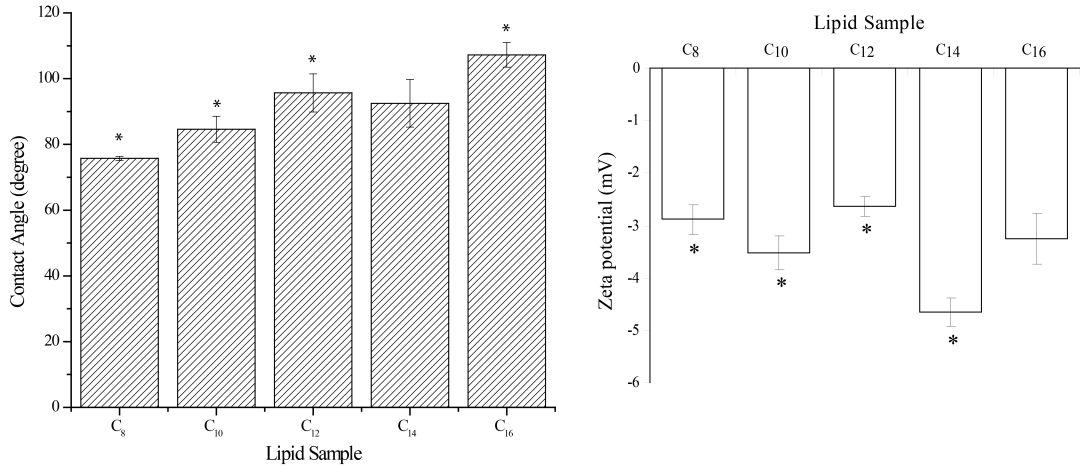

Figure C.2. Left, a) The sessile contact angle with PBS buffer (n=3,$p<0.05$, ±SEM). Columns marked by asterisk (*) are statistically significant compared to the subsequent more hydrophobic lipid (i.e.C_{10} compared to C_{12}). Right, b) Zeta potential of lipid microparticles in 1:10 dilutions of PBS:water, (n=3, $p<0.05$, ±SEM). All lipid particle surfaces retain a negative charge.

The particles are negatively charged as well, likely from hydrolyzed ester groups at the surface (Figure C.2b.). The negative charge is advantageous because very hydrophobic particulates are prone to aggregation, but Coulombic charge repulsion can facilitate singular particle dispersion with little input energy.

Both the mean hydrodynamic and mean aerodynamic particle sizes were measured. The effect of lipid concentration and surfactant concentration on the hydrodynamic particle size, with constant stirring rate and temperature, was determined by serial variation of both parameters. The results showed that increasing the lipid concentration led to an increase in mean diameter, and increasing the surfactant concentration decreases the mean diameter (Table C.2.). The aerodynamic diameters showed particle sizes varying from 8μm to 32μm with minimum calculated density of 0.08 to 0.79 g/cm^3, suggesting their potential application for pulmonary drug delivery since these densities lie within the desired range for favorable deep lung deposition [41].

Table C.2. Particle size measurement results using Coulter counter

Sample	Low Conc Lipid Soln 2.5 % PVA (μm)	High Conc Lipid Soln 2.5 % PVA (μm)	Low Conc Lipid Soln 5 % PVA (μm)	High Conc Lipid Soln 5 % PVA (μm)
C_8	39.6	41.2	28.8	37.8
C_{10}	32.3	35.6	22	33.6
C_{12}	29.7	36.6	27.3	28.4
C_{14}	26.2	29.7	29	17.6
C_{16}	25.3	24	21.7	26.1

Inspection of surface morphology by SEM supports the hydrodynamic and aerodynamic diameter data, revealing porous structures on the surface and throughout the matrix (Figure C.3.). Interestingly, particle porosity is a function of the lipid length, with the shorter lipids giving denser particles. Particles from both C_8 and C_{10} show a relatively smooth surface compared to C_{12} through C_{16}. Additionally, the surface structures become more prominent as the lipid chain length increases.

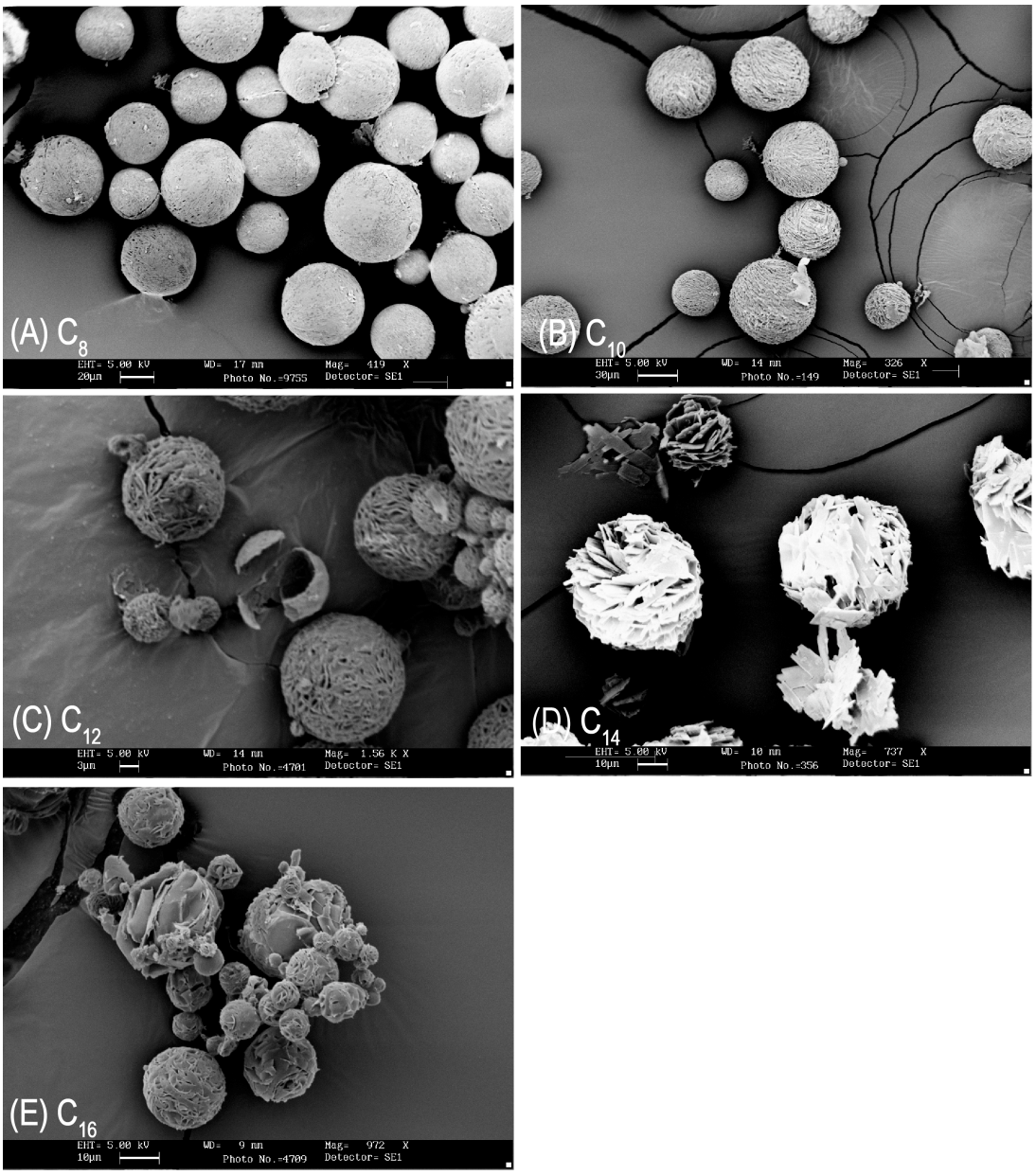

Figure C.3. Lipid microparticles morphology as a function of lipid chain length. Clockwise from top-left, (A) C_8 particle morphology showing a smooth surface followed by (B) C_{10}, (C) C_{12}, (D) C_{14}, and (E) C_{16}. Note the increasing porosity with increasing lipid chain length.

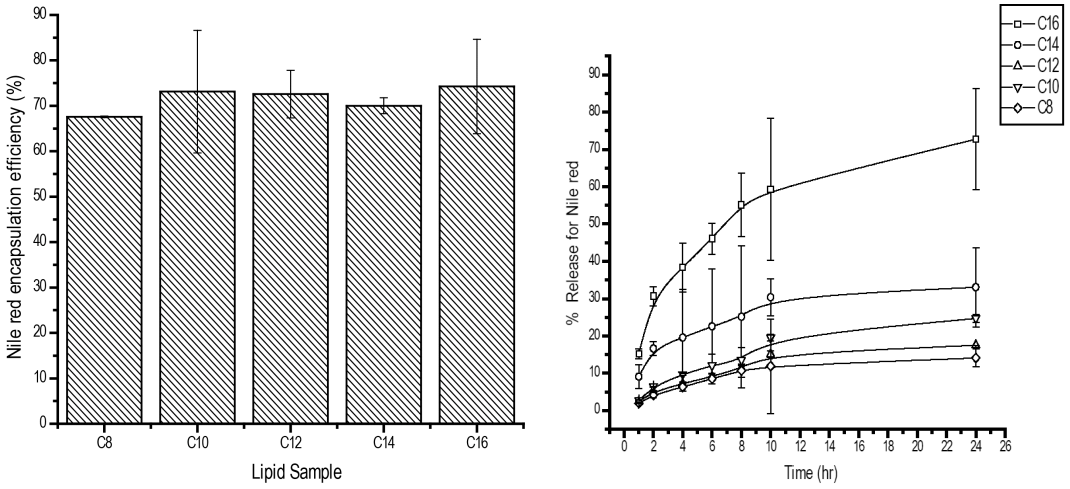

Figure C.4. Left, (a) Encapsulation efficiency measurements for particles containing nile red as hydrophobic model drug. Right, (b) Nile red release from lipid microparticles. All lipids display slow release for the duration of 24 hours (n=3, ±SEM). Release rates increase with increasing lipid chain length.

Microparticles containing nile red were successfully fabricated from all lipids in the series using the method of spontaneous emulsification. Encapsulation efficiencies exceeded 70% for all lipids (Figure C.4a.). The in vitro release characteristics of lipid microparticles encapsulating nile red, a model for hydrophobic drugs, was observed over a 24 hour period at 37 °C. The microparticles exhibited chain length-dependent release behavior, but in an unexpected manner with microparticles fabricated from longer chain lipid particles giving faster release kinetics (Figure C.4b.). Based on the SEM images and particle density calculations, it appears that this release behavior is governed more strongly by microparticle porosity, and subsequently the surface area, than by lipid hydrophobicity.

However, the observed release kinetics could also be influenced by the distribution of the nile red within the microparticle. To ascertain whether the intra-particle drug distribution was driving the release behavior from the lipid

microparticles, confocal microscopy was used to visualize the spatial deposition of nile red within particles of each lipid length (Figure C.5.). The images show that nile red is deposited near the surface for all microparticles, but the interior content increases with increasing lipid length, particularly with C_{16}. These results support the premise that microparticle porosity and surface area governs nile red release kinetics from the microparticles since greater interior content of the more hydrophobic particles would retard nile red release whereas the opposite is observed in Figure 4b.

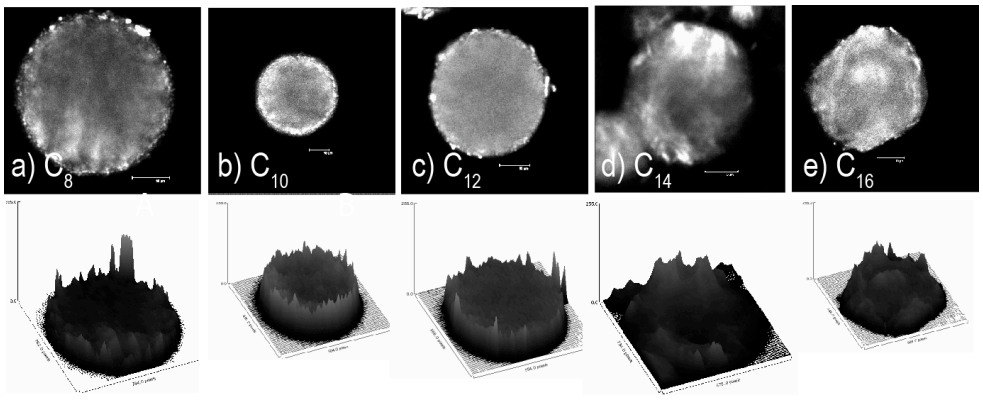

Figure C.5. Model drug distribution within lipid microparticles, clockwise from top-left, (a) nile red encapsulated C_8 particles (b) nile red encapsulated C_{10} particles, (c) nile red encapsulated C_{12} particles, (d) nile red encapsulated C_{14} particles, (e) nile red encapsulated C_{16} particles. It is apparent that with increasing lipid chain length the hydrophilic model drug distribution moves toward the surface of the particle, whilst the hydrophobic model drug remains homogenously distributed.

D. Conclusion

In conclusion, a family of DHA derived symmetrical lipids with varying hydrocarbon chain length were synthesized to systematically analyze how lipid length influences microparticle fabrication, microparticle morphology, and drug release kinetics. Our results are somewhat surprising in that the release kinetics of a hydrophobic drug model increased with increasing lipid length. SEM and confocal microscopy images, as well as particle density calculations collectively suggest that

the microparticle porosity is the primary factor that controls release kinetics, as microparticle porosity increases with increasing lipid length.

E Liquid hydrophobic matrices for controlled drug delivery

E. 1. Materials and methods

Acetic anhydride, butyric anhydride, hexanoyl anhydride, terahydrofuran, pyridine, 1,3-Dihydroxyacetone dimer 97% (DHA), sodium borohydride , anhydrous pyridine and rhodamine-B were all obtained from Sigma-Aldrich (Saint Louis, MO) and used without further purification. Dichloromethane (DCM), acetone, tetrahydrofuran (THF) and diethyl ether were purchased from J.T.Baker (West Chester, PA). All reagents and solvents were used as received without additional purification

E.2. Synthesis and characterization

Synthesis and characterization of symmetrical diglycerides

1,3-dihydroxypropan-2-one 1,3-dialkylate

Symmetrical lipids were synthesized through modification of a previously reported method by Bentley and McCrae [39]. The general procedure for short length lipids is as follows, using the synthesis of C_2 symmetrical lipid as an example: DHA (15.0 g, 153 mmole) was stirred in anhydrous pyridine (50 mL) under flow of N_2 at room temperature, followed by sequential dropwise (1 drop/sec) addition of acetic anhydride (50 ml, 453 mmol), in that order. The mixture was stirred for 1 hrs at room, after which all solvents were removed as completely as possible by vacuum distillation. The residue was dissolved in ethyl acetate, and washed with water (1 × 50 mL), and 3% aqueous hydrochloric acid (1 × 75 mL), and water (1 × 75 mL) and dried. Solvent removal by rotoevaporation in vacuo and crystallization with toluene-hexanes (1:1) resulted in long colorless needles as product. ^{1}H-NMR spectra were

recorded at room temperature with a Brucker AF-300 spectrometer operating at 300.13 MHz, and elemental analyses were obtained through QTI (Whitehouse, NJ).

A series of symmetrical diglycerides were synthesized via modification of previously suggested synthetic routes by Bentley and McCrae [39]. The protocol is as follows (for C_2 diglyceride as an example), the above synthesized solid lipid (10.0 g) was dissolved in a mixture of tetrahydrofuran:water (150:10) and treated portionwise with neutral sodium borohydride (2 g) at 5^{o}C. After 30 minutes excess sodium borohydride was destroyed via dropwise addition (1 drop/s) of glacial acetic acid (1 mL). The solution was diluted with chloroform, washed with DI-water, and aqueous sodium bicarbonate solution, and DI-water and subsequently dried over sodium sulfate, scheme E.2. Finally the solvent was removed by rotary evaporation in vacuo to obtain the final diglycerides product. As mentioned above, ^{1}H-NMR spectra were recorded at room temperature with a Brucker AF-300 spectrometer. Products were stored on dry conditions at 4^{o}C until further use.

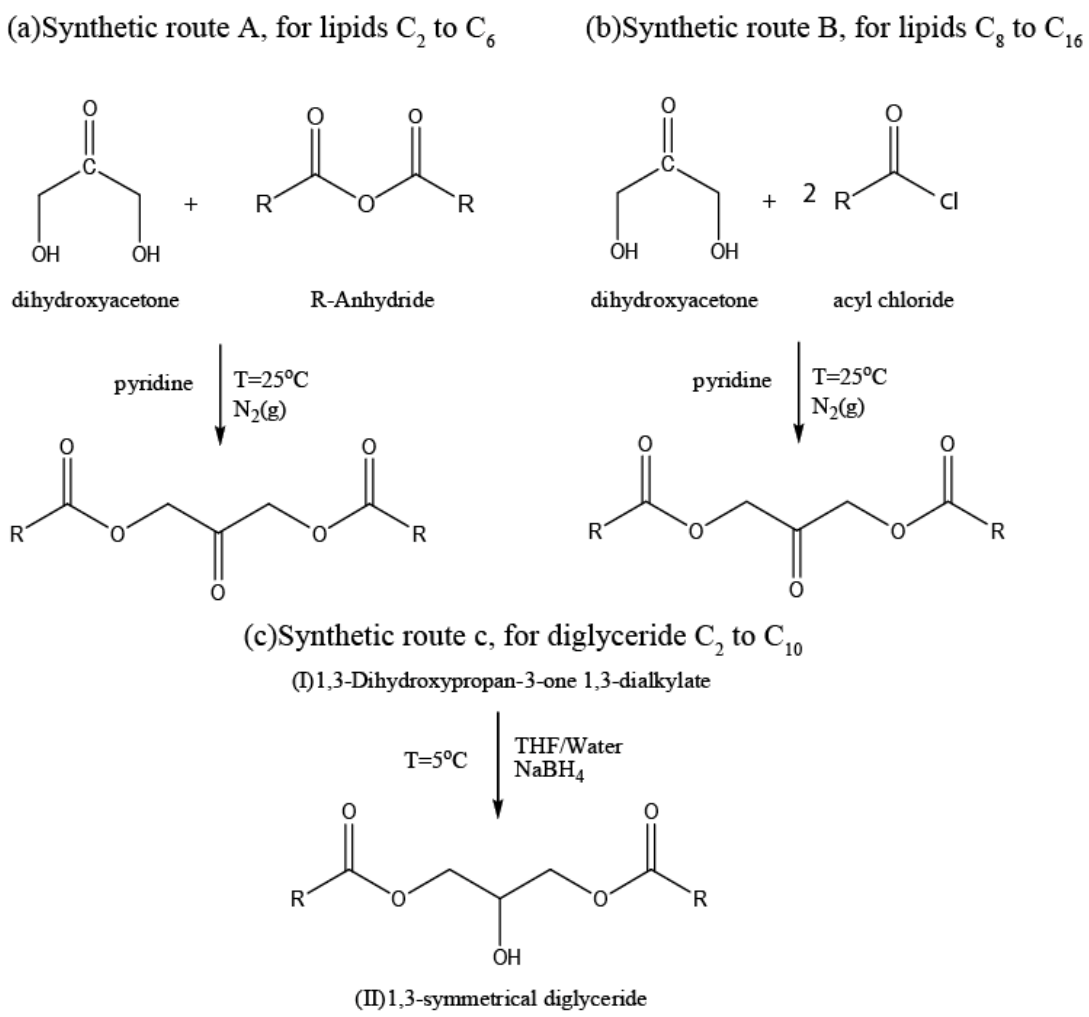

Scheme E.2. Synthesis of symmetrical 1,3-diglycerides

E.3. In vitro controlled release of Rhodamine-B

In vitro release kinetics were determined by dissolving rhodamine-B as a model drug in intended lipid, 1-mL of PBS buffer was added to the solution (total volume=2 mL). The oil in water (o/w) biphasic suspension was incubated at 37 °C and placed under gentle rotation. PBS buffer was removed for fluorescence measurement after certain time intervals to determine the amount of release, and replenished with fresh buffer. Rhodamine-B concentration was measured at λ_{Exc}=540 nm and λ_{Em}=565 nm and quantified according to a standard curve of rhodamine-B in PBS.

E.4. Cytotoxicity

Cell viability and proliferation in the presence of each diglycerides were examined using HeLa cells (Human epithelial carcinoma cell line) that were grown in Dulbecco's modified Eagle's medium (DMEM) with 10% Fetal Bovine serum (FBS) and 1% penicillin/streptomycin. All cells were maintained at 37 ^{o}C in a humidified atmosphere of 95% air, 5% CO_2. Cells were then seeded into 96-well plates at an approximate density of 5000 cells per well (25000 cells/ml). Dilutions of model drug that were prepared with dimethyl sulfoxide to avoid phase separation upon addition of the drug into the wells were added 24 hrs later. The cells were incubated with the dilutions for 4 hrs, after which the drug dilution was removed and replaced with fresh media. The MTT reagent (20 μL) was added 24 hrs later, cells were incubated with the reagent for 1 hr. The concentration of the viable cells in each well was determined by UV absorbance at λ=490 nm using a microplate spectrafluorometer.

F. Results and discussion

A series of symmetrical diglyceride were successfully synthesized by using wet-THF as a suitable solvent and $NaBH_4$ as a mild reducing agent (Scheme 3). The final diglycerides range from liquid (C_2-C_8) to waxy solid (C_{10}) at room temperature (Table 3). Physical characterization using thin layer chromatography showed presence of 1,3 and 1,2 isomers, the results were confirmed by ^{1}H NMR (300 MHz, $CDCl_3$), (Figure F.6).

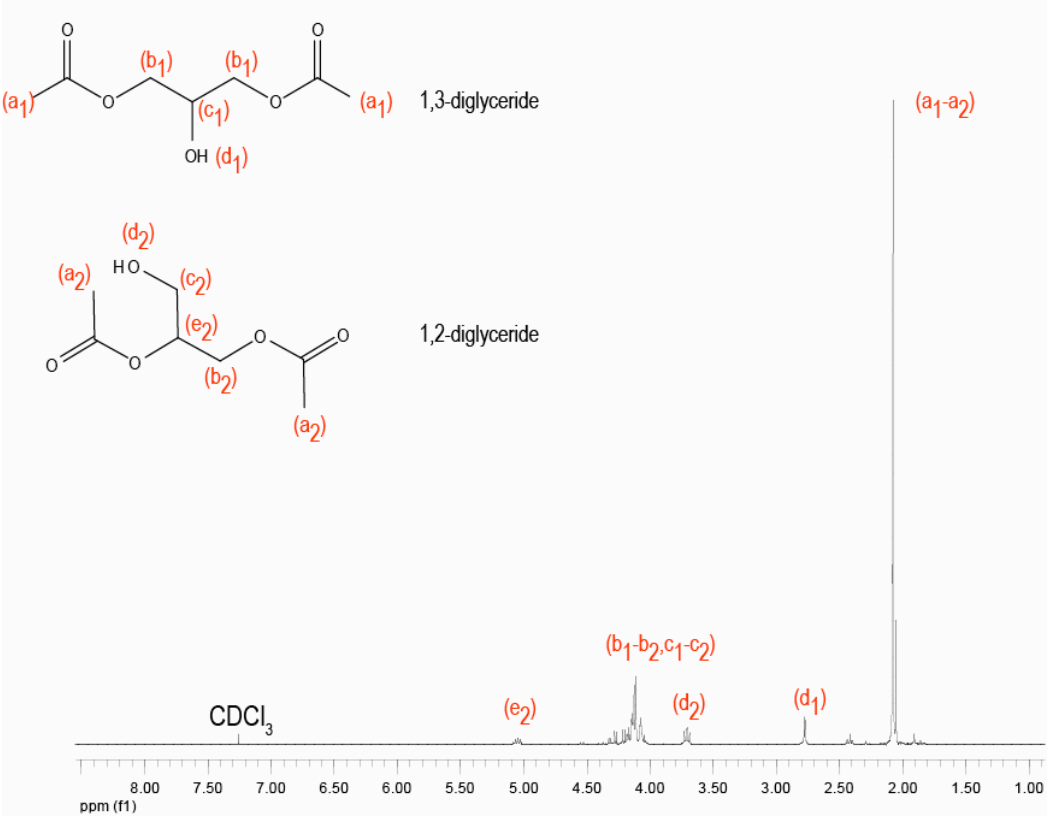

Figure F.1. ^{1}H NMR (300 MHz, $CDCl_3$, δ) of C_2 diglyceride. Other diglycerides decidedly look exactly the same with the exception of the large peak at 2.21 ppm. The peaks for [C_2 diglyceride] are 2.20 (m,12H), 2.8 (s,1H), 3.8 (s,1H), 4.10-4.30 (m,4H), and 5.10 (p,1H).

Table F.1. Elemental analysis of symmetrical diglycerides

Sample	Log P (Chem draw ®)	Experimental E. analysis		Theoretical E. analysis	
		%C	%H	%C	%H
C_2 Diglyceride	-0.87	47.79	6.99	47.72	6.87
C_4 Diglyceride	1.27	56.82	8.79	56.88	8.68
C_6 Diglyceride	2.94	62.19	10.06	62.47	9.79
C_8 Diglyceride	4.61	65.92	10.76	66.24	10.53
C_{10} Diglyceride	6.28	68.94	11.37	68.96	11.07

The level of hydrophobicity was estimated using via calculations of the partition coefficient (LogP) using ChemDraw software (Table F.1.). Reasons behind

estimation of hydrophobicity are two-fold. First, Log P values show whether the diglyceride is miscible with water or not. Second, similar to symmetrical DHA lipids, the variation of diglycerides hydrophobicity can be used to regulate the rate of the drug release.

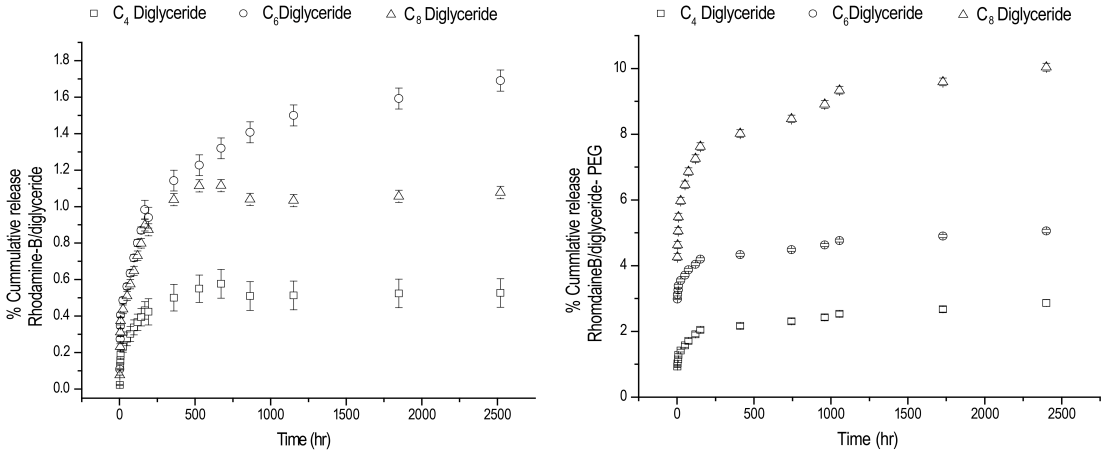

Figure F.2. Left, a) Release profiles of rhodamine-B from rhodamine-B/diglycerides into aqueous phase (PBS buffer). Right, b) Release profiles of rhodamine-B from rhodamine-B/diglycerides/PEG(M_W~200) into PBS buffer.

The in vitro release characteristics of rhodamine-B dissolved in diglycerides, a model for hydrophilic drugs, was observed over an extended period of time at 37 °C. The diglycerides exhibited chain length-dependent release behavior, similar to lipid microparticles, more hydrophobic diglycerides namely C_8 and C_6 released faster than less hydrophobic C_4 diglyceride. Additionally, C_6 diglyceride formed a double interface with the PBS buffer, thus resulting in faster release kinetics compared to more hydrophobic C_8 diglyceride (Figure F. 2a. -left, Figure F.3.).

To determine whether the rhodamine-B and diglcyeride interaction was driving the release behavior from the lipid microparticles, polyethylene glycol (PEG) with M_W of 200 was added to the binary heterogeneous mixture under identical conditions to

the original experiment. The results showed that the more hydrophobic diglycerides (C_8) released faster compared to C_6 and C_4 diglyceride. The cumulative release of each mixture compared to the binary mixture of drug and diglycerides/PBS buffer was higher, up to 10% in case of C_8-diglyceride (Figure F.2b. -right). These results support the premise that interactions between the hydrophobic matrix and hydrophilic model drug are the main driving forces behind the release kinetics observed in this experiment.

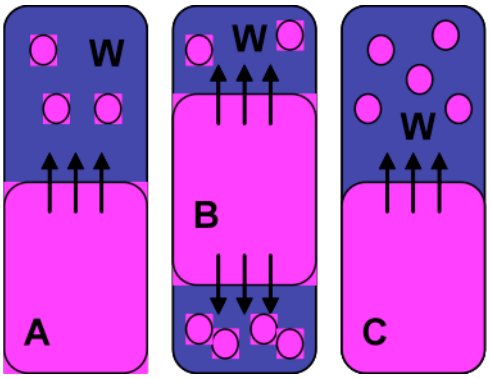

Figure F.3. Formation of interfaces between oily and aqueous layers

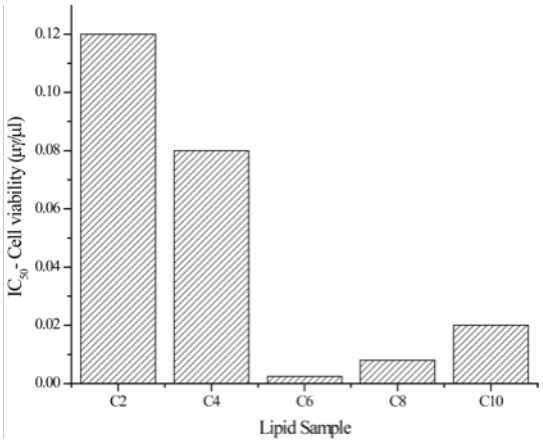

Figure F.4. Cell viability and IC_{50} after the diglycerides treatment

Presence of low molecular weight PEG impacts the initial release readings more strongly compared to the later ones, mainly because PEG is more miscible with PBS buffer rather than the diglycerides (Figure F.2b. -right).

Lastly, cells treated with free diglycerides showed decreasing viability with increasing hydrophobicity (Figure F.4.). Previously obtained results by Malhi *et al.* and Feldstein *et al.* showed that free fatty acids induce lipoapoptosis in hepatocyte cells (HepG2) [43], presuming that the diglycerides enzymatically degrade into their building blocks of fatty acids and dihydroxyacetone, the resulting fatty acids may act as cellular toxins and thus cause apoptosis. According to Feldstein *et al.* over-accumulation of fatty acids in non-adipose tissue, will lead to their entry into the nonoxidative deleterious pathways causing cell injury and death [44].

G. Conclusion

In conclusion, a family of DHA derived symmetrical lipids and their glyceride analogs with varying hydrocarbon chain length were synthesized to systematically analyze how lipid length influences drug release kinetics. Our results are somewhat surprising in that the release kinetics of model drugs increased with increasing lipid hydrophobicity. In case of microparticles, SEM and confocal microscopy images, as well as particle density calculations collectively suggest that the microparticle porosity is the primary factor that controls release kinetics, as microparticle porosity increases with increasing lipid length. As for the diglycerides, the inability to control the number of interfaces formed between the oily phase and the aqueous phase complicate our efforts for in further understanding the process of release from liquid hydrophobic matrices. In addition, the cytotoxic nature of the diglycerides makes them unsuitable for our intended applications of drug delivery.

REFERENCES

[1] R. Langer, Drug delivery: drugs on target, Science 2001, 293, 58-59.

[2] H. Rosen, T. Abribat, The rise and rise of drug delivery, Nat. Rev. Drug Discov. 2005, 4, 381-385.

[3] D. Kohane, Microparticles and Nanoparticles for drug delivery, Biotechnology and Bioengineering 2007, 96, 2, 203-209

[4] W. Jiang, R.K. Gupta, M.C. Deshpande, S.P. Schwendeman, Biodegradable poly(lactic-co-glycolic acid) microparticles for injectable delivery of vaccine antigens, Adv. Drug Del Rev 2005, 57, 391-410

[5] V.R. Sinha, A. Trehan, Biodegradable microspheres for parenteral delivery. Crit Rev Ther Drug Carrier Syst 2005, 22, 535-602

[6] S.S. Davis, Coming of age of lipid-based drug delivery systems, Adv. Drug Del Rev 2004, 1241-1242

[7] C.J.H.Porter, N.L.Trevaskis and W.N. Charman, Lipids and lipid-based formulations: optimizing the oral delivery of lipophilic drugs, Nature reviews, 2007, 6, 231-248

[8] C.W. Pouton, C.J.H. Porter, Formulation of lipid-based delivery systems for oral administration: Materials, methods and strategies, Advanced drug delivery reviews, 2007

[9] S. Jaspart, P. Bertholet, G. Piel, J.-M. Dogne, L. Delattre, B. Evrard, Solid lipid microparticles as a sustained release system for pulmonary drug delivery, Eur. J. Pharm. Biopharm. 2007, 65, 47-56.

[10] G. Jiang, B.H. Woo, F. Kang, J. Singh, P. DeLuca, Assessment of protein release kinetics, stability and protein polymer interaction of lysozyme encapsulated poly(D,L-lactide-co-glycolide) microspheres, J. Controlled Release 2002, 79, 137-145

[11] M.M. Arnolds, E.M. Gorman, L. J. Schieber, E.J. Munson, C. Berkland, NanoCipro encapsulation in monodisperse large porous PLGA microparticles, J. Controlled Release 2007, 121,1-2, 100-109

[12] S.A. Wissing, O. Kayser, R.H. Muller, Solid lipid nanoparticles for parenteral drug delivery, Adv. Drug Deliv. Rev. 2004, 56, 1257-1272.

[13] M. DelCurto, D. Chicco, M. D'Antonio, V. Ciolli, H. Dannan, S. D'Urso, B. Neuteboom, S. Pompili, S. Schiesaro, P. Esposito, Lipid microparticles as sustained

release system for a GnRH antagonist (Antide), J. Controlled Release. 2003, 89, 297-310

[14] R. Pandey, G.K. Khuller, Solid lipid particle-based inhalable sustained drug delivery system against experimental tuberculosis, Tuberculosis 2005, 85, 227-234

[15] S. Saraf, D. Mishra, A. Asthana, R. Jain, S. Singh, N. Jain, Lipid microparticles for mucosal immunization against hepatitis B, Vaccine 2006, 24, 45-56

[16] E. Gavini, V. Sanna, R. Sharma, C. Juliano, M. Usai, M. Marchetti, J. Karlsen, P. Giunchedi, Solid lipid microparticles (SLM) containing juniper oil as anti-ace topical carriers: preliminary studies, Pharm. Dev. Technol 2005, 10, 479-487.

[17] S. Jaspart, G. Piel, L. Delattre, B. Evrard, Solid lipid microparticles: formulation, preparation, characterization, drug release and applications, Expert Opin. Drug Deliv. 2005, 2, 75-87.

[18] H. K. Frederiksen, H. G. Kristensen, M. Pedersen, Solid lipid microparticle formulations of the pyrethroid gamma-cyhalothrin-incompatibility of the lipid and the pyrethroid and biological properties of the formulations, J. Controlled Release 2003, 86, 243-252

[19] R. Cortesi, E. Esposito, G. Luca, C. Nastruzzi, Production of lipospheres as carriers for bioactive compounds, Biomaterials 2002 , 23, 2283-2294.
C. Erni, C. Suard, S. Freitas, D. Dreher, H.P. Merkle, E. Walter, Evaluation of cationic solid lipid microparticles as synthetic carriers for the targeted delivery of macromolecules to phagocytic antigen-presenting cells, Biomaterials 2002 ,23, 4667-4676.

[20] B. Heurtault, P. Saulnier, B. Pech, J.-E. Proust, J.-P. Benoit, Physico-chemical stability of colloidal lipid particles, Biomaterials 2003, 24, 4283-4300.

[21] W. Mehnert, K. Mader, Solid lipid nanoparticles: Production, characterization and applications, Adv. Drug Deliv. Rev. 2001, 47, 165-196.

[22] H. Reithemeier, J. Herrmann, A. Gopferich, Development and characterization of solid lipid microparticles as drug carrier for somatostatin. Int. J. Pharm 2001, 218, 133-143

[23] M. Savolainen, J. Herder, C. Khooc, K. Lövqvist, C. Dahlqvist, H. Glad, A. M. Juppo, Evaluation of polar lipid-hydrophilic polymer microparticles, Int. J. Pharm 2003, 262, 1-2, 47-62

[24] N. Passerini, B. Perissutti, B. Albertini, D. Voinovich, M. Moneghini. L. Rodriguez, Controlled release of verapamil hydrochloride from waxy microparticles prepared by spray congealing, J. Controlled Release 2003, 88, 263-275

[25] Y. Akiyama, M. Yoshioka, H. Horibe, S. Hirai, N. Kitamori, H. Toguchi, Novel controlled-release microspheres using polyglycerol esters of fatty acids, J. Controlled Release 1993, 26, 1-10

[26] B. Gaucher, M. Rouquayrol, D. Roche, J. Greiner, A. Aubertin and P. Vierling, Prodrugs of HIV protease inhibitors-saquinavir, indinavir and nelfinavir-derived from diglycerides or amino acids: synthesis, stability and anti-HIV activity, Org. Biomol. Chem., 2004, 2, 345 – 357

[27] M.S.Y. Khan, M. Akhter, Synthesis, pharmacological activity and hydrolytic behavior of glyceride prodrugs of ibuprofen, European Journal of Medicinal Chemistry, 2005, 40, Issue 4, 371-376

[28] L. Rodriguez, N. Passerini, C. Cavallaria, M. Cinia, P. Sancinb and A. Finic, Description and preliminary evaluation of a new ultrasonic atomizer for spray-congealing process, Int. J. Pharm 1999, 183, 133-143

[29] M. Demirel, Y. Yazan. R. H. Muller, F. Killice and B. Bozan, Formulation and in vitro-in vivo evaluation of piribedil solid lipid micro-nanoparticles, J. Microencapsulation 2001, 18, 359-371

[30] S. Vanna , N. Kirschvink, P.Gustin, E. Gavini, I. Roland, L. Delattre, and B. Evrard, Preparation and In Vivo Toxicity Study of Solid Lipid Microparticles as Carrier for Pulmonary Administration, AAPS PharmSciTec 2003, 5, Article 27

[31] T. Eldem, P.Speiser, A. Hincal, Optimization of spray-dried and congealed lipid micropellets and characterization of thier surface morphology by scanning electron microscopy, Pharm. Res.1991, 8, 47-54

[32] F.Q. Hu, H. Yuan, H.H. Zhang, M. Fang, Preparation of solid lipid nanoparticles with clobetasol propionate by a novel solvent diffusion method in aqueous system and physicochemical characterization, Int. J. Pharm. 2002, 239, 121-128.

[33] J.M. Berg, J.L. Tymoczko, L. Stryer: Biochemistry, W.H. Freeman and Co., New York, 1995

[34] V. Esmann, Dihydroxyacetone as an intermediate during the metabolism of glycerol and glyceraldehyde in leukocytes from the rat. , Acta. Chemica. Scandinavica.1968 , 22, 2281-2288

[35] P.N. Zawaneh, A.M. Doody, A.N. Zelikin, D. Putnam, Diblock copolymers based on dihydroxyacetone and ethylene glycol: synthesis, characterization, and nanoparticle formulation, Biomacromolecules 2006, 7 ,3245-3251

[37] A.N. Zelikin, D. Putnam, Poly(carbonate-acetal)s from the dimer form of dihydroxyacetone, Macromolecules 2005, 38, 5532-5537

[38] A.N. Zelikin, P.N. Zawaneh, D. Putnam, A functionalizable biomaterial based on dihydroxyacetone, an intermediate of glucose metabolism, Biomacromolecules 2006, 7, 3239-3244.

[39] P.H. Bentley, W. McCrae, An efficient synthesis of symmetrical 1,3-diglycerides, J. Org. Chem. 1970, 35, 2082-2083.

[40] M.A. Tracy, K.L. Ward, L. Firouzabadian, Y. Wang, N. Dong, R. Qian, Y. Zhang, Factors affecting the degradation rate of poly(lactide-co-glycolide) microspheres in vivo and in vitro, Biomaterials 1999, 20, 1057-1062

[41] D.A. Edwards, J. Hanes, G. Caponetti, J. Hrkach, A. B. Ben-Jebria, M. L. Eskew, J. Mintzes, D. Deaver, N. Lotan, R. Langer, Large porous particles for pulmonary drug delivery, Science ,1997, 276: 1868-1871.

[42] R.A. Jain, The manufacturing techniques of various drug loaded biodegradable poly(lactide-co-glycolide) (PLGA) devices, Biomaterials 2000, 21, 2475-2490.

[43] H. Malhi, S. F. Bronk, N. W. Werneburg, and G. J. Gores, Free Fatty Acids Induce JNK-dependent Hepatocyte Lipoapoptosis. Biol. Chem., 2006, 281, Issue 17, 12093-12101

[44] A.E. Feldstein, N.W. Werneburg, A. Canbay, M.E. Guicciardi, S.F. Bronk, R. Rydzewski, L.J. Burgart, G.J. Gores, Free fatty acids promote hepatic lipotoxicity by stimulating TNF- expression via a lysosomal pathway, Hepatology, 2004, 40, Issue 1,185-194